FABRICATION AND CHARACTERIZATION OF HIGH T_C BULK MATERIALS AND FILMS FOR SUPERCONDUCTING DEVICES

THESIS

Submitted in partial fulfilment

of the requirements for the degree of

DOCTOR OF PHILOSOPHY

by

AJAY AGARWAL

Under the Supervision of

Dr. Ram P Gupta

BIRLA INSTITUTE OF TECHNOLOGY AND SCIENCE

PILANI (RAJASTHAN) INDIA

1997

DEDICATED

TO

MY

FATHER

and

MOTHER

ACKNOWLEDGEMENT

Howsoever formal or ritualistic the Acknowledgements may seem, it is necessary. A person on the threshold of a life-time achievement approaches the moment with a tremulous heart - pulsating with excitement, expectation and apprehension; with hope and trepidation. The moment is significant and full of tremendous possibilities for a future, bright and rosy. At such a crucial moment it is only natural and proper to remember one and all of those who have been instrumental in putting him in his present situation. It is for this reason that this formality is not all that formal and ritualistic; it is as much the expression of a genuinely grateful heart. It is, frankly and honestly, in this spirit that I proceed to record my gratitude. My words, I know, will fall far short in giving adequate expression to the range and depth of my gratitude but I am also aware and confident of the generosity and magnanimity of my benefactors and well-wishers.

With all the humility and earnestness I am capable of, I bow to my guide Dr. Ram P. Gupta, Scientist/ Deputy Director, Central Electronics Engineering Research Institute, Pilani, whose debt I shall never be able to gauge and repay. Who has ever repaid a kindness? Respected Dr Gupta's enlightened supervision has really enabled me to complete my endeavour. His immense knowledge, vast experience in the field of conducting and guiding research endeavours and constant encouragement and support have been my proud privilege. supervision this work has been accomplished. His knowledge, experience, constant encouragement and support has helped me tremendously in completing this work.

The technical discussions and suggestions from Dr. W. S. Khokle (Ex-Director, CEERI, Pilani), Dr. P. D. Vyas, Dr. Chandra Shekhar and Dr. R. K. Garg (Scientists, CEERI, Pilani) and Prof. (Mrs) Aparna Gupta, Prof. L. K. Maheshwari, Prof. G. P. Srivastava, Prof. S. Kumar (Deans, BITS, Pilani) have enlightened my way to successful

completion of this thesis. Their words of advice and encouragement have been of great help at various points of time.

I am extremely grateful to Dr. P. R. Deshmukh, Mr. Mulayam Singh and Mr. Kamaljeet Rangara for the EDAX analysis and SEM Micrography, which they have done at utmost priority, every time I approached them. Without their help it was very difficult

research. I have always felt their blessings and encouragement throughout my endeavour. I would like to record my debt of gratitude to my wife Dolly, who apart from other materialistic supports, has given me the much needed emotional support from the core of her heart. Her constant inspiration had been the source of great boost during the tough days of writing and compiling the thesis. I profoundly acknowledge the limitless love and constant inspiration/ guidance I have got from my brothers-in-law Dr. Ravindra and Er. Devesh and my sisters Alpana, Kalpana and Priyanka.

Finally, I thank all mighty God, unknown powers and human beings who have contributed in their own way towards the realization of this research work. As these noble spirits have been my sustenance so far, I hope and pray that they still give me their sincere best wishes and blessings as I need them now and always.

AJAY AGARWAL

Central Electronics Engineering Research Institute
Pilani - 333 031, Rajasthan, India
Phone : 91-1596-43483 (O) 42757 (R) Fax : 91-1596-42294
E-Mail : rpg@ceeri.ernet.in Gram : "ELECTRONIC"

Dr. R.P. Gupta
Group Leader
Sensors & Microsystems Group

CERTIFICATE

This is to certify that the thesis entitled **Fabrication and Characterization of High T_c Bulk Materials and films for Superconducting Devices** and submitted by ***Ajay Agarwal*** ID. No. 90PZYF019 for award of Ph.D. Degree of the Institute, embodies original work done by him under my supervision.

Signature in full of the Supervisor

Name in capital block letters **DR. RAM P GUPTA**

Date: 16 Dec '97 Designation **Scientist F**

List of Abbreviations

A - contact area

APCVD - Atmospheric Pressure Chemical Vapour Deposition

ARE - Activated Reactive Evaporation

AVFT - Abrikosov Vortex Flow Transistor

B - magnetic field

B-2212 - $Bi_2Sr_2CaCu_2O_y$

BPSCCO - Bismuth Lead Strontium Calcium Copper Oxide

BSCCO - Bismuth Strontium Calcium Copper Oxide

C - Celcius

C_G - gate capicitance

CGRs - Carbon Glass Resistors

CMF - Compressed Magnetic Field

CVD - Chemical Vapour Deposition

d - inter planer spacing

DBTs - Dielectric Base Transistors

dil. - dilute

E_{kin} - kinetic energy

E/B/C - Emitter-Base-Collector

ECR - Electron Cyclotron Resonance

EDAX - Energy Dispersive Analysis of X-rays

e.g. - example

emf - electromotive force

f - frequency of AC field

FET - Field Effect Transistor

FTS - Facing Target Sputtering

g.b. - Grain boundary

GHz - Giga Hertz

GPa - Giga Pascal

GRT - Germanium Resistance Thermometer

H - RMS magnetic field

H_c - critical magnetic field

H^* - reversible field

HTS - High Temperature Superconductivity

HTSC - High Temperature Superconductor

HWE - Hot Well Epitaxy

I_{ct} - transport critical current

I_G - Gate current

IBAD - Ion Beam Assisted Deposition

I-V - current-voltage

J_b - inter-granular critical current density

J_c - Critical current density

J_{ct} - transport current density

J_d - depairing critical current density

J_{fp} - flux pinning critical current density

J_p - percolation critical current density

JJ - Josephson Junction

JOFET - Josephson Field Effect Transistor

JVFT - Josephson Vortex Flow Transistor

K - Kelvin

kcal - kilo calories

kohm - kilo ohm

kV - kilo volt

LHe - liquid helium

LN_2 - liquid nitrogen

LPCVD - Low Pressure Chemical Vapour Deposition

LPE - Liquid Phase Epitaxy

LTS - Low Temperature Superconductors

MBE - Molecular Beam Epitaxy

MHz - Mega Hertz

MIS - Metal Insulator Superconductor

MOCVD - Metallorganic Chemical Vapour Deposition

MRI - Magnetic Resonance Imaging

mV - milli volt

n - an integer (for order of diffraction)

nA - nano Ampere

NMR - Nuclear Magnetic Resonance

OPT - Oxygen Plasma Treatment

PRT - Platinum Resistance Thermometer

psec - pico second

Q - quality factor

QPIDs - Quasiparticle Injection Devices

R - resistance

R_s - surface resistance

R-123 - $RBa_2Cu_3O_{7-x}$ where R= rare earth elements

RABiTS - Rolling Assisted Biaxial Texturing

R-T - resistance-temperature

SBTs - Superconducting Base Transistors

SD - source drain

SEM - Scanning Electron Microscopy

SQUID - Superconducting Quantum Interference Device

STO - strontium titanate

STM Scanning Tunnelling Microscopy

SUBSITs - Superconducting Base Semiconductor Injection Transistors

Su-FET - Superconducting Field Effect Transistor

super-CIT - superconducting- Current Injection Transistor

super-HETs - superconducting- Hot Electron Transistors

T_c - critical temperature

$T_{c,ON}$ - onset temperature

$T_{c,zero}$ - zero dc temperature

TBCCO - Thallium Barium Calcium Copper Oxide

UHP - ultra high pure

UHV - ultra high vacuum

v - measured RMS voltage

V - sample volume (for susceptibility)

V_{CROSS} - cross over voltage

V_G - gate voltage

VFTs - Vortex Flow Transistors

XRD -X-Ray Diffraction

YBCO - Yittrium Barium Copper Oxide

YSZ - Yttria Stabilized Zirconia

1-2-3 - $Y_1Ba_2Cu_3O_7$

2223 - $Bi_2Sr_2Ca_2Cu_3O_y$

Å - Angstrom

° - degree

α - calibration coefficient, thermal coefficient

β - current gain

χ - volume susceptibility

χ' - real part of susceptibility

χ'' - imaginary part of susceptibility

ε - dielectric constant

λ - wave length, penetration depth

λ_{el} - electric penetration depth

θ - Bragg's diffraction angle

μm - micro meter

μA - micro ampere

ξ - coherece length

ρ_c - contact resistivity

Δ - energy gap

ΔG - free energy

ΔH - change in enthalpy

ΔH_{298} - heat of reaction at 298K

$\Delta H_{reaction}$ - heat of reaction

ΔS - change in entropy

ΔT - temperature change

ΔT_c - transition width

ΔV - voltage change

CONTENTS

CHAPTER-ONE

ELECTRONICS WITH SUPERCONDUCTING DEVICES

1.1 INTRODUCTION

The electronic applications of high temperature superconductors (HTS) have received enormous attention since their discovery in 1986. Although the euphoria around the discovery has faded away, the basic understanding of this fascinating phenomenon of superconduction in ceramic oxides and the applications of these materials are steadily making progress. In fact, electronics with superconducting devices belongs to low temperature electronics, also known as cold electronics, cryogenic electronics or cryo-electronics, which involves operation of devices, circuits and systems at temperatures significantly below room temperature. The motivation for low temperature electronics is the improved performance compared to conventional electronics operating at normal ambient temperature. At low temperatures, the disruptive thermal effects that cause power waste, noise and wear-out are greatly reduced. The increased speed of digital system, better signal-to-noise ratio and greater bandwidth of analog system, improved sensitivity of sensors and greater precision of measuring instruments are some of the obvious advantages of cryo-electronics. In this connection, the uses of superconducting devices, which only operate at low temperatures, i.e. below their critical transition temperature (T_c) of superconduction, are being explored since the discovery of superconductivity in 1911. However, it is only after development of reliable niobium superconducting junctions towards the end of 1983, that various kinds of useful integrated circuits and systems, operating at liquid helium temperatures, were realized.

One of the major hurdles that prevented the wide use and rapid development of low temperature electronics is carrier "freeze-out" problem in silicon devices, which even today constitute a major part of circuitry associated with a cry-electronic system. At temperatures below about 40K, silicon devices exhibit radical changes in characteristics due to carrier freeze-out, i.e. the current carriers in the device become inactive in want of sufficient thermal energy. The discovery of high temperature ceramic superconductors having superconducting temperature above boiling point of liquid nitrogen, has, however, opened up possibilities of raising the temperature of cold electronics to a level where associated semiconductor-based electronics also operates efficiently. Consequently, better performance is expected by combining matured semiconductor electronics with high T_c superconducting devices. From cryogenic point of view, liquid nitrogen (LN_2) usage as coolant in field applications is much cheaper in comparison to liquid helium (LHe). This is attributed to the difference in their latent heats. The latent heat of LN_2 is about 60 times to that of LHe. Therefore, the boil rate of LN_2 is much slower. This is one of the main reasons for researchers interest on development of HTS devices in laboratories around the world.

1.2 SUPERCONDUCTING ELECTRONICS

Superconductivity is considered to be the most remarkable phenomenon of condensed matter physics. Two basic properties of superconductors are: (i) Zero dc resistance below T_c, i.e. perfect conduction and (ii) Meissner effect or expulsion of magnetic field in the superconducting state, i.e. perfect diamagnetism. The transition temperature of known superconducting metals and alloys, now named as low temperature superconductors (LTSs) are limited to 23K, i.e. liquid helium temperatures. However, the ceramic superconductors have shown superconduction well above 100K. Therefore, these HTS can possibly bring the benefits of superconductivity to a more practical domain and thus likely to cause great changes in the conventional cryo-electronics.

In general, the applications of superconductors are of two kinds. The first category is that of low-power electronic application, where the involved current (only few mA) and magnetic fields (< 1 Tesla) are relatively small. The second class of applications employs bulk material in the form of wires etc. of large cross-section to support high current in high magnetic field environment. In the present work, we are only concerned with the low-power electronic applications of superconductors.

1.2.1 Superconducting passive components

The criterion of zero resistance of a superconductor is no more valid at radio frequency. At these frequencies, surface current predominates and therefore, surface resistance (R_s) controls the high frequency behaviour of the material. For normal conductors, the current penetration depth is determined by 'skin effect' and is proportional to the square root of frequency. In case of a superconductor, it is independent of frequency and is equal to 'London penetration depth'. Since 'London penetration depth' is small compared to 'skin depth', particularly at low frequencies, the thickness of a superconductor can remain very small at low frequencies. However,even at radio frequencies the resistance of superconducting films is low compared to conventional conductors. So for the microwave applications such as filters, delay lines, low-loss transmission lines, ultra-high Q (quality factor) resonator and other passive components, superconductors are useful.

The superconducting transmission lines can also store signal without much attenuation or distortion. On coupling with other devices, the line can be configured to perform complex functions such as filtering, convolution, correlation, pulse compression/ expansion, Fourier transformation and spectral manipulation. Circuits based on superconducting films have demonstrated real time analog processing of signals having gigahertz bandwidths that could be applied to radar, communications or spectral analysis. Compared to circuits using normal conductors, superconductors can provide an order of magnitude greater bandwidth. A 19-pole HTS thin film has been designed (Zhang et al., 1995). Nisenoff et al. (1991) and Kawechi et al. (1996) have also reported extensive work on microwave applications of HTS materials. Sze et al. (1989) have also fabricated a

microstrip transmission line by sandwiching a mylar dielectric between two HTS films operating from 2 to 25 GHz.

1.5.2 Superconducting active devices

There is a whole range of active electronic circuits and systems based on Josephson junction (JJ), the foremost active device of superconductivity. The device possesses a number of attributes, such as fast switching, low power dissipation, wide frequency range, low noise and high sensitivity, which are valuable for electronic applications. The JJ digital gates switch rapidly within a few picoseconds and dissipate extremely low power (only a few microwatt). There is no semiconductor device that can match both at once. Thus, digital systems and computers based on JJs could outperform those based on semiconductor devices.

A high quality niobium-based JJ has been realized after the termination of IBM Josephson supercomputer programme in September 1983. The $Nb/AlO_x/Nb$ junctions are now frequently being used in almost all liquid helium-based electronics. The JJs have three important features for digital applications: (i) high switching speed (1-10 ps/gate) (ii) low power consumption (1-10 μW/gate), and (iii) low dispersion signal transmission (transmission velocity is 100 μm/ps). The development of high speed superconductive computing system is attributed to these three important characteristics of a JJ.

In addition to the difficulties in materials and process development, device design and circuit simulation, progress in superconductive electronics is hindered by lack of a good active device like semiconductor transistor. To obtain the basic functions, several JJ configurations are used in a superconductive digital circuit. Thus building a practical electronic system such as a computer from JJ device is more challenging than one from semiconductor devices. Nonetheless, a JJ-based random-access non-destructive read-out memory cell suitable for fast cache applications in a Josephson computer was developed with an access time of 4 ns (Duzer, 1980; Henkels and Zappe, 1978). A single-flux-quantum memory cell for main memory application was first investigated for a Josephson

computer at IBM (Guéret, et al., 1980). In 1988 Kotani et al. reported a 4-bit microprocessor at Fujitsu, which was the equivalent of the well-known silicon AM 2901 bit-slice processor. Later, they produced a 8-bit digital signal processor (Kotani et al., 1990). Recently, an almost perfect (99.8% bit yield) random access 4-kbit memory chip has been reported by NEC (Tahara et al., 1996). For various applications voltage-state logic circuit have been used (Hatano et al., 1989; Numata et al., 1996; Feld et al., 1996; Spooner et. al., 1996; Hosoya et al., 1996; Bradley et al., 1996; Jeffery et al., 1996). Several families and applications of single-flux-quantum logic circuits have also been reported (Likharev et al., 1985; Herr et al., 1996; Rylov et al., 1996; Przybysz et al., 1995; Semenov et al., 1996; Dubash et al., 1996; Worsham et al., 1996; Mukhanov , 1993; Deng et al., 1995; 1996; Kirichenko et al., 1996). A new approach to memory in which CMOS memory is adapted to Josephson system was utilised by Ghoshal et al. (1993, 1995a, 1995b). A small number of digital circuits have been made with various types of Josephson junction in YBCO technology (Shokor et al., 1995; Kaplunenko et al., 1995; Wiegerink et al., 1995; 1996; Zhang et al., 1996; Cambridge et al., 1996; Berkowitz et al., 1996).

The SQUID magnetometer is based on an element consisting of a superconducting loop containing either one or two Josephson junctions. It is the most sensitive instrument to detect extremely small magnetic field of the order of 10^{-10} gauss/$(Hz)^{1/2}$. The so-called rf-SQUID magnetometer employs a loop with one junction. The loop is inductively coupled to an RF-driven circuit which can detect the changes of the reactance of the loop produced by changes of flux linking it. It thus acts as a flux-to-reactance converter. The so-called dc-SQUID magnetometer is based on a loop interrupted by two junctions which serves as a flux-to-voltage converter. Both type of SQUID magnetometer employ electronic system to complete their functions as measurement systems. In the mid-1980's LTS-SQUID using Niobium/Aluminium-oxide/Niobium Josephson junctions, were well developed and in use for laboratory measurements and cardiological and geophysical measurements. There are now systems with 32-SQUID detectors for cardiac measurements and with over 100 sensors for brain measurements (Clarke, 1993).

Dimos et al. (1988) used HTS film epitaxially deposited on bicrystal, to make SQUID magnetometer. Drung et al. (1996a) have made magnetocardiogram using an HTS-SQUID magnetometer with the input transformer on a separate chip flipped on the SQUID chip. Both LTS and HTS SQUID loops have been used for non-destructive evaluation and microscopy of corrosion pits, fatigue cracks, voids, subsurface features and stress (Donaldson et al., 1993; Jeffery et al., 1995). A monolithic combination of the SQUID and its transformer was used to measure brain activity (Drung et al., 1996b).

Since 1972, standard volt has been maintained using the relationship between voltage and frequency in a Josephson junction and the highly precise measurement of frequency. The early systems only produce voltages in the milli volt range at constant voltage steps in junction I-V characteristics; these had to be compared through a precise potentio-meter to volt-level outputs of secondary standards. A new concept was introduced in 1984 using properly designed tunnel junctions irradiated by microwaves develop constant voltage steps (Nieneyer et al., 1984; Hamilton et al., 1985). The present standard for 1.2 V is maintained by an array of about 2000 junctions irradiated by a 94 GHz microwave source. The concept was latter extended to a much larger array with a voltage of 10 V (Lloyd et al., 1987). A recent work is aiming to make a digital-to-analog converter in order to make an volt standard capable of producing arbitrary time-depended signals of high frequency and precise values (Benz and Hamilton, 1996).

The motivation for developing a three terminal superconducting device like a semiconductor transistor is attributed to unmatched characteristics of transistors. These are input-output isolation, inversion and well defined gain. The replacement of JJs by a three-terminal superconducting device reduces the complexities of the circuit design to a great extend. Also, since the carrier density in high T_c materials is lower by an order of magnitude compared to low T_c materials, the electric field penetration depth is larger. These properties along with high dielectric constant make these materials promising for electric field effect devices like the semiconductor-FETs. The study of high T_c based FET is the main objective of present work and it is described in detail in chapter six of this thesis.

CHAPTER - TWO

MEASUREMENT TECHNIQUES

2.1 INTRODUCTION

The characterization of superconductors requires familiarity with a number of measurement techniques. The measurement of resistivity and magnetic susceptibility are primary ones while other characterizations include x-ray diffraction, EDAX, scanning electron microscopy (SEM), scanning tunnelling microscopy (STM), surface profiling, etc. Since many of these properties are measured as a function of temperature, the knowledge of thermometry at cryogenic temperatures is very important for the experimentalists. This chapter deals with these techniques in brief.

2.2 TEMPERATURE MEASUREMENT

The measurement and control of temperature is pivotal to experiments or applications involving superconductivity. In case of high temperature superconductors, the temperature monitoring and control is very important during material processing, which involves various heat treatments and the same is true for characterizing the samples for its temperature dependent properties. Hence, a wide range of temperature sensors are required which are capable of recording temperature as high as 1000°C in muffle/ air furnace on one hand, and others that are particularly sensitive at or below liquid nitrogen temperature i.e. 77K, on the other hand. In this section, we summarize the properties of different sensors which are commonly used for synthesis and characterization of high temperature superconductors.

2.2.1 Thermocouples

A thermocouple is formed when two dissimilar wires are joined together at two ends. One end namely hot junction is used to measure the temperature while, the other end is called cold/ reference junction. A measuring device usually milli-voltmeter is connected between the dissimilar wires. The working principle of such a couple is that when its two junctions are at different temperatures, an electromotive force (emf) is set up due to algebraic sum of:

(i) An emf developed between two different metals placed in contact to form a junction, known as "Seebeck" effect.

(ii) An emf developed between the ends of a homogeneous wire when one of its ends is heated, it is known as "Thompson" effect.

The magnitude of the emf therefore depends on the metals/ alloys used to construct the thermocouple and on the temperature difference of the junctions.

Thermocouples are particularly useful for applications where a small sensor is required for high spatial resolution or where low thermal capacity of the sensor is important. When high accuracy is required, thermocouples may be calibrated against a temperature standard over the range of interest. Thermocouples also have the advantage that the circuitry required for temperature measurement is simple, for e.g., a micro/ milli voltmeter and a water-ice bath for the reference junction. A thermoelectric refrigerator may replace the ice bath and cold-junction "compensation" circuits are also available in the modern temperature measuring devices. The data pertaining to common couples are given in Table-2.1.

Most of the thermocouples are quite effective at high temperatures only, typically above 600K but type T couple may be used down to about 20K with reasonable accuracy. We have mainly used K type and R type thermocouples for monitoring (i) furnace temperature during material processing, (ii) substrate temperature during deposition of high T_c films, and for some other high temperature applications.

Table-2.1 Thermocouples and related data.

Thermocouple Wires	Type	Upper Limit (°C)
Copper/Constantan (60%Cu + 40% Ni)	T	400
Iron/Constantan	J	800
Chromel (90%Ni + 10%Cr)/ Alumel (98%Ni + 2%Al)	K	1100
Platinum/ Platinum with 10%Rhodium	S	1450
Platinum/ Platinum with 13%Rhodium	R	1450

2.2.2 Carbon and Carbon-Glass Resistors (CGRs)

The property of change in resistance with temperature is used in resistor sensors. Carbon and carbon-glass resistors are the favourite temperature sensors for cryogenic applications. These devices are quite rugged and show a very high sensitivity to temperature in the range below approximately 20K, where increase in its resistance with temperature is large. For accurate measurement, the voltage drop on the current-supplying wires should be avoided. Hence, carbon resistors are generally used in a four-lead measurement configuration. Carbon-glass resistors are highly stable carbon resistors designed especially for thermometry. Also, CGRs are relatively insensitive to magnetic fields up to about 10 Tesla, hence, are suitable for superconductor measurements performed in the presence of magnetic field.

2.2.3 The Germanium Resistance Thermometer (GRT)

The germanium resistance thermometer (GRT) is particularly useful at temperatures below 0.05K and is commonly used up to 100K. A standard GRT is a germanium chip mounted in a strain-free manner, in a cylindrical copper enclosure. The conventional `four terminal' resistance measurement technique is used. The sensor has typically 10-100 Kohm resistance at low temperatures and as little as a few ohm at higher

temperatures. The device is specially recommended for applications below 30K, where high accuracy is required. Thus a reproducibility of 0.001K is possible, at the low temperatures, with GRT. The sensor is not the best for use in high magnetic fields.

2.2.4 Rhodium - Iron (Rh-Fe) Resistance Thermometers

The rhodium-iron resistance sensor has an anomalous temperature response near 40K that leads to good sensitivity at low temperatures. The device is useful from less than 1K to levels of 800K with ± 0.01K stability. However, Rh-Fe sensor is expensive to construct.

2.2.5 Platinum Resistance Thermometer (PRT)

Platinum Resistance Thermometers (PRTs) are precise, rugged and wide range temperature sensors. PRT can be used to measure temperatures between 70K to 1000K. The accuracies achieved are up to 10 milli-kelvins.

2.2.6 Diode Temperature Sensors

Ordinary silicon and gallium arsenide diodes have sufficient sensitivity to temperature to allow their voltage drop (at constant current of ≅100μA) to be a reliable thermometer for many applications. The typical sensitivity ($\Delta V/\Delta T$) of voltage drop versus temperature for a silicon diode is of the order of 2-3 mV/K at 300K, which increases as the temperature decreases. A sudden increase in $\Delta V/\Delta T$ at temperatures in the range of 30K results in a rather high sensitivity at the low temperatures. Diode sensors may be used to achieve sensitivity of the order of 0.1K at cryogenic temperatures.

A summary of the important characteristics of some commonly used cryogenic temperature sensors is listed in Table 2.2 and the Table 2.3 contains various types of temperature sensors used, in our laboratory, for different purposes.

Table 2.2 Characteristics of some cryogenic thermometers

Type	Temperature range	Typical Reproducibility	Magnetic field Limitation
Germanium Resistance Thermometer (GRT)	<0.05 to 100K	<0.001K	B <2.5 T
Carbon-Glass Resistor (CGR)	1.4 to 330K	0.001K	B upto 19 T
Platinum Resistance Thermometer (PRT)	14K to 850°C	0.01K	Poor Reproducibility
Rhodium-Iron (Rh-Fe) Thermometer	1 to 800K	0.01K	Limited use
Silicon Diode	1 to 473K	0.03K	B < 2.5K
GaAlAs Diode	1 to 325K	0.05K	---
Capacitance Sensor	1 to 330K	0.3K	Superior at Highest fields

Table 2.3 Different temperature sensors used with their application

Equipment/ system	Temperature sensor used
(i) Furnaces	Type K, R and NiCr/Ni thermocouple
(ii) Sputtering system, for monitoring substrates temperature	Type K thermocouple
(iii) R-T measurement Set-up	Platinum Resistance Thermometer (PRT 100)
(iv) A.C.Susceptometer	Silicon diode
(v) Helium closed cycle refrigeration system	GaAlAs diode/Silicon diode

2.3 RESISTIVITY MEASUREMENT IN SUPERCONDUCTORS

The measurement of resistivity of superconductor samples is, atleast in principle, not different from measurement of the same of the metals. The main difference is that, as

temperature falls below critical temperature (T_c), the resistance to be measured reduces to zero value, theoreticaly. However, the very small resistance values, approaching zero are difficult to measure. Zero resistances are, in principle, impossible to measure. At best, one can determine that the resistance is below a certain upper limit, determined by the resolution of the measuring equipment. For the determination of T_c in superconducting samples, four probe measurement technique is usually employed. The method is also known as Kelvin measurements. Here, four terminals are attached to the sample, as shown in the Fig. 2.1. Through the outer two probes a constant current is applied, whereas, the potential drop is measured between inner terminals. The technique is useful since the contact resistance between the superconductor-metal interface is eliminated from the measured values.

A typical resistance-temperature (R-T) measurements of a Y-Ba-Cu-O sample are plotted in Fig. 2.2. The two important points defined in this graph are 'onset temperature' ($T_{c,ON}$) and the temperature for zero dc resistance ($T_{c,zero}$). However, in a common convention used for superconductors where the transition region is quite narrow, T_c is simply the transition temperature corresponding to zero resistance. Onset temperature for superconducting phenomena is the level where the resistance versus temperature curve just begins to depart from the normal metallic behaviour, whereas, $T_{c,zero}$ is defined as the highest temperature where the material is considered to be fully superconducting, that is, where dc resistance is zero. Another important term i.e. the transition width (ΔT_c) is defined as the difference in $T_{c,ON}$ and $T_{c,zero}$.

A set-up which we have used for the measurement of resistance as a function of temperature is shown in Fig. 2.3. It consists of a nano-voltmeter (model 181 from Keithley Instruments Inc.), a current source (model 120 of Lake Shore Cryotronics or model 220 from Keithley Instruments Inc.), platinum resistor thermometer (PRT-100) with temperature indicator (model 195A multimeter from Keithley Instruments Inc.), measuring probe and cryostate with liquid nitrogen or helium closed cycle refrigeration station (model 22 refrigerator from CTI Cryogenics).

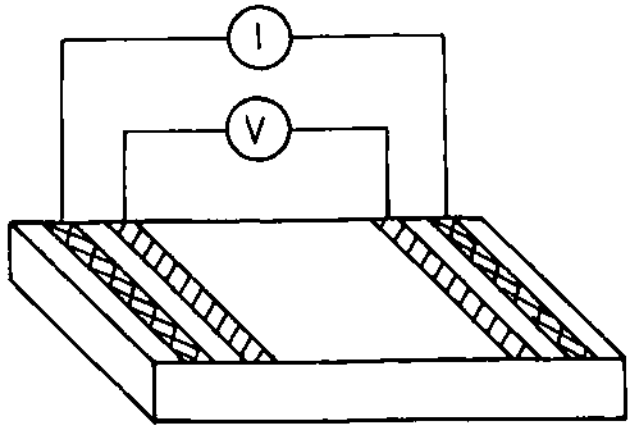

Fig. 2.1 Standard four probe resistance measurement technique

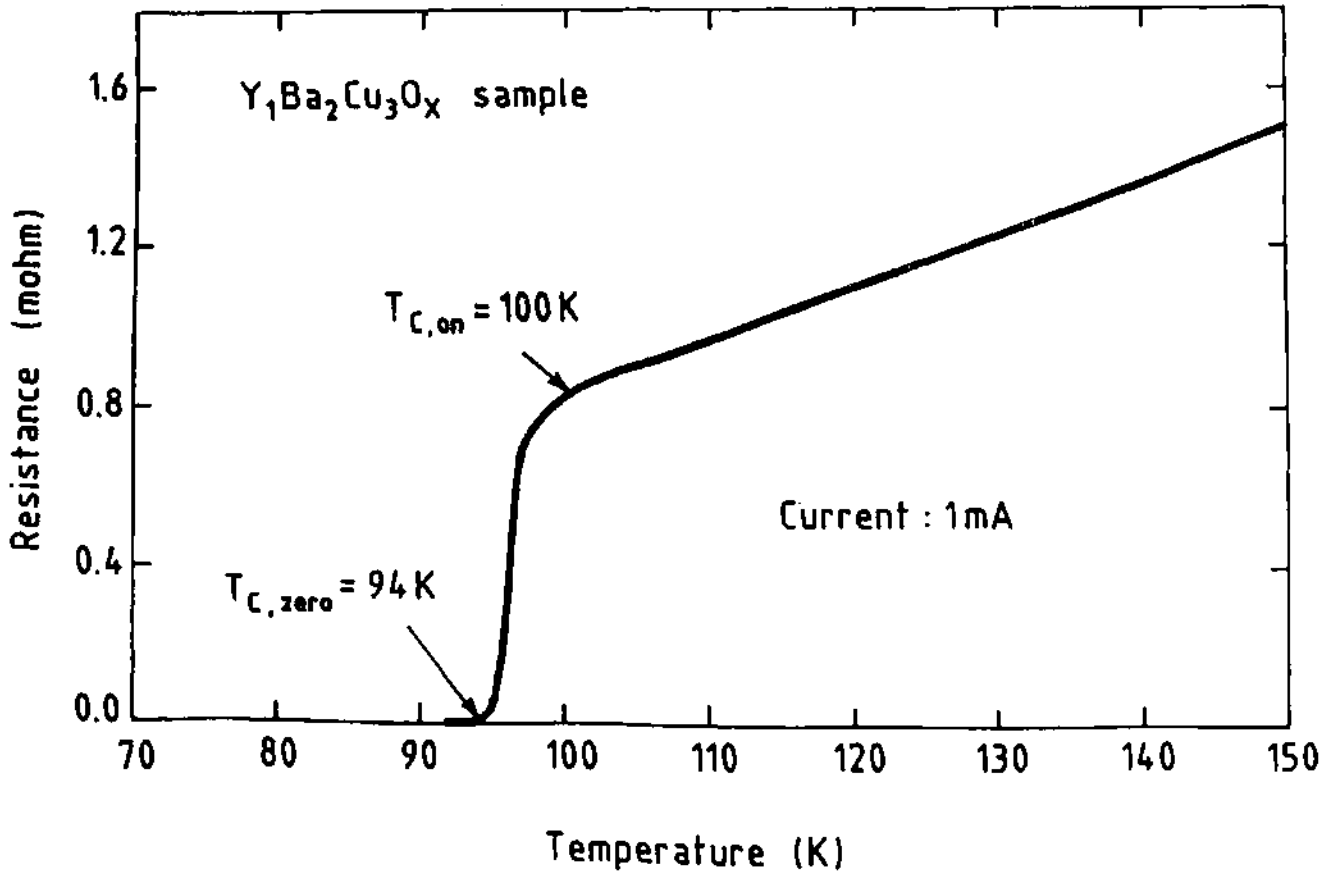

Fig. 2.2 A typical resistance plot of Y-Ba-Cu-O sample as a function of temperature

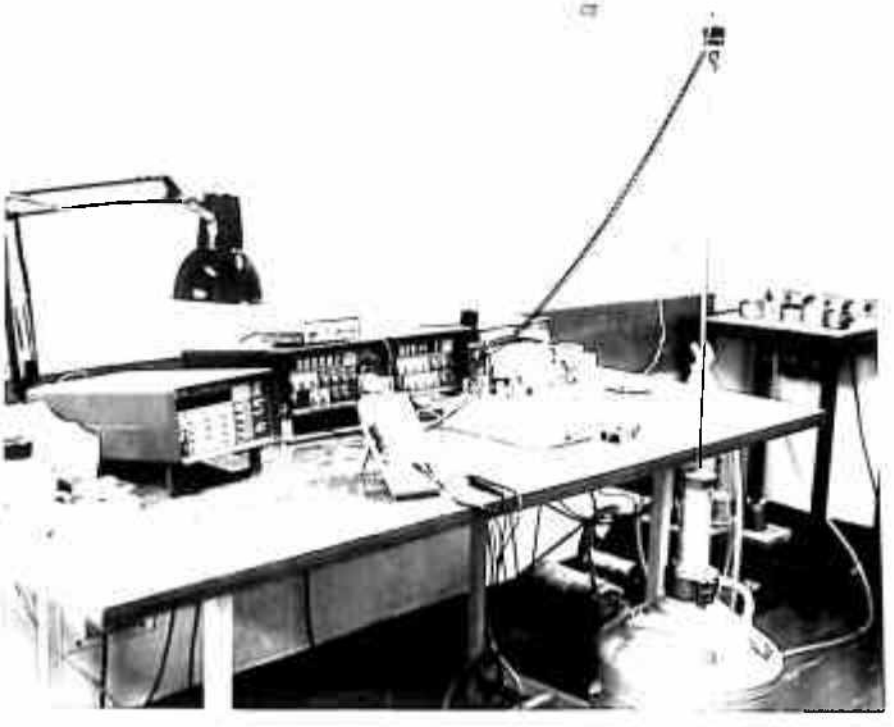

Figure 2.3: Resistance measurement set-up.

2.4 MAGNETIC SUSCEPTIBILITY (χ) MEASUREMENTS

Magnetic susceptibility characterization is generally performed to study magnetic properties of the materials. The susceptibility measurements are crucial for determining whether a material is actually superconducting, as the material transforms from paramagnetic to diamagnetic state at or below transition temperature. Also, the value of χ is often treated as an indicative of the percent volume of a sample that is superconducting. The dc resistivity does not provide such an information, since a single percolation path will lead to zero resistance in a sample that may be primarily composed of non-superconducting phase or low T_c phase.

AC susceptometers are quite extensively used in the study of magnetic properties of superconducting materials. Its principle of operation involves subjecting the sample material to a small alternating field. The flux variation due to the sample is picked up by a sensing coil surrounding the sample and the resulting voltage induced in the coil is detected. This voltage is directly proportional to the magnetic susceptibility of the sample. The voltage also depends on a number of other experimental parameters as given by the following relationship (Instruction manual):

$$v = (1/\alpha)VfH\chi \qquad \ldots\ldots (2.1)$$

where, v = measured RMS voltage

α = calibration coefficient

V = sample volume

f = frequency of AC field

H = RMS magnetic field

χ = volume susceptibility of sample.

The calibration coefficient depends on the sample and coil geometry. The magnetic field H is the RMS field at the center of the sensing coils and is determined from the physical parameters of the solenoid and the operating current. Rearranging Eq.

2.1, the relationship for determining the sample susceptibility, χ from the experimental parameters can be obtained as:

$$\chi = \alpha v / (VfH) \qquad \ldots\ldots (2.2)$$

The schematic block diagram of the AC susceptometer is shown in Fig. 2.4. The alternating magnetic field is generated by a solenoid which serves as the primary in a transformer circuit. The solenoid is driven with an AC current source with variable amplitude and frequency. Two identical sensing coils are positioned symmetrically inside of the primary coil and serve as the secondary coils in the measuring circuit. The two sensing coils are connected in opposition in order to cancel the voltages induced by the AC field itself or voltages induced by unwanted external sources. Figure 2.5 shows the front view of the Lake shore (model 7000) AC susceptometer used in our investigations.

A typical ac susceptibility data for a sintered high T_c superconductor sample is plotted in Fig. 2.6. It consists of two distinct plots, namely, real (χ') and imaginary (χ'') parts, which represents two complementary aspects of flux dynamics in polycrystalline superconductors. The sharp drop in χ' below the T_c has been related, in single crystals (Fig. 2.7), to the temperature at which the flux penetrates to the centre of the sample (Nikolo and Goldfarb, 1989). In granular materials, the same argument can be extended for the matrix and the weak links to postulate two drops in χ' at two temperatures (Nikolo and Goldfarb, 1989). One of the two temperatures is intrinsic to the superconductor and the other is characteristic of the coupling among the grains. The coupling component also supports supercurrents and has its own T_c and J_c values which are less than the values corresponding to the intrinsic component of the superconductor. The reason for this has been assumed to be the lack of stoichiometry at the grain boundaries which could give rise to normal metal barriers (Chiang, et al., 1988; Babcock, et al., 1988; Dubots and Cave, 1988) and proximity-effect coupling among the grains (Hein, et al., 1992; Finnemore, et al., 1987; Ekin, et al., 1987; Suenaga, et al., 1987; Larbalestier, et al., 1987). Another coupling mechanism in sintered materials is through micro bridges between grains (Ishida and Mazaki, 1981). The imaginary part (χ'') represents the losses

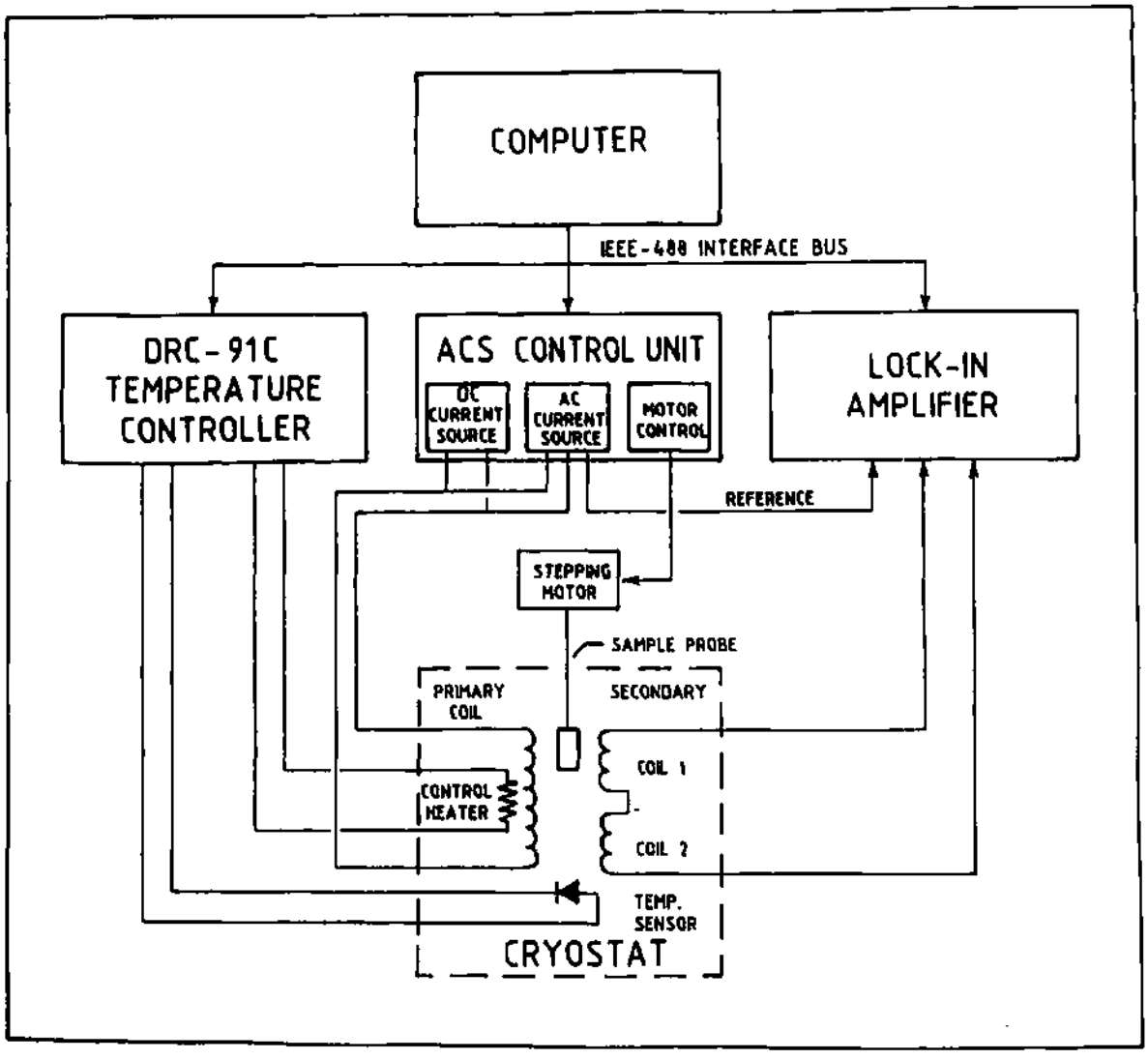

Fig. 2.4 Schematic block diagram of AC Susceptometer (Model 7000)

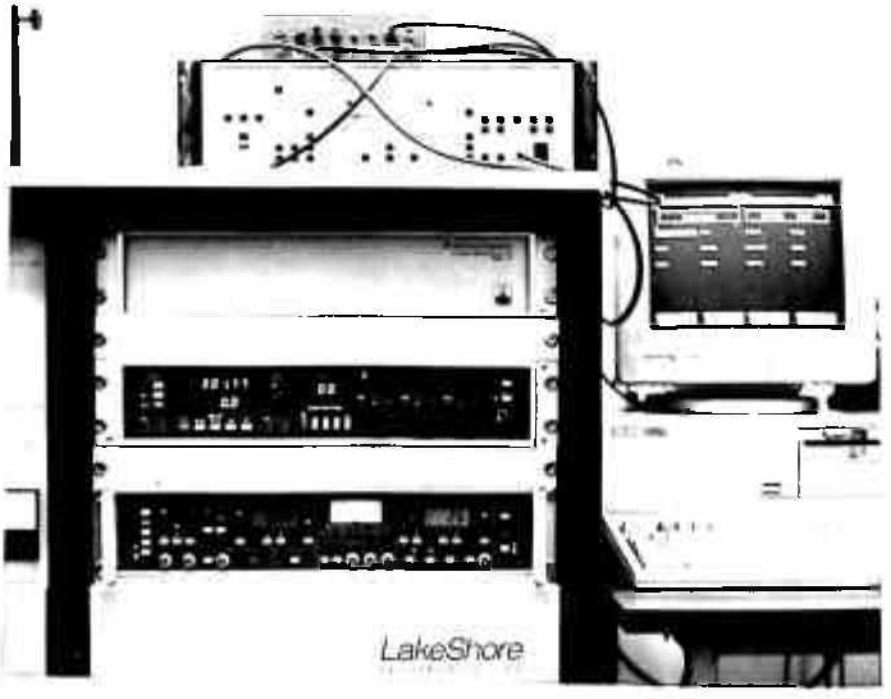

Figure 2.5: Front view of the AC susceptometer.

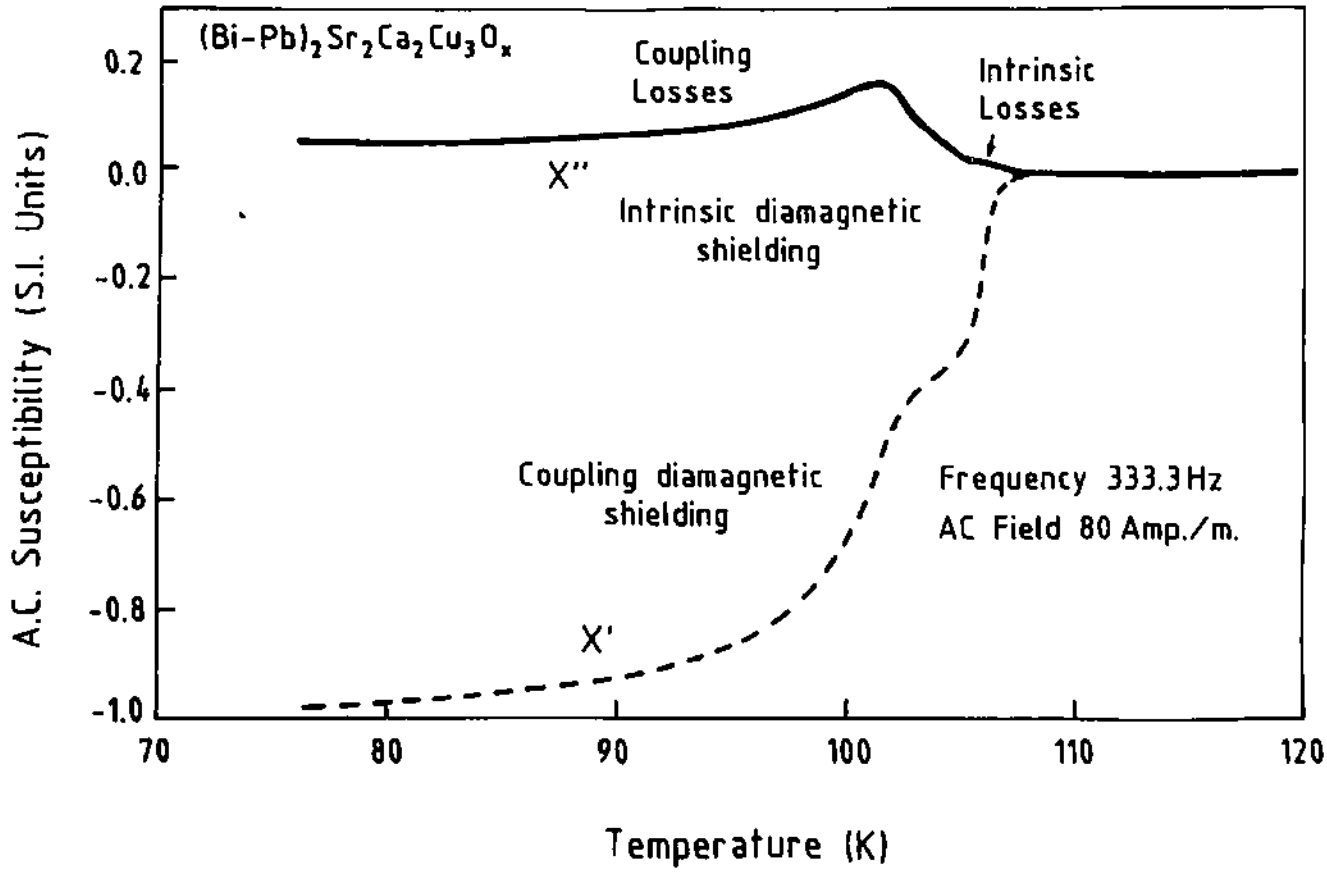

Fig. 2.6 A typical a.c. susceptibility data for a sintered high T_c superconductor

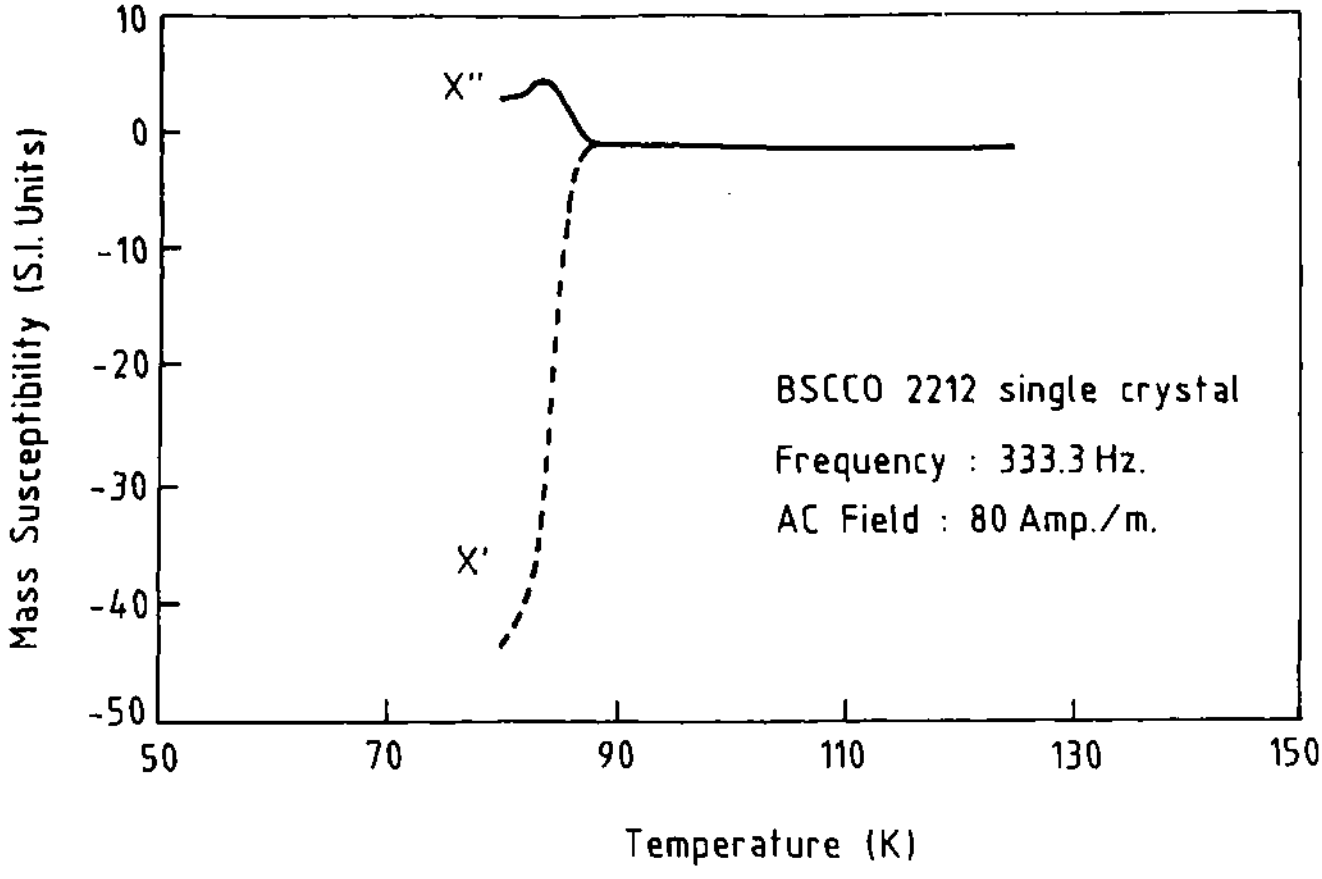

Fig. 2.7 AC susceptibility plot for a high T_c single crystal (BSCCO - 2212)

in the superconductor, and the peaks observed in χ'' can be interpreted in terms of losses incurred due to flux motion in the matrix and/ or along the weak links in the polycrystalline microstructure (Nikolo and Goldfarb, 1989; Hein, et al., 1992).

At T_c of the coupling component, there is striking change in susceptibility because of the large change in shielded volume. But, the change in resistivity is minor because the coupling component forms a small part of the conduction path. A crushed sample yields isolated grains with only intrinsic characteristics (Chen, et al., 1988; Küpfer, et al., 1987; Suenaga, et al., 1987; Mazaki and Ishida, 1987) also shown in Fig. 2.8. Both intrinsic and coupling critical temperatures are ac field dependent, however the effect is much more pronounced in the latter case (Nikolo and Goldfarb, 1989; Goldfarb, et al., 1987; Garcia, et al., 1987). This field dependence can be examined with increasing ac measurement field as depicted in Fig. 2.9.

For a high quality, strongly coupled, sintered superconductor, the two critical temperatures coincide for small measuring fields (Goldfarb, et al., 1987). The coupling T_c is not depressed much with increasing measurement field compared to a poor quality, weakly coupled sample.

2.5 X-RAY DIFFRACTION (XRD) ANALYSIS OF SUPERCONDUCTORS

An analysis of the angular position and intensity of x-ray beams diffracted by crystalline material gives information on the crystal structure or/ and phases present in the material. High temperature superconductors are prepared by reacting various metal oxides and carbonates and the totality of materials reacted can be ascertained by the XRD analysis of the final product. Also the high T_c compounds tend to crystallize in various phases having different critical properties. Hence, to develop a process for the synthesis of a particular phase, of a superconducting system, XRD is very useful.

For diffraction of x-rays by a crystal lattice the Bragg's relation must be satisfied which states:

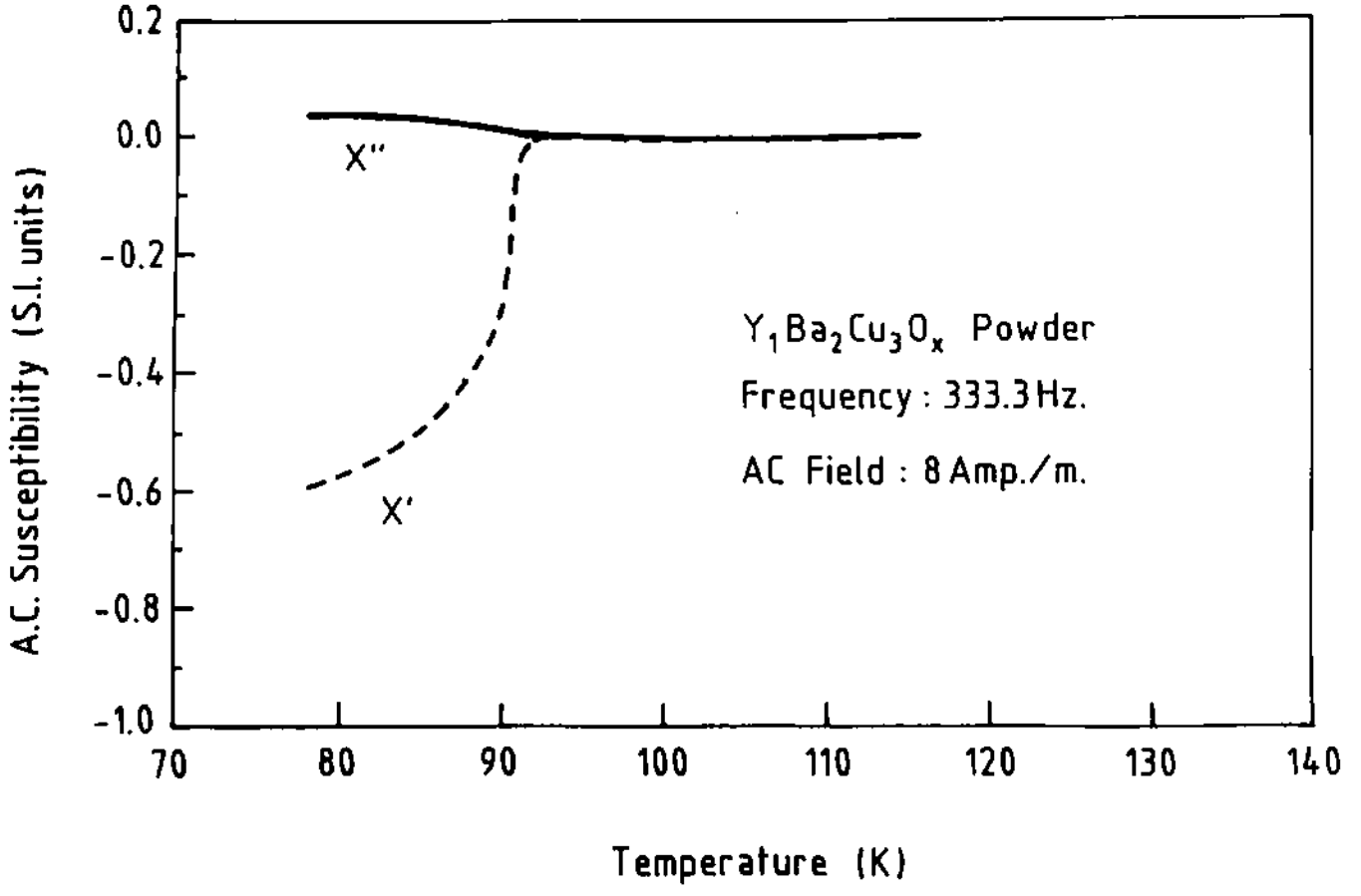

Fig. 2.8 AC susceptibility plot for a high T_c powder

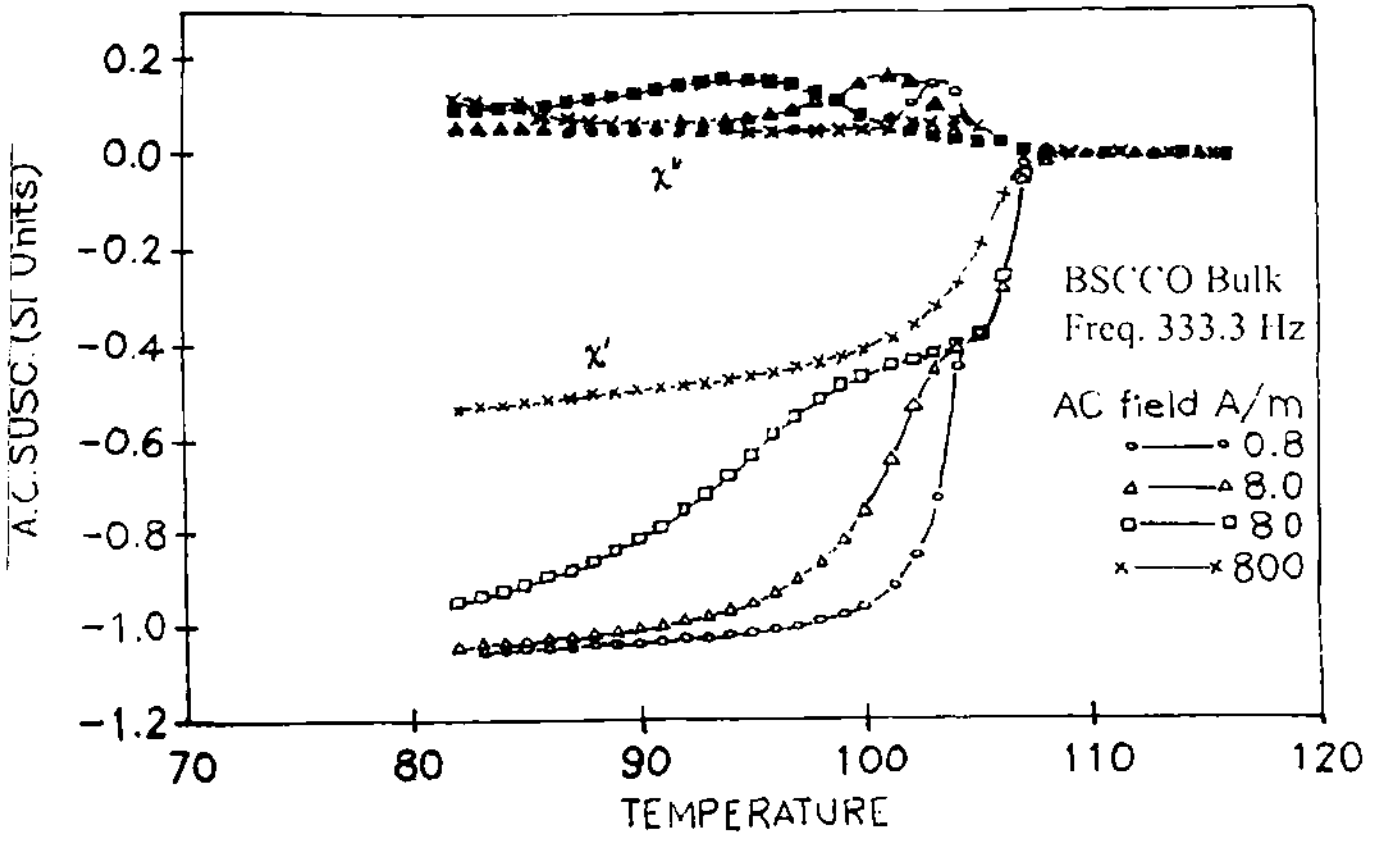

Figure 2.9: AC Susceptibility plots of a High T_c Sample at various ac fields.

$$n\lambda = 2d \sin\theta \ldots\ldots\ldots (2.3)$$

where, λ is the x-ray wavelength, d is the interplaner spacing, θ is the Bragg diffraction angle, and n is an integer giving the order of the diffraction.

There are three standard methods of x-ray diffraction, namely (i) the Laue method, it involves a stationary single crystal and 'white' x-rays (ii) the rotating crystal method involving a single crystal rotated in a beam of monochromatic x-rays and (iii) the powder method where a polycrystalline sample rotates in a beam of monochromatic x-rays. We have used the rotating crystal and powder methods for the identification of crystal structures/ phases present in the high T_c films and bulk materials respectively. In these methods, different sets of atomic planes with spacing 'd', diffract the x-ray beam of wavelength λ at an appropriate angle of incidence θ. Hence, a spectra of maxima peaks, corresponding to various planes, as a function of 2θ values is obtained. Monochromatic x-rays generally used for the purpose are Cu (K_α) [λ=1.54Å] and Fe ($K_{\alpha 1 \alpha 2}$) [λ=1.937Å].

A typical x-ray diffraction data of a multiphasic BSCCO thin film on a single crystal MgO substrate along with other unreacted material are listed in Table 2.4. The peaks numbering 1, 4, 8, 12, and 13 which are corresponding to 2θ equal to 4.941, 19.298, 34.008, 49.221 and 59.968 degrees respectively, represent high T_c phase (i.e. 2223 compound), whereas, peaks 6 and 7 at 2θ values of 24.115 and 29.014 degrees indicate the presence of 2223 and 2212 phases together. The peaks pertaining to T_c = 10K phase (2201 compound) are also present at 2θ = 14.382° and 21.505°. Also, the peak corresponding to the substrate (MgO) was observed at 43.113° and that of unreacted CuO at 38.283°. Some unidentified compounds/ phases also showed their signatures at 10.858°, 37.628°, 64.645° and 67.836 degrees.

Table 2.4 X-ray diffraction pattern of a BSCCO thin film (λ = 1.54Å)

Seq.	2θ	Phase(s) indicated
1.	4.941	2223
2.	10.858	unidentified
3.	14.382	2201
4.	19.298	2223
5.	21.505	2201
6.	24.115	2223& 2212
7.	29.014	2223 & 2212
8.	34.008	2223
9.	37.628	unidentified
10.	38.283	CuO
11.	43.113	MgO
12.	49.221	2223
13.	59.968	2223
14.	64.645	unidentified
15.	67.836	unidentified

2.6 SCANNING ELECTRON MICROSCOPY (SEM) AND ENERGY DISPERSIVE ANALYSIS OF X-RAYS (EDAX)

Scanning electron microscopy is a standard analytical method as it provides increased spatial resolution and depth of field compared with optical microscopy, and also because chemical information can be obtained from the x-ray spectra generated by electron bombardment. Resolution better than 100Å can be achieved under optimum conditions.

For our investigations on high T_c materials and films, we have found SEM to be an important tool. SEM micrograph of a superconductor provide information regarding the size of the grains, their shape and connectivity, which is also an indicative of the growth pattern and the current density of the sample as discussed in the subsequent chapters.

As the electrons strike the sample surface, in SEM, the x-rays are also produced. The spectroscopy of these x-rays using energy dispersive detector is known as energy

dispersive analysis of x-rays (EDAX). EDAX analysis is useful for chemical analysis both qualitatively i.e. for detecting elements present in the sample and quantitatively i.e. for knowing the atomic or weight percentage of each of the elements present. Such an information is very crucial for the optimization of process parameters, to grow a particular phase in either, a superconducting bulk or a film.

2.7 FILM THICKNESS AND SURFACE SMOOTHNESS MEASUREMENT

Surface profiler provides a wealth of topographic information on features such as film thickness, etched depths, surface defects, roughness and flatness etc. These information are important for the fabrication of high T_c superconducting thin films and their application to microelctronic devices.

The surface profile measurement system, Dektak II A, Sloan Technology division, California has been used. It is a microprocessor based instrument capable of measuring very small vertical features ranging in height from less than 100 angstroms to 655,000 angstroms, with a vertical resolution of 5Å. A typical plot of the surface of a MgO substrate is depicted in the Fig. 2.10(a) which shows smooth surface with roughness less than 50Å while the step in the Fig. 2.10(b) indicate the high T_c film thickness with respect to the substrate.

2.8 SCANNING TUNNELING MICROSCOPY

The surface topography on an atomic scale is done using scanning tunneling microscope (STM). The STM works by positioning a sharp metallic tip (in the best case, atomically sharpened) a few atomic diameters above a conducting sample. A bias voltage is applied between the tip and the specimen. At a distance under 10 Å, a tunneling current flows between the sample and the tip. In operation, the bias voltages are typically from 10 to 1000 mV and the tunneling currents from 0.2 to 10 nA. The system works in two modes i.e. constant current mode or constant tip-sample separation or constant height

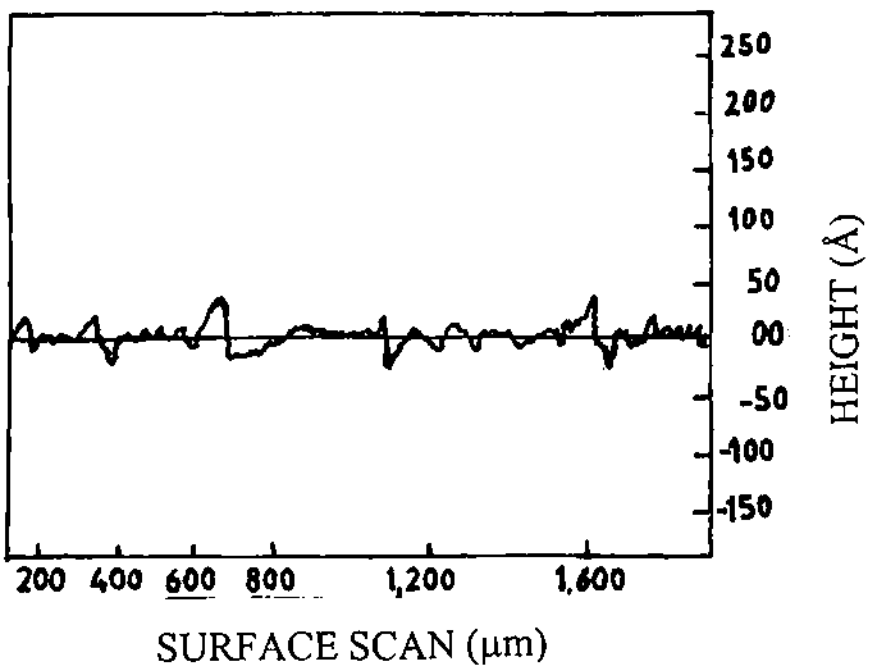

Figure 2.10(a): Surface profile of a MgO substrate

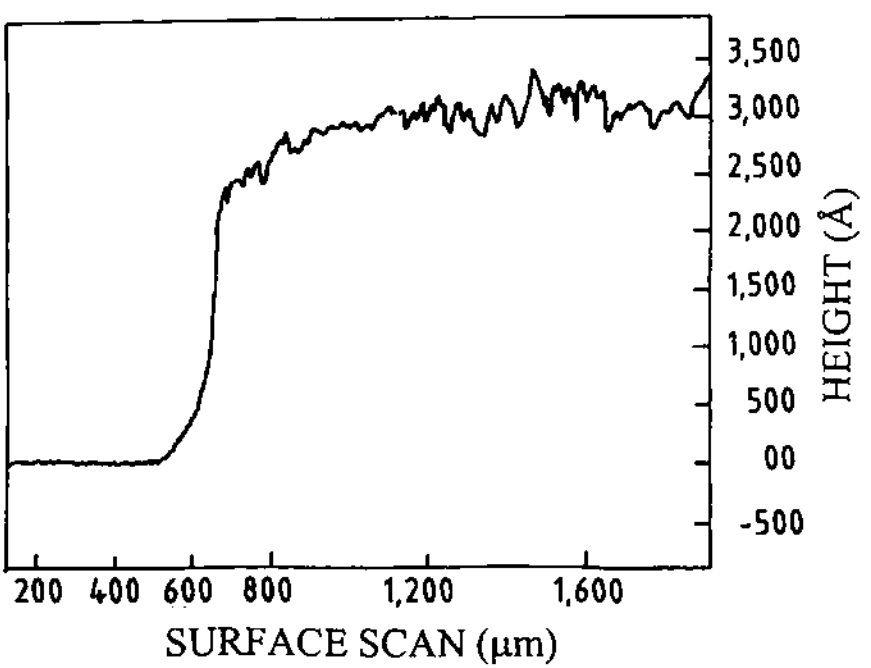

FIG 2 10 (b) PROFILE INDICATING FILMTHICKNESS WITH RESPECT TO THE SUBSTRATE

mode. An electric feedback loop is used to keep the tunneling current constant by adjusting the tip- sample separation in the first case, or the tip-sample separation is maintained constant by adjusting the tunneling current.

The phenomenon of electron tunneling underlines the operation of the STM. An electron cloud occupies the space between the surface of the sample and the needle tip. The cloud is a consequence of the indeterminacy of the electron's location (a result of its wavelike properties); because the electron is "smeared out", there is a probability that it can lie beyond the surface boundary of the conductor. The density of the electron cloud decreases exponentially with distance. A voltage-induced flow of electrons through the cloud is therefore extremely sensitive to the distance between the surface and the tip. As the tip is swept across the surface a feedback mechanism senses the flow (called the tunneling current) and holds constant the height of the tip above the surface atoms. In this manner the tip follows the contours of the surface. The motion of the tip is read and processed by a computer and displayed on a screen or a plotter. Sweeping the tip through a pattern of parallel lines yields a high-resolution, three-dimensional image of the surface.

CHAPTER - THREE

SYNTHESIS OF HIGH T_c SUPERCONDUCTING BULK MATERIALS

3.1 INTRODUCTION

The discovery of superconductivity in $YBa_2Cu_3O_{7-x}$ at 93K by Chu and Wu in early 1987 (Wu et al., 1987) surpassed the liquid nitrogen temperature barrier of 77K and made applications of superconductivity appear more practical than ever before. These observations in 1986-87 thus heralded in the modern era of high temperature superconductivity (HTS). In the ensuing decade after the discovery of HTS, more than one hundred non-intermetallic compounds have been found to superconduct above 23K, the record for conventional low-temperature intermetallic superconductors.

To determine the role of Y in 90K superconductivity, Y was replaced with some magnetic rare earth trivalent elements. T_c remained unaffected even with a large fraction of Y replaced. This suggested that Y in Y-123 is electronically isolated from the superconducting electron system and serves mostly as a stabilizer in the compound. Thus a new series of 90K superconductors $RBa_2Cu_3O_{7-x}$ (R-123) with R=rare earth elements except for Ce and Tb was discovered (Hor et al., 1987).

As 1987 drew to a close, T_c did not budge from 93K, regardless of the extensive world-wide efforts devoted to the search for higher T_c's. Some pessimistically concluded that $T_c > 93K$ could only be found in non-cuprate materials, if it existed at all. Their premature prediction was shattered by Maeda et al. (1988) who announced the discovery of superconductivity in the Bi-Sr-Ca-Cu-O (BSCCO) system in January 1988. They

replaced the trivalent rare-earth elements in R-123 with elements from the V-B group in the Periodic Table, such as Bi and Sb, which are trivalent and have ionic radii similar to the rare earths. They succeeded in observing superconductivity above 105K in multiphase samples of BSCCO which was also confirmed by Chu et al. (1988). The three members of the homologous series B-22(n-1)n with n=1, 2, and 3 were soon determined (Hazen et al., 1988a; Veblen et al., 1988). The new record T_c = 110K was attributed to the n=3 member; and 80 and 22K to members of n=2 and 1, respectively.

Following a similar rationale to Maeda et al.'s, Sheng and Hermann started to substitute the non-magnetic trivalent Tl for R in R-123. By reducing the reaction time to a few minutes to overcome the high volatility problem associated with Tl_2O_3, they detected superconductivity above 90K (Sheng and Hermann, 1988) in their nominal $TlBa_2Cu_3O_x$ samples in November 1987. By partially substituting Ca for Ba, they discovered (Sheng et al., 1988) a T_c ~ 120K in their multiphase sample of Tl-Ba-Ca-Cu-O (TBCCO) in February 1988, only a few weeks after Maeda et al. announce their discovery of T_c ~ 110K in BSCCO. T_c = 90, 110, and 125K were assigned to the n = 1, 2, and 3 members of the series Tl-22(n-1)n, respectively, setting a new record. Another homologous series Tl- 12(n-1)n was soon synthesised and found (Morosini et al., 1988; Parkin et al., 1988) to be superconducting at T_c = 50, 82, 110, and 120K for the n = 1, 2, 3, and 4 members, respectively. In September 1992, the T_c of Tl-2223 was further enhanced to 131K (Berkeley et al., 1993) by the application of pressure.

The T_c stagnated at ~ 125K. In late 1989, some predicted again that T_c in layered cuprate might never exceed 160K. However, the prediction tumbled in mid 1993 when pressure enhanced the new record T_c of 134K in $HgBa_2Ca_2Cu_3O_x$ (Hg-1223) (Schilling et al., 1993) at ambient pressure, to 164K at 30 GPa (Chu et al., 1993; Gao et al., 1994). In April 1993, Schilling et al. (1993) reported the detection of superconductivity at temperatures up to 133K in samples consisting of members of Hg-12(n-1)n with n = 1, 2, and 3 respectively (Gao et al., 1993; Putilin et al., 1993; Antipov et al., 1993; Meng et al., 1993; Radaelli et al., 1993; Huang et al., 1993). The T_c of Hg-1223 was further enhanced

by the application of pressure and found an onset T_c to 164K at ~30GPa in the summer of 1993 (Chu et al., 1994).

It was recognised (Gao et al., 1995) that the T_c of the various homologous series $A_mX_2Ca_{n-1}Cu_nO_{2n+m+2+y}$ increases as A changes from Bi through Tl to Hg in the Periodic Table. Further change of A to Au, or even Ag or Cu, was therefore carried out. No efforts succeeded in synthesising compounds with A = Au or Ag due to their chemical inertness. However, Cu-12(n-1)n with n = 3 and 4 was formed under high pressure by Ihara et al. (1994) and Wu et al. (1994) with T_c = 60 and 117K respectively. After proper annealing, the T_c of Cu-1223 was raised to 120K (Marezio et al., 1996).

In this chapter, we describe the methodology for the synthesis of YBCO and BSCCO superconducting bulk samples. The synthesis of TBCCO compound was not attempted due to its toxic character. The techniques discussed here are for the preparation of polycrystalline materials only as our prime objective has been to use this technology to make the targets for the preparation of high T_c films and to explore their applications to superconducting devices. Hence, the techniques dealing with the growth of single crystals of ceramic superconductors were not pursued and therefore not discussed here. Primarily, there are two approaches to prepare high T_c superconducting samples, namely (i) solution techniques and (ii) solid state or ceramic method. We have employed widely used solid state technique to prepare YBCO and BSCCO superconducting materials. However in this chapter, we briefly describe the various techniques of 'solution method' prior to the solid state procedures developed in our laboratory.

3.1.1 Solution techniques

The solution techniques are used for the synthesis of micro-crystalline particles and clusters. These methods begin with the preparation of aqueous solutions of the desired constituents in appropriate stoichiometry. The solutions are then atomized and the heat or mass transfer is achieved in milli-seconds. Depending on the atomisation process, the techniques can be classified into sol-gel, co-precipitation, spray drying, freeze drying or a similar technique. It is generally felt that solution techniques produce better quality

products, as they permit reactions at lower temperatures, produce materials with particle size of less than 0.5 μm and having a narrow size dispersion. The smaller and uniformly sized particle produces denser compacts on sintering. Also, the solution derived high T_c materials have a narrower transition width (< 1K).

Sol-gel powder preparation technique starts with the preparation of the aqueous solution containing proper ratios of various metal nitrates. This aqueous solution is then emulsified with the help of a water immiscible organic compound such as heptane. A stable emulsion is formed by ultrasonic agitation. Subsequently, the metal hydroxides in the emulsion droplets are co-precipitated using suitable organic amines. These amines can be used to extract the anions and the pH of the aqueous phase rises so that the hydrous oxides of the cations precipitate to form an amorphous gel. The gel is then dried to get fine grained homogeneously mixed powder in right ratio. However, the sol-gel is a time consuming method and requires expensive chemicals. A typical sol-gel procedure for the synthesis of YBCO superconductor, as followed by Wu et al. (1988), is mentioned here. They first prepared yttrium and barium methoxyethoxides from Y-isopropoxide and B-metal respectively by reacting them with methoxyethanol. Cu(II) ethoxide was partially dissolved in toluene. A clear solution of Y-methoxyethoxide and Ba-methoxyethoxide in methoxyethanol was then added to the Cu(II) ethoxide/ toluene solution to further enhance the solution solubility. The stock solution was stirred in an inert atmosphere for 10 hours, then taken out and divided into two parts. The first part was opened to the atmosphere and the second was mixed with 1 mol metal alkoxide to 1 mol water (diluted in methoxyethanol). A gel-like paste was formed within 48 hours. These gels were first slowly vacuum dried and then fired at 800°C to 850°C for 15 hours. From this temperature, the samples were cooled to 650°C at the rate of 10°C/min, holding for 5 hours at 650°C and then cooled to room temperature at 5°C/min. Both the samples showed critical temperature above 90K.

In co-precipitation process, the required metal cations are co-precipitated from a common medium, usually hydroxides, carbonates, oxalates, formates or citrates, which are subsequently heated at appropriate temperatures to yield the final products. In this

technique, precipitation can be non-uniform or incomplete and the material may be lost during washing. Also, the precipitation agent such as alkali is likely to remain till end. Precipitation routes have another limitation as the solution homogeneity can be lost during process due to differential solubility. However, Varma et al. (1988) have successfully prepared $YBa_2Cu_3O_{7-x}$ superconducting ceramic with $T_{c,zero}$ = 90 K, using co-precipitated powders. They dissolved stoichiometric amount of $BaCO_3$, Y_2O_3, and CuO (3% excess) in nitric acid (1N) to obtain approximately 1 molar solution. In this solution, aqueous ammonia was added till pH became 6.0 - 6.5. This resulted in the precipitation of yttrium and copper as hydroxides but, $Ba(OH)_2$ was precipitated after addition of excess amount of isopropyl alcohol to the solution. The mixture was continuously stirred for half an hour on a magnetic stirrer. The precipitate was filtered, dried at 110°C, and calcined at 750°C. The black calcined powder was further heat treated at 750°C for 12 hours in flowing oxygen to obtain superconducting compound.

In spray drying, suitable constituents dissolved in a solvent are sprayed in the form of fine droplets into a hot chamber. The solvent evaporates instantaneously leaving behind an intimate mixture of the reactants. This technique can be utilized to synthesize polycrystalline thick films also. A typical example of the process was successfully demonstrated by Kawai et al. (1988). They prepared aqueous solution of Y, Ba and Cu nitrates to achieve atomic ratio of Y, Ba and Cu to be 1:2:3. The solution was sprayed over substrates which were kept at 400°C. The samples were then heated at 800°C in air. The process of spraying and heating were repeated until desired material thickness was obtained. Films thus obtained were heated in furnace upto 950°C in an oxygen ambient for 5 minutes. The specimen showed $T_{c,zero}$ at 83K.

3.1.2 Solid state reaction or ceramic technique

This is the most widely used method for the synthesis of ceramic superconductors. It requires less familiarity with the physico-chemical processes involved in the transformation of a mixture of compounds into a superconductor (Rao and Gopalakrishanan, 1986).

It is a conventional ceramic preparation technique in which chemicals, in solid-state, react to form the desired compound. The various steps involved in the processing of high T_c material are illustrated in Fig.3.1. In this process, appropriate amount of chemicals are weighed and mixed. The proper mixing is achieved during grinding, using a mortar and pestal or a ball mill. The well mixed mixture is subjected to calcination. Calcination is defined as the dissociation and driving off of some constituent in the form of gas from the compounds by subjecting them to a heat treatment. The Calcined material is re-pulverized by mechanical means to obtain fine powder. This powder is subsequently pelletized and annealed to obtain superconducting material. Annealing is a process of heating and cooling the reacted powder to obtain superconducting compound of desired composition, phase and micro-structure. This is the most important step of superconductor synthesis technology as superconducting properties are profoundly dependent on this step. The temperature and the rate of the cooling depends upon the material and its composition. These are required to be optimized in each individual case to form superconducting compound of desired stoichiometry and phase during the annealing process.

In solid-state reaction technique, the basic chemicals used for the synthesis of these high T_c superconductors are oxides, carbonates, nitrates or hydroxides of the constituent elements. The purity of these compounds is very important and they should be free from impurities such as Al, Fe, etc. Desired amount of powder chemicals are pulverized for several hours to ensure proper mixing. This also increases surface area for better solid state reaction among various species. The thoroughly mixed powder is then calcined in the powder or pellet form. The calcined material is again pulverized and the pellets, of diameter 10-15 mm and thickness 2-3 mm, were formed at 100 to 150 Kg/cm^2 pressure using a hydraulic press. The pellets are then subjected to annealing. All heat treatments are accomplished in muffle furnace having quartz tube with ceramic boats and microprocessor based temperature controllers. The samples thus produced are characterized for various properties. This is the general procedure followed in our laboratory for the preparation of YBCO and BSCCO compounds.

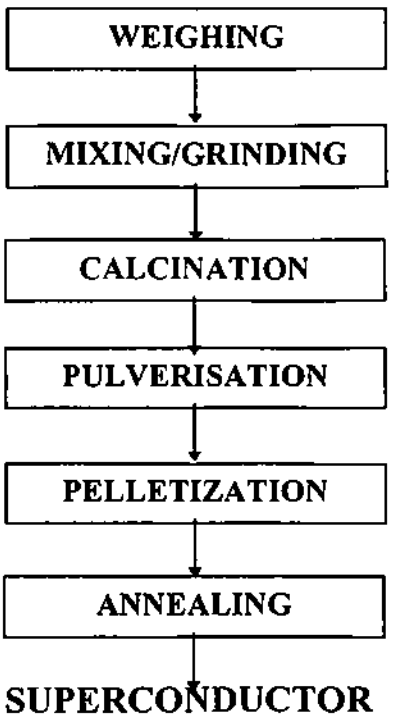

Figure 3.1 Process flow steps of high T_c superconductors fabrication

In solid-state reaction technique, the basic chemicals used for the synthesis of these high T_c superconductors are oxides, carbonates, nitrates or hydroxides of the constituent elements. The purity of these compounds is very important and they should be free from impurities such as Al, Fe, etc. Desired amount of powder chemicals are pulverized for several hours to ensure proper mixing. This also increases surface area for better solid state reaction among various species. The thoroughly mixed powder is then calcined in the powder or pellet form. The calcined material is again pulverized and the pellets, of diameter 10-15 mm and thickness 2-3 mm, formed at 100 to 150 Kg/cm^2 pressure using a hydraulic press. The pellets are then subjected to annealing. All heat treatments are accomplished in muffle furnace having quartz tube with ceramic boats and microprocessor based temperature controllers. The samples thus produced are characterized by various properties. This is the general procedure followed in our laboratory for the preparation of YBCO and BSCCO compounds.

3.2 SYNTHESIS OF YBCO SUPERCONDUCTING COMPOUNDS

We have used calculated amount of high purity Y_2O_3 (99.99% pure of CDH Chemie, USA), $BaCO_3$, and CuO (both 99.999% pure of Vin Karola Instruments, USA) for the synthesis of stoichiometric $YBa_2Cu_3O_{7-x}$ compound. The chemicals were weighed according to the molecular weight of the chemicals and the reaction as shown in equation 3.1.

$$1/2Y_2O_3 + 2BaCO_3 + 3CuO \xrightarrow{\Delta} YBa_2Cu_3O_{7-x} + 2CO_2 \quad ...(3.1)$$

or, 1/2(225.808) 2(197.349) 3(79.545)

or, 112.904 394.698 238.635

The amount of each reactant was taken, in above proportions by weight. For example, for a typical process 1.129 gm of Y_2O_3, 3.947 gm of $BaCO_3$ and 2.386 gm of CuO were taken. The chemicals were thoroughly mixed and pounded using an agate mortar and pestle. The fine pulverized powder was then subjected to calcination at 940 ± 5°C for approximately 10 hours in oxygen ambient. The gas flow was maintained at 1 l/min. Calcined material was re-weighed. From the weight lost, during the process, the percentage calcination was ascertained. The process was repeated to obtain nearly 100% calcination which is generally achieved in two to three calcination cycles.

The calcined powder was repulverised and pellets (15 mm diameter and 3-4 mm thick) were formed. The pellets were subjected to various annealing heat treatments to optimize the process, in flowing oxygen. Through a large number of experiments we realized that the annealing cycle, particularly cooling, had profound effect on the superconducting properties of the sample. The $T_{c,zero}$ as well as superconducting volume fraction in the sample are significantly influenced by the parameters of the cooling scheme. Through a large number of experiments, we have optimized these parameters. These experiments have led to three kinds of processes as summarized in the Table-3.1. The sample Y01 was first heat treated at 900°C for 13 hours and subsequently at 950°C for 7 hours. The pellet was then cooled at the rate of 1°C/min. upto 150°C. The specimen

Y02 was annealed at 940°C for 15 hours and cooling was done by simply putting the furnace off. And the third pellet Y03 was given treatment at 950°C for 24 hours and it was cooled from 950°C to 150°C at the rate of 10°C/min. with holding the sample at constant temperatures for one hour, after every 100°C cooling. This process, in which cooling is performed in 'steps' is developed in our laboratory to prepare the highest T_c superconducting YBCO samples. This cooling procedure is depicted in Fig. 3.2. The resistivity, susceptibility and other characterizations on these samples are mentioned in the subsequent section.

Table 3.1 Annealing cycles for various YBCO samples.

Sample No.	Annealing Temperature and time	Cooling Procedure
Y01	900°C for 13 hours + 950°C for 7 hours	950°C to 150°C at the rate of 1°C/min.
Y02	940°C for 15 hours	Furnace cooling
Y03	950°C for 24 hours	Steps cooling (Fig.3.2)

3.3 CHARACTERIZATION OF $YBa_2Cu_3O_{7-x}$ SAMPLES

The annealed pellets are mainly characterized through resistance versus temperature (R-T) and a.c. susceptibility versus temperature (χ-T) measurements as explained in the previous chapter. The grain size, shape, its connectivity etc. are studied with the aid of micro graphs obtained from the scanning electron microscope (SEM) and the presence of various phases/ compounds in the final products are determined through x-ray diffractometry (XRD).

The resistivity and susceptibility curves for the sample Y01 are shown in Fig.3.3. The R-T plot indicates $T_{c,ON}$ and $T_{c,zero}$ equal to 98K and 91K respectively whereas, χ-T data suggest intrinsic onset temperature equal to 92.5K and coupling superconduction starts about 91.0K. The R-T plot of sample Y02, in Fig.3.4, shows $T_{c,ON}$ = 97K and $T_{c,zero}$

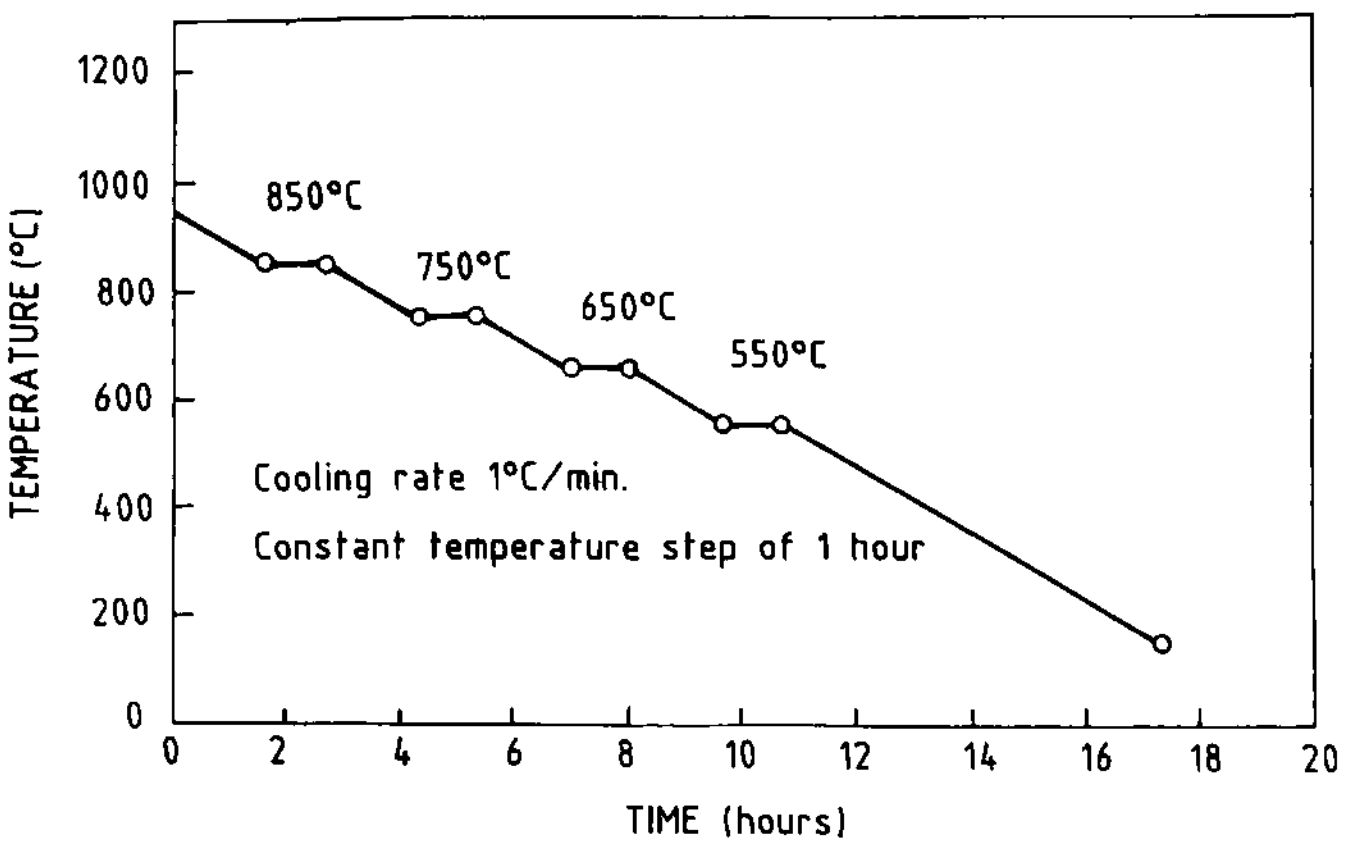

Fig.3.2 Steps Cooling for sample Y03

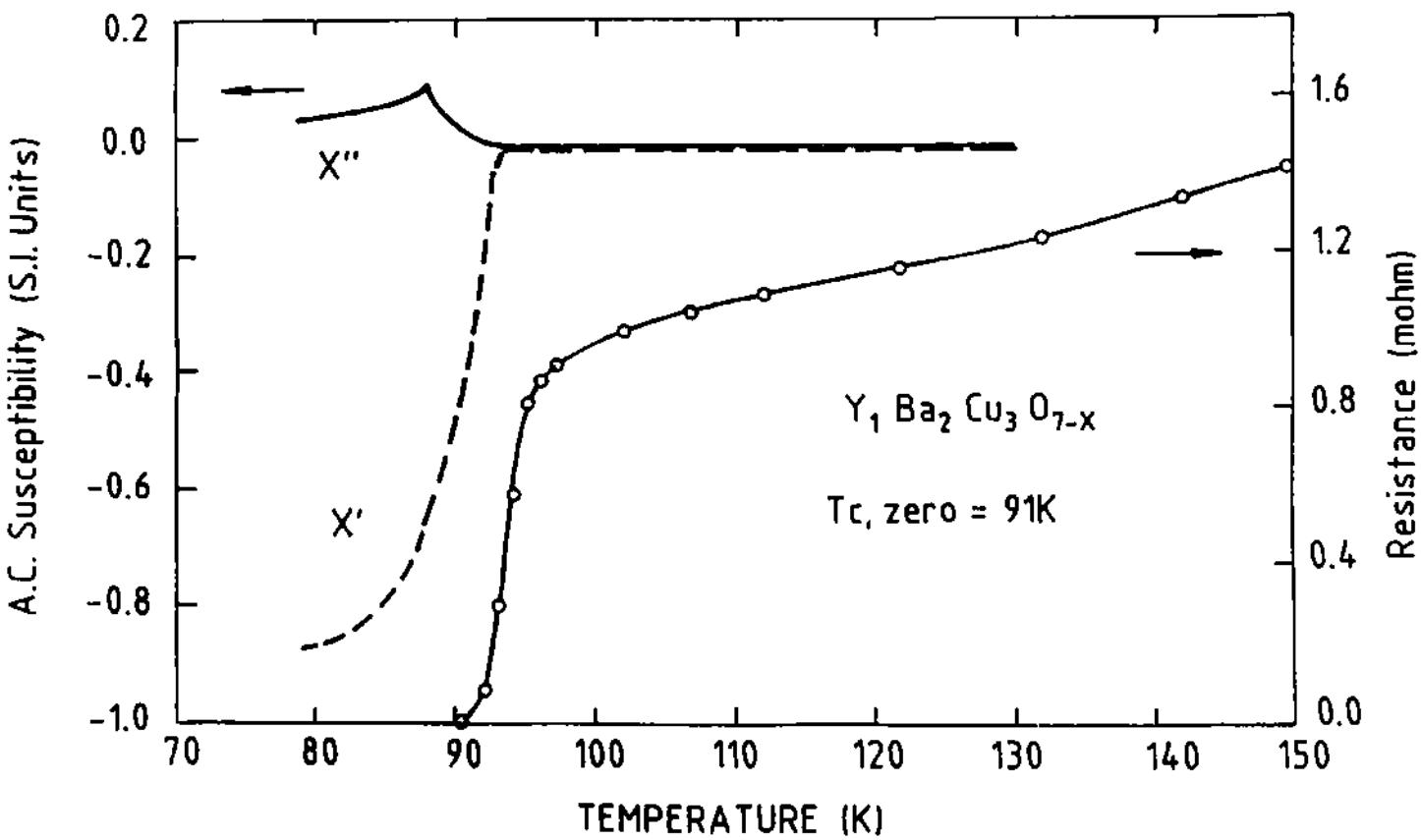

Fig. 3.3 A.C. Susceptibility and resistance as functions of temperature for sample Y01.

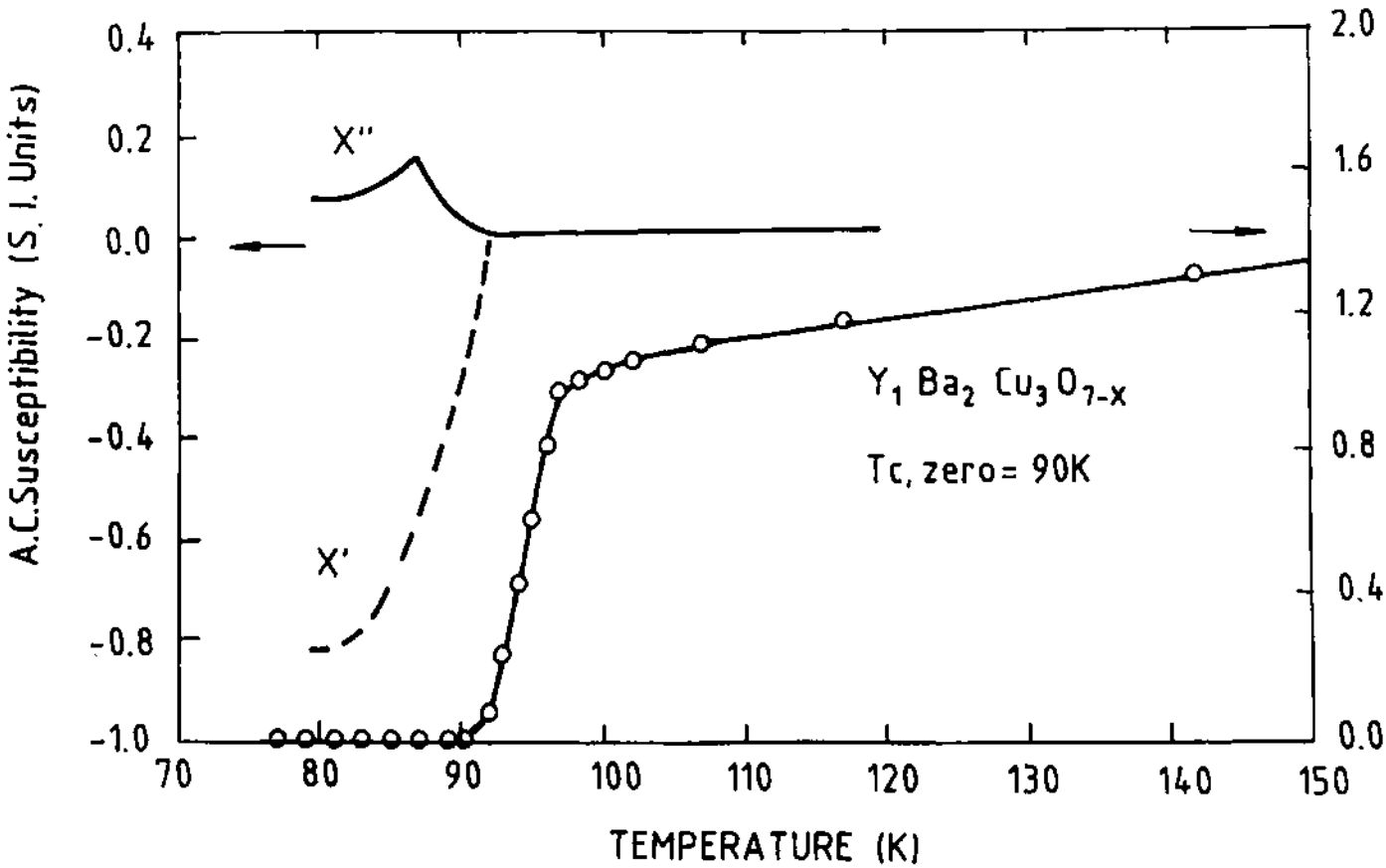

Fig.3.4 A.C. Susceptibility and resistance as functions of temperature for sample Y02.

= 90K while, χ-T indicates onset of intrinsic component at 92K and that of grains coupling around 90K. And in Fig.3.5, R-T plot of sample Y03 indicates $T_{c,ON}$ and $T_{c,zero}$ equal to 98K and 94K respectively. χ-T graph of the sample suggests onset temperature equivalent to 93.0K for the intrinsic component of the grains but the onset temperature corresponding to the coupling of the grains is not distinguishable as large fraction of the sample turns diamagnetic sharply at the onset of the intrinsic superconductivity of the grains. This characteristic is similar to that of single crystal sample (shown in the previous chapter) and it indicates a high quality, strongly coupled ceramic superconductor (Goldfarb, et al., 1987). The critical temperature data are also listed in Table 3.2.

Table 3.2 Critical temperature data of YBCO samples

Sample No	Resistivity data (K)			Susceptibility data (K)	
	$T_{c,ON}$	$T_{c,zero}$	ΔT_c	Intrinsic onset	Coupling onset
Y01	98	91	7	92.5	91.0
Y02	97	90	7	92.0	90.0
Y03	98	94	4	93.0	absent

Although the three samples showed zero resistance at or above 90K, the highest critical temperature (94K) and almost complete transition of the material, into superconducting phase above boiling point of liquid nitrogen, is only achieved in the steps cooled sample (i.e. sample Y03). Narrow peak in the χ'' plot of sample Y03 also suggests the coupling of the grains in a small temperature range, whereas, figures 3.3 and 3.4 show comparatively wider coupling peaks. The transition width ΔT_c is also minimum in Y03 which may be attributed to nearly simultaneous superconducting transition in the grains and their interconnections.

SEM micro graph of the continuous cooled [Fig.3.6(a)] and step cooled [Fig.3.6(b)] samples clearly demonstrates the difference in granularity of the samples. The steps cooling produces flat and bigger sized grains which are very well connected. Powder x-ray diffractometry data on sample Y03 is shown in Fig.3.7. Table 3.3 lists 'd'

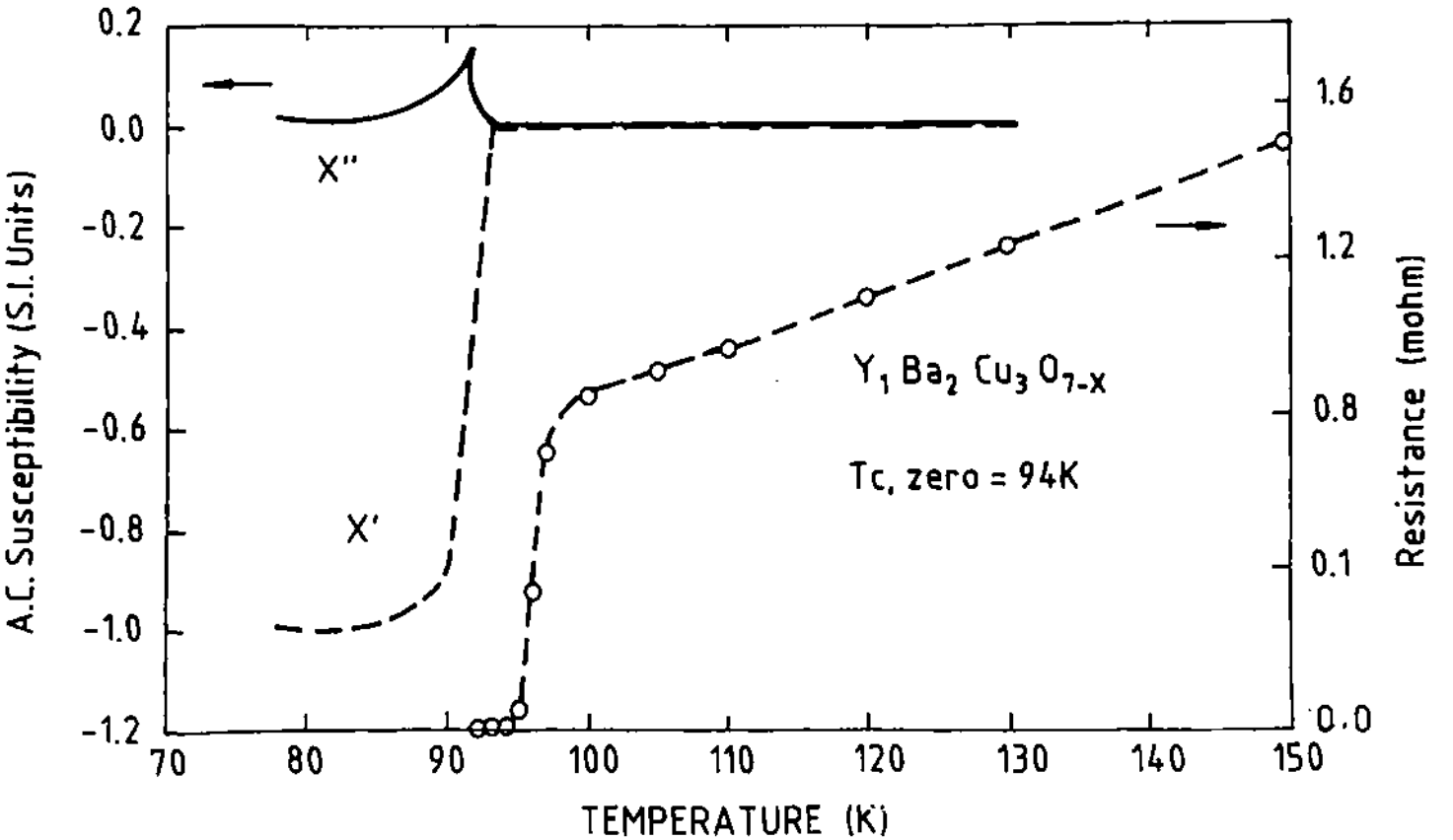

Fig3.5 A.C. Susceptibility and resistance as functions of temperature for sample Y03.

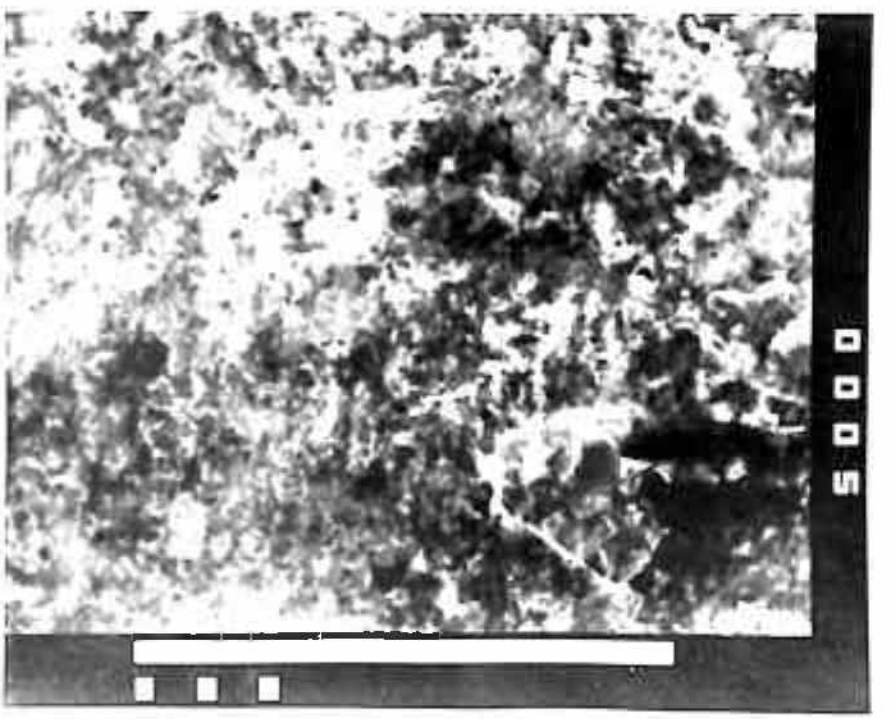

Figure 3.6(a): SEM micrograph of sample Y01.

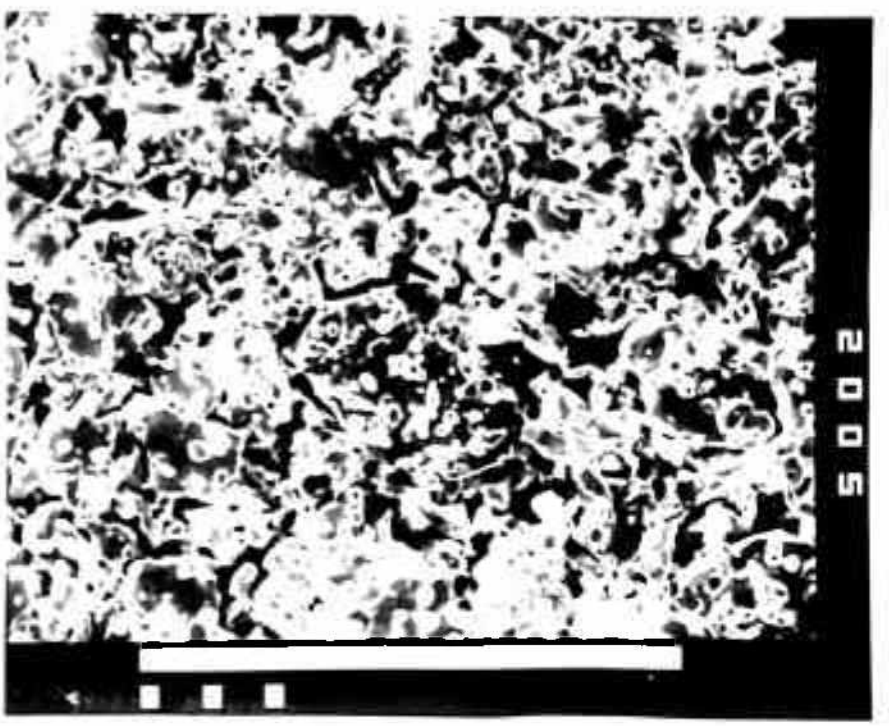

Figure 3.6(b): SEM micrograph of sample Y03.

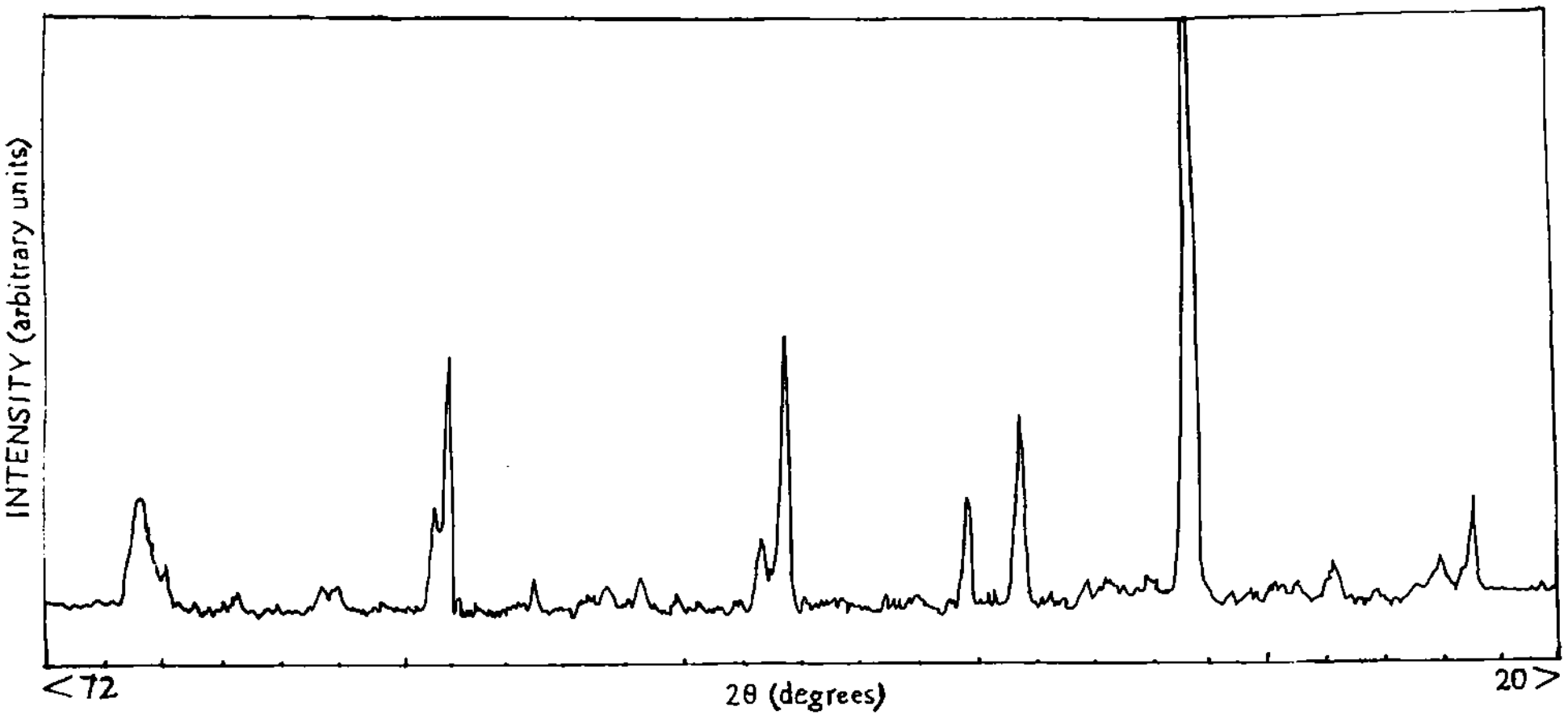

Figure 3.7: Powder X-ray diffraction plot for the sample Y03.

3.4 PREPARATION OF BPSCCO SUPERCONDUCTING MATERIAL

The chemicals used for the synthesis of high T_c phase, Bi_{2-x} Pb_x $Sr_2Ca_2Cu_3O_y$, of BPSCCO (2223) system are high purity Bi_2O_3 (99.9% pure of Aldrich chemical, USA), PbO, $SrCO_3$, $CaCO_3$, and CuO (all more than 99% pure of Loba chemie, India). In our laboratory, we synthesized Pb doped BSCCO samples for different contents of lead. Through a number of experiments, we determined that the $T_{c,zero}$ above 100K is obtained for $0.4 \leq x \leq 0.8$. Thus we believed that the formation of high T_c (2223) phase is enhanced by, lead in this range. The results of only two types of specimen i.e. samples with x=0.4 and 0.8 are reported in this text. The reaction equations for x=0.4 and x=0.8 are

(i) for x = 0.4

$$0.8\,Bi_2O_3 + 0.4PbO + 2SrCO_3 + 2CaCO_3 + 3CuO \xrightarrow{\Delta}$$

or, 0.8(465.96) 0.4(223.19) 2(147.63) 2(100.09) 3(79.54)

or, 372.77 89.28 295.26 200.18 238.62

$$Bi_{1.6}\,Pb_{0.4}\,Sr_2Ca_2Cu_3O_{9+y} + 4CO_2 \uparrow \ldots\ldots (3.2)$$

(ii) for x = 0.8

$$0.6\,Bi_2O_3 + 0.8PbO + 2\,SrCO_3 + 2CaCO_3 + 3CuO \xrightarrow{\Delta}$$

or, 0.6(465.96) 0.8(223.19) 2(147.63) 2(100.09) 3(79.54)

or, 279.58 178.55 295.26 200.18 238.62

$$Bi_{1.2}\,Pb_{0.8}\,Sr_2Ca_2Cu_3O_{9+y} + 4CO_2 \uparrow \ldots\ldots (3.3)$$

According to above equations, we took Bi_2O_3= 7.4554 gm, PbO = 1.7856 gm, $SrCO_3$= 5.906 gm, $CaCO_3$= 4.0036 gm and CuO = 4.7724 gm for x = 0.4. And for x = 0.8, Bi_2O_3 and PbO weighed 5.592 gm and 3.572 gm respectively whereas, amount of the other chemicals remained same. In either case, all the compounds are pounded together in agate mortar with pestle. The fine pulverized powder is then subjected to calcination at 850 ± 5°C for approx. 18 hours in air.

In an another approach, separate calcination of $SrCO_3$ and $CaCO_3$ is also attempted as shown in equations 3.4 and 3.5, to achieve better decomposition of

carbonates into oxides. Here, calcium and strontium carbonates are decomposed at 900°C to obtain their oxides. These oxides are then mixed with the oxides of Bi, Pb, and Cu and subsequently heat treated at 850 ± 5°C for nearly 18 hours in air.

$$SrCO_3 \xrightarrow{900°C/2hrs} SrO + CO_2 \uparrow \quad \ldots\ldots (3.4)$$

$$CaCO_3 \xrightarrow{900°C/2hrs} CaO + CO_2 \uparrow \quad \ldots\ldots (3.5)$$

Both the calcination processes, however, produced the similar results, i.e. the net loss in weight due to carbon-di-oxide evolution was equal in both the cases. Hence, separate calcination of $SrCO_3$ and $CaCO_3$ is seldom practiced. Alike the YBCO processing, the calcined powder is repulverised and pelletized. The pellets are then subjected to annealing cycles. A typical set of five annealing cycles is summarized in Table 3.4. All the samples were annealed at 860°C in air for 60 hours except for sample B01, which was heat treated for 40 hours only. Samples B01, B02 and B04 were cooled at the rate of 1°C/ min. But while cooling, the pellet B04 was also kept at constant temperatures for 1 hour after every 100°C decrease in temperature i.e. 'steps cooling' (fig. 3.8) as described in the section 3.2 for the preparation of YBCO samples. Specimen B03 and B05 were cooled at the rate of 0.5°C/min. but the two contained different amounts of bismuth and lead. Bi:Pb ratio for sample B03 has been 1.2:0.8 while that of B05 it is 1.6:0.4. The various measurements done on the BSCCO samples are described in next section.

Table 3.4 Annealing cycles for various BPSCCO samples.

Sample No.	Bi:Pb Ratio	Annealing Temperature and Time	Cooling Procedure
B01	1.2:0.8	860°C for 40 hours	860°C to 160°C at 1°C/min.
B02	1.2:0.8	860°C for 60 hours	860°C to 160°C at 1°C/min.
B03	1.2:0.8	860°C for 60 hours	860°C to 60°C at 0.5°C/min.
B04	1.2:0.8	860°C for 60 hours	Steps cooling (Fig.3.8)
B05	1.6:0.4	860°C for 60 hours	860°C to 60°C at 0.5°C/min.

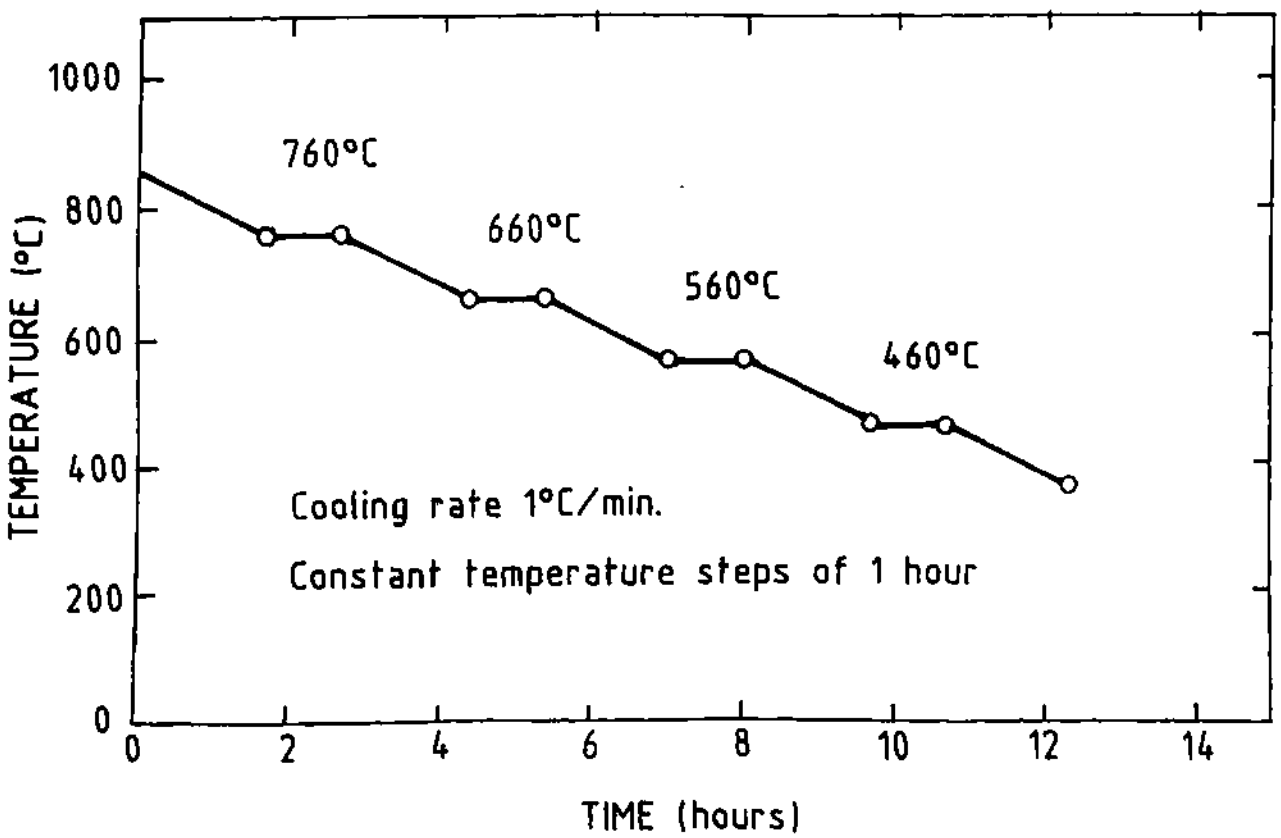

Fig.3.8 Steps Cooling for sample B04

3.5 CHARACTERIZATION OF Bi_{2-X} Pb_X $Sr_2Ca_2Cu_3O_Y$ PELLETS

The annealed BSCCO specimen are characterized through resistivity and a.c. susceptibility measurements, as a function of temperature, and x-ray diffraction analysis for detecting the presence of different phases. The R-T plots of the samples B01 to B04, in figures 3.9 to 3.12, indicates $T_{c,ON}$ = 116K, whereas, data corresponding to pellet B05 (Fig. 3.13) suggests that the superconducting transition commenced at 118K. The $T_{c,zero}$ of the samples varied from 98K to 107K. All these critical temperatures pertaining to resistivity curves and their corresponding susceptibility data are tabulated in Table 3.5.

The lowest value, 98K, was obtained in sample B01, may be due to the presence of low T_c phase in large quantity. The fact was confirmed by susceptibility data (Fig. 3.9) which show prolonged intrinsic transition and only 30% volume fraction of the material transforming into superconducting state at 77K. Hence, the coupling transition could hardly got initiated in this specimen upto boiling point of liquid nitrogen however sample turned into zero resistance state through percolation path. As illustrated in Fig.3.10, the onset of intrinsic and coupling transitions in sample B02 are at 107K and 102K respectively. Also, $T_{c,zero}$ = 105K, denoted by R-T results in Fig. 3.10 for this sample, is much higher than 98K of B01. This suggests that annealing of merely 40 hours at 860°C is not enough for the complete transition of the material into high T_c superconducting (2223) phase of this compound. The complete transition is therefore achieved after 60 hours of annealing. The heat treatments of more than 60 hours have also been attempted (Nobumasa, et al., 1988; Sato, et al., 1988) in order to produce higher fractions of high T_c phase in the BSCCO material. Further, the comparison of χ-T and R-T data of the sample B02 with specimen B03 and B04 reveal that there was no significant change in properties introduced due to either slow cooling or steps cooling as is evident from figures 3.10 to 3.12. Susceptibility curves of all the three samples show same onset temperatures (Table 3.5). However, transition width, ΔT_c , is equal to 10K and 12K in slow cooled and steps cooled pellets respectively as compared to ΔT_c = 11K in sample B02. Sample B05 (with

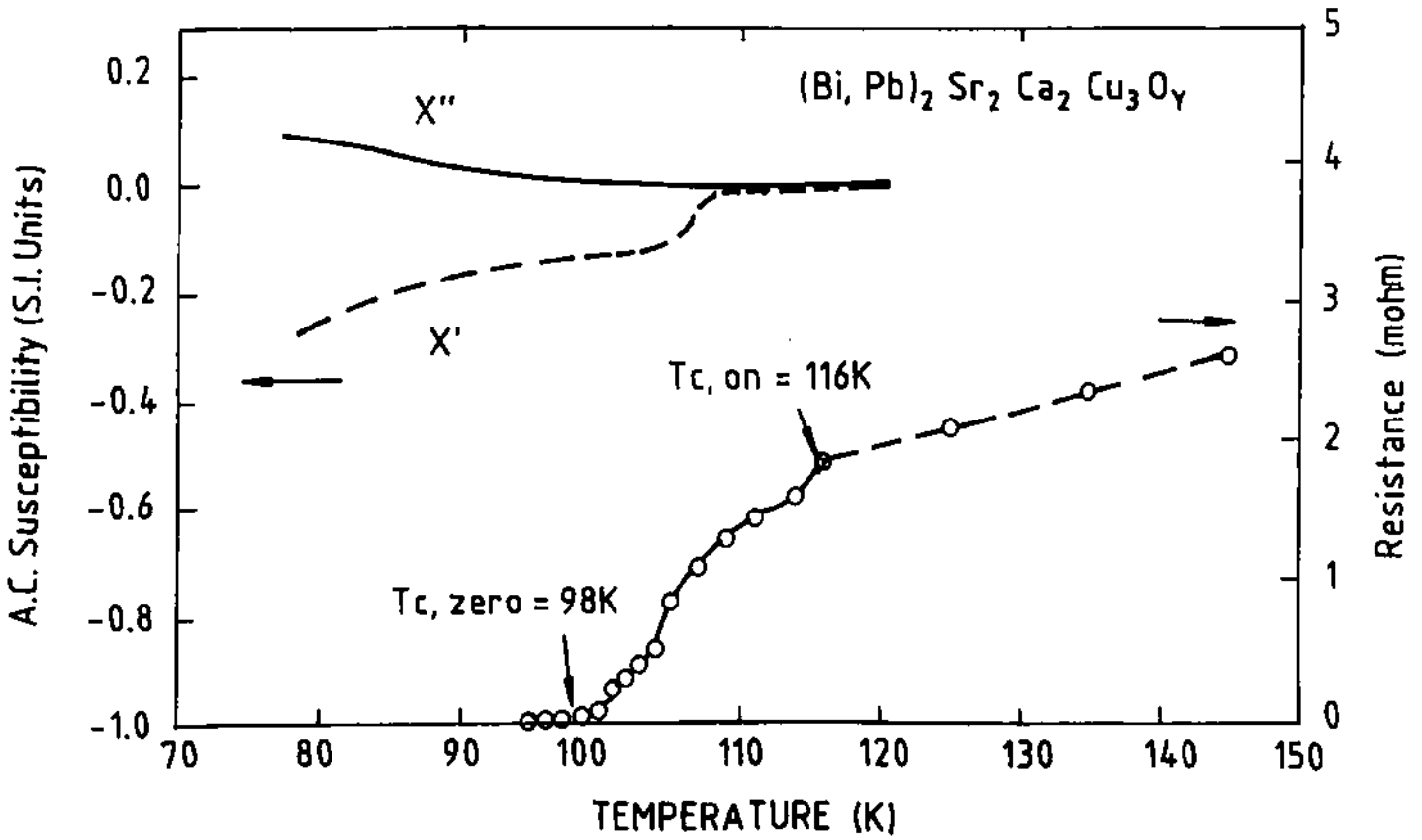

Fig.3.9 A.C. Susceptibility and resistance as functions of temperature for sample B01.

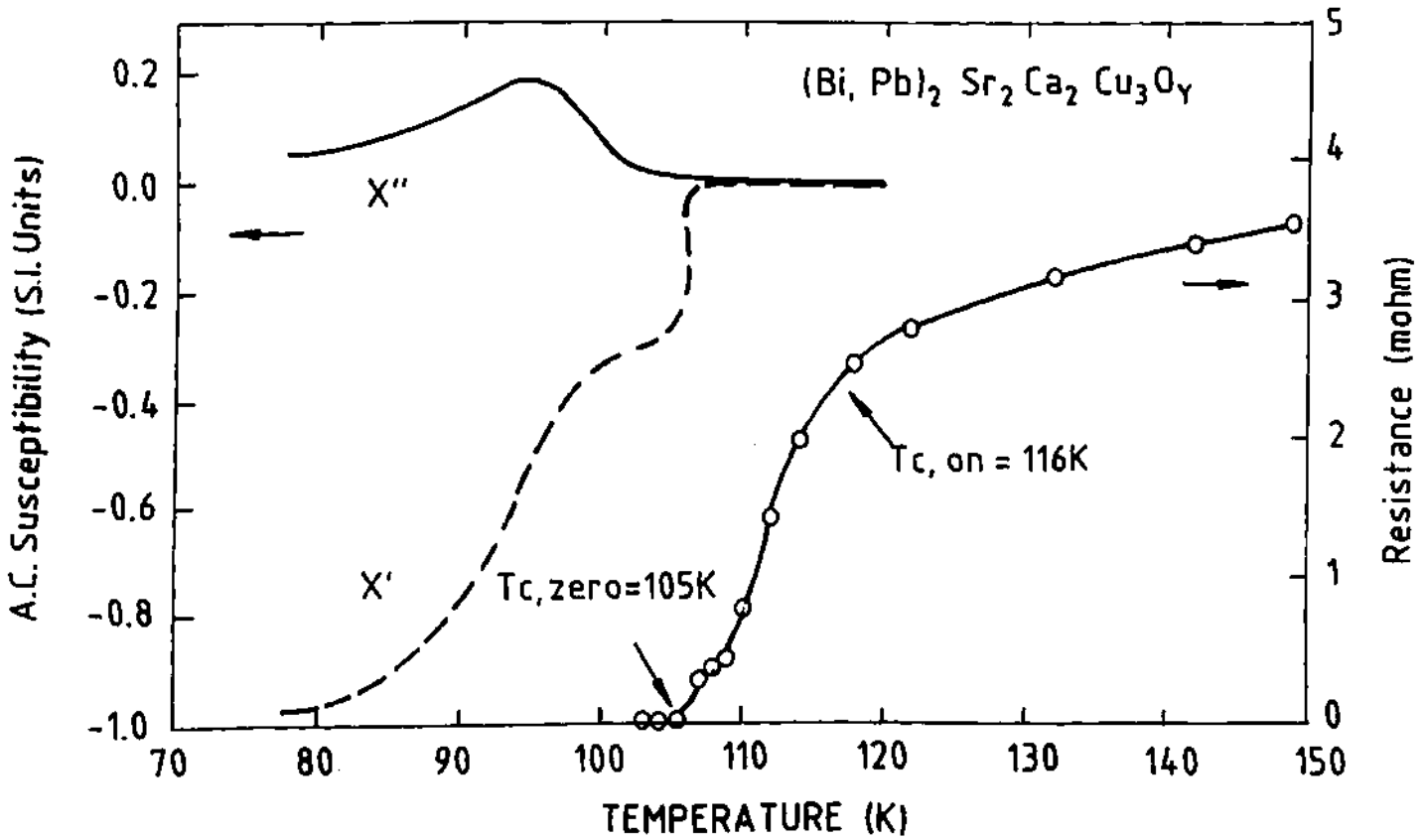

Fig.3.10 A.C. Susceptibility and resistance as functions of temperature for sample B02.

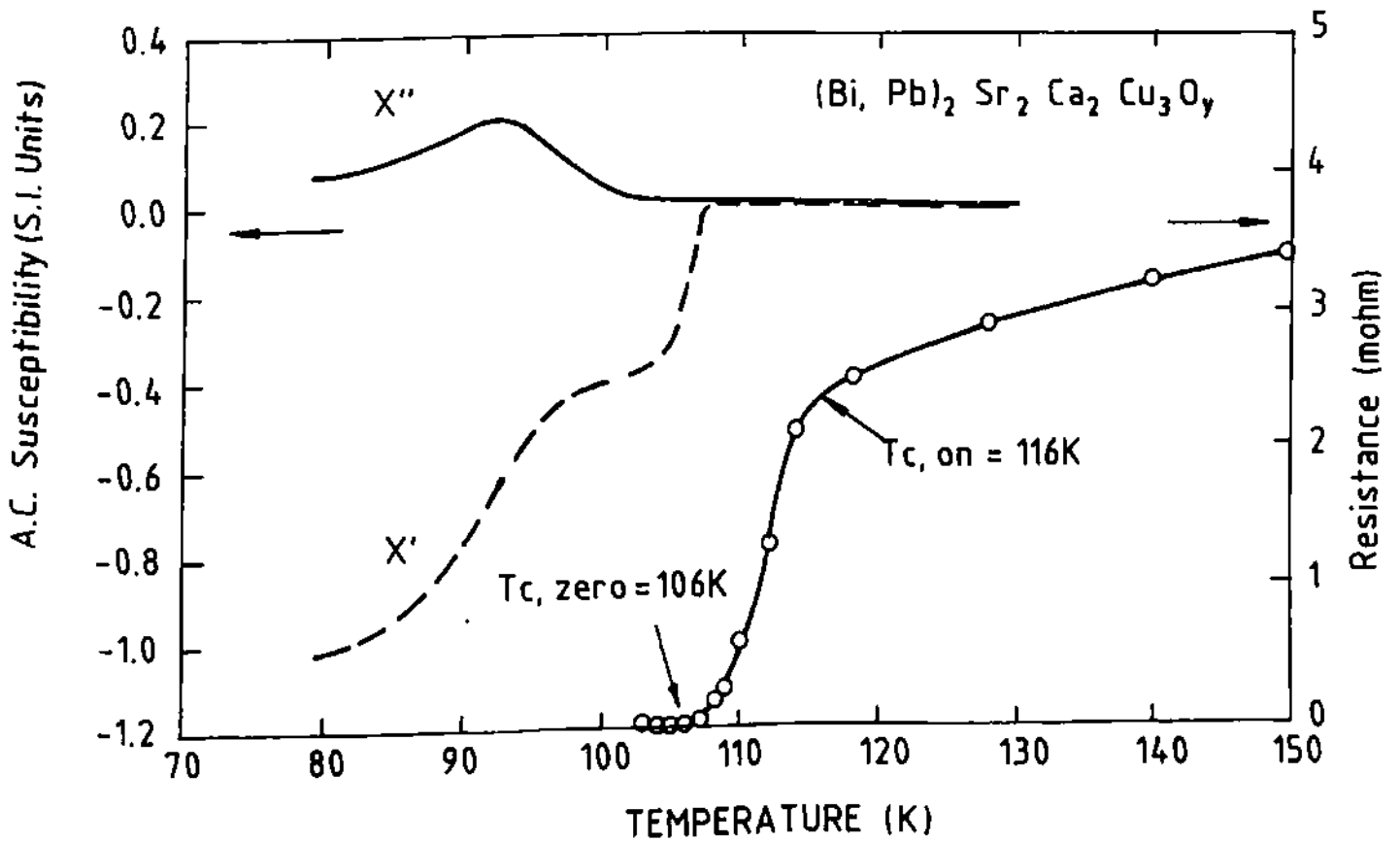

Fig.3.11 A.C. Susceptibility and resistance as functions of temperature for sample B03

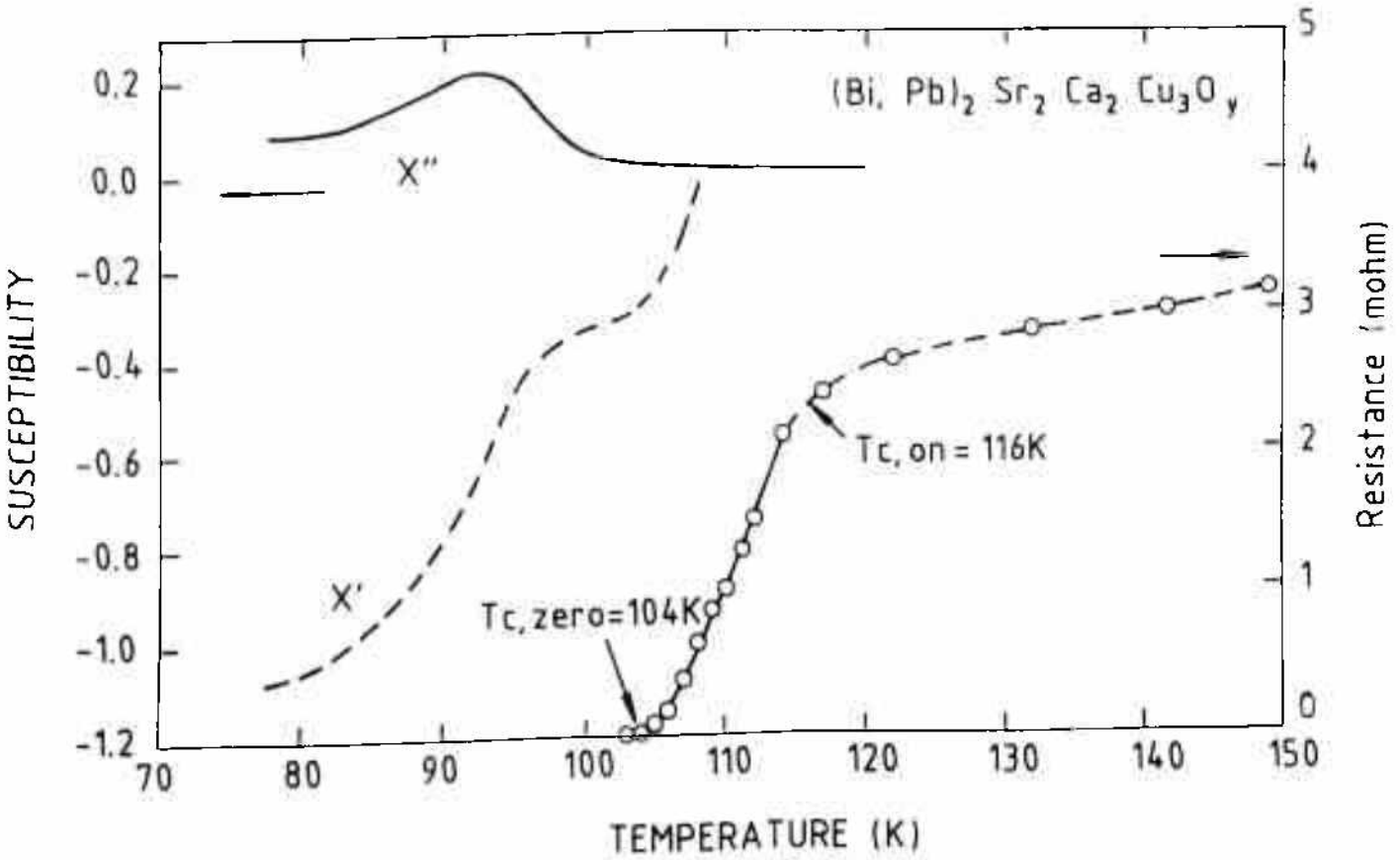

Fig.3.12 A.C. Susceptibility and resistance as functions of temperature for sample B04.

x=0.4), in Fig. 3.13, shows higher $T_{c,ON}$ = 118K and $T_{c,zero}$ = 107K in resistivity curve while, susceptibility plot shows intrinsic and coupling onset temperatures equal to 108K and 105K respectively. Also, the peak in χ'' plot of the sample, which corresponds to about 60% transition (by volume) of the material into superconducting phase, is at 101.5K in sample B05 whereas, for other samples it lies between 92.5K to 95.0K. Also, comparatively sharper peak in χ'' curve of sample B05 clearly indicates much stronger inter granular coupling among the grains of this pellet than that of other processes.

Table 3.5 Critical temperature data of BPSCCO samples

Sample No	Resistivity data (K)			Susceptibility data (K)	
	$T_{c,ON}$	$T_{c,zero}$	ΔT_c	Intrinsic onset	Coupling onset
B01	116	98	18	107	< 77
B02	116	105	11	107	102
B03	116	106	10	107	102
B04	116	104	12	107	102
B05	118	107	11	108	105

The sample B05 was also characterized through x-ray powder diffractionc The 2θ versus intensity plot of the specimen indicated peaks corresponding to both high T_c (2223) and low T_c (2212) phases, as shown in Fig. 3.14. The indices and phases corresponding to the peaks, in Table 3.6, suggests that the majority of the material has crystalized in the high T_c phase with lattice parameters a, b, and c equal to 3.8117 Å, 3.7879 Å, and 37.17 Å respectively showing slight orthogonality. However, some amount of low T_c phase with lattice constants a, b, and c equal to 3.8041 Å, 3.8142 Å, and 30.7291 Å respectively and a few unknown peaks are also present.

These analysis suggests that the proper amount of lead, in place of bismuth, is essential for the synthesis of high T_c phase in BSCCO compounds although, the annealing

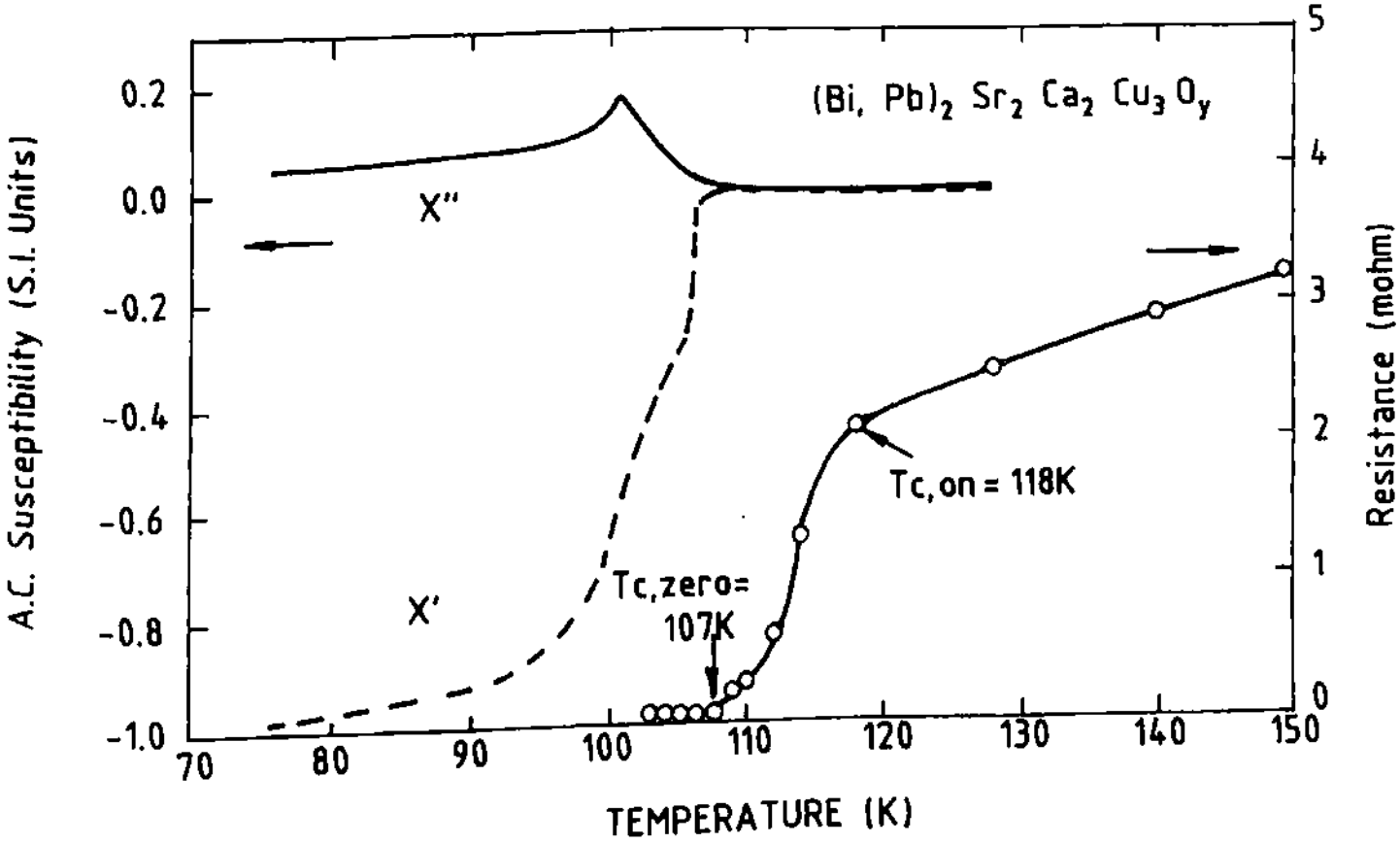

Fig.3.13 A.C. Susceptibility and resistance as functions of temperature for sample B05.

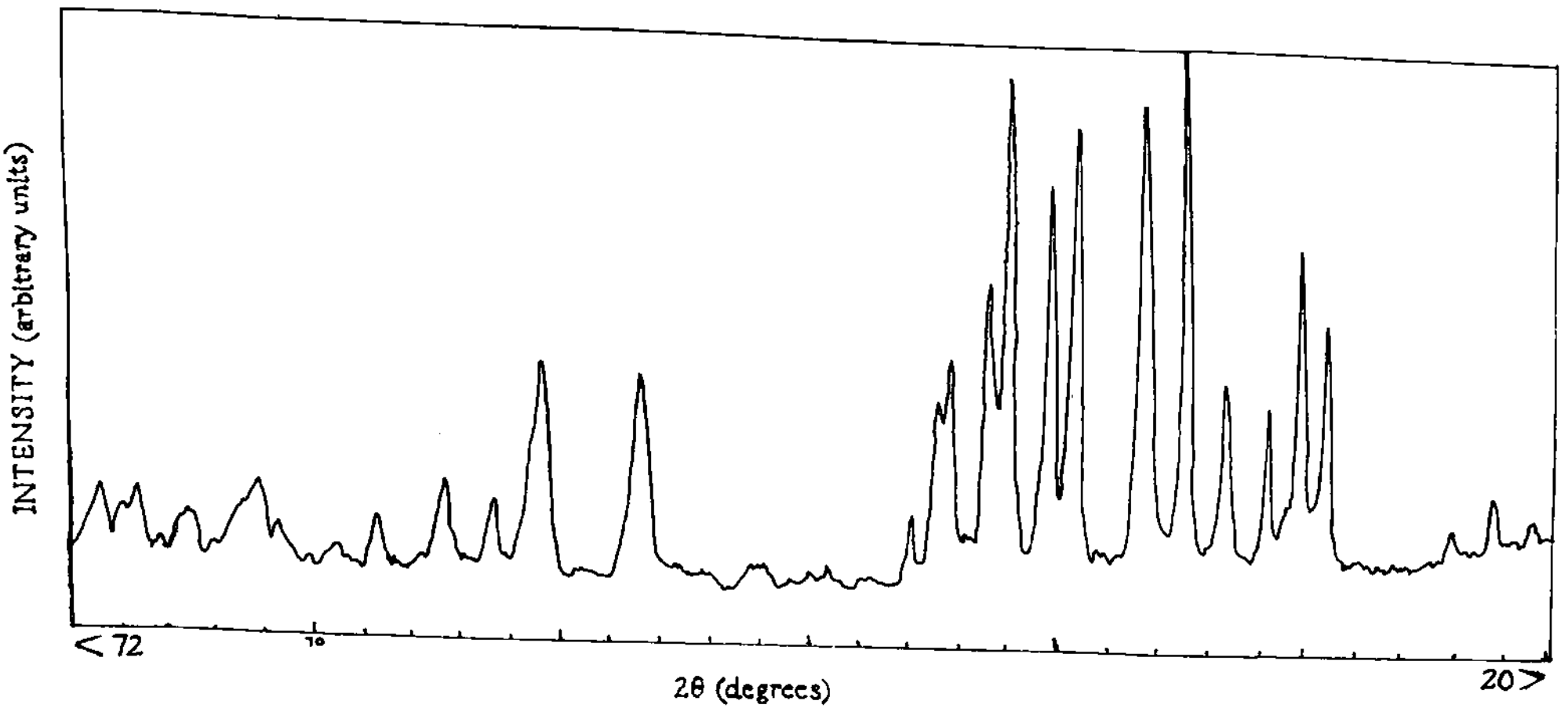

Figure 3.14: Powder X-ray diffraction plot for the sample B05.

cycle along with the cooling pattern also plays an important role in the grain growth, their connectivity and the formation of high T_c phase. In BSCCO system, instead of 'step cooling', slow cooling (at the rate of 0.5°C/min.) has been found to be more effective for the growth of 2223 phase.

Table 3.6 X-ray powder diffraction data of BPSCCO samples B05

S. No.	2θ	d	Phase (Plane)
1.	20.9	5.3368	High T_c (007)
2.	22.4	4.9836	Unidentified
3.	24.0	4.6557	High T_c (008)
4.	29.1	3.8531	Low T_c
5.	30.2	3.7158	High T_c (0010)
6.	31.4	3.5772	Low T_c
7.	33.0	3.4082	High T_c
8.	34.8	3.2370	Low T_c
9.	36.4	3.0992	High T_c (0012)/ Low T_c (0010)
10.	39.2	2.8856	Low T_c (117)
11.	40.4	2.8033	High T_c (119)
12.	42.0	2.7011	High T_c (200)/ Low T_c (200)
13.	42.8	2.6529	High T_c
14.	44.4	2.5619	Low T_c (0012)
15.	44.8	2.5402	High T_c
16.	45.9	2.4825	High T_c
17.	57.0	2.0286	High T_c (1112)
18.	61.0	1.9072	High T_c / Low T_c
19.	62.8	1.8575	High T_c (0020)
20.	64.8	1.8065	Low T_c (0115)
21.	67.6	1.7400	Unidentified
22.	69.2	1.7047	Low T_c (208)
23.	71.5	1.6568	High T_c (215)
24.	72.4	1.6390	Low T_c
25.	73.2	1.6235	High T_c (2012)
26.	75.2	1.5865	Low T_c (217)
27.	77.4	1.5482	High T_c (0022)
28.	78.4	1.5283	Low T_c (2012)

3.6 CONCLUSIONS

The single phase $YBa_{2.}u_3O_{7-x,}$ with $T_{c,zero}$ about 94K can be produced by processing the material at 950°C for 24 hours followed by cooling in steps. These cuprates contain more than 80 percent superconducting material, by volume at 90K. While the growth of high T_c phase (Bi_{2-x} Pb_x $Sr_2Ca_2Cu_3O_y$) in BSCCO compounds depends on the lead content and the process cycle. In this case continuous slow cooling at the rate of 0.5°C/min. and Bi:Pb ratio of 1.6:0.4 was found most suitable for the growth of 2223 phase in bismuth cuprates. The stronger inter granular coupling was also observed in these samples.

CHAPTER -FOUR

DEPOSITION OF SUPERCONDUCTING THIN FILMS OF YBCO AND BSCCO COMPOUNDS

This chapter is broadly divided into three sections. The first one briefly describes various thin film preparation techniques which are used in semiconductor device fabrication technology and are being employed globally for the synthesis of HTSC films too. The second section presents some global issues in substrate selection for high T_c films and a review of HTSC film preparation work of various research groups. The work is classified according to the techniques used for film deposition. The final section describes the high T_c thin film synthesis techniques developed, their analysis, results and conclusions.

4.1 TECHNIQUES FOR THIN FILM PREPARATION

Thin films deposition techniques may be broadly classified under three categories, namely, evaporation, chemical deposition and sputtering.

4.1.1 Evaporation

The thin film deposition by the evaporation is simple and very convenient and is at present the most widely used for numerous applications. The principle of thermal evaporation is that the solid materials vaporize when heated to sufficiently high temperature. The condensation of the vapour onto substrates yields thin solid films of that material. Depending on the various heat energy sources, the evaporation methods can be classified as flash, arc, laser, r.f., electron beam and exploding-wire evaporation

techniques. The film deposition by these methods is carried out in a high vacuum system, usually below 10^{-6} Torr, to avoid contamination in the films.

4.1.2 Chemical depositions

Chemical methods may be classified in two categories, namely, electro-deposition and chemical vapour deposition (CVD). These techniques enable coating thickness to be varied from few angstroms to hundreds of microns in a well controlled fashion. Although the impurities and their effects vary with the material to be deposited, most refractory metals and several non-metals are obtained chemically in a purer form than by conventional metallurgical practices. Electro-deposition techniques can further be classified as electrolytic, electroless and anodic oxidation deposition. Chemical vapour deposition techniques are suitable for volume production and deposition on large area. A number of CVD techniques have been developed for example, low pressure CVD (LPCVD), atmospheric pressure CVD (APCVD) and metallorganic CVD (MOCVD). Although special organic compounds have limited shelf life, required for MOCVD, it is widely being used in semiconductor industries.

4.1.3 Sputtering techniques

The ejection of atoms from the surface of a material, called target, by bombardment with energetic particles is called "sputtering". Inert gas argon is generally used to generate energetic particles for bombardment. If ejection is due to positive ion bombardment it is refereed to as "cathodic sputtering". The ejected or sputtered atoms can be condensed on a substrate to form a thin film. Sputtering technique has been dealt with in details here, as it was used by us to fabricate HTSC thin films in the present work.

In sputtering method, the ions for sputtering are provided by the well-known phenomenon of glow discharge resulting due to an applied electric field between two electrodes in a gas at low pressures. The gas breaks down to conduct electricity when a certain minimum voltage is reached. Effective sputtering is possible only when both the

number of ions and their energy is large. Some of the factors which influence the sputter deposition of films are discussed below:

(a) Pressure: As the gas pressure is increased, the discharge current increases, the voltage falls. The number of ions increases proportionally with the number of ions and electrons created at the breakdown, but their density decreases with decreasing ion energy linearly or less than linearly in the practical range of a few kilo volts. Thus, a net increase in the total number of ejected atoms results. Also, with increasing pressure, ejected atoms suffer more collisions and are thus prevented from reaching the anode.

(b) Deposit Distribution: Because of collisions with the ambient gas atoms at high pressures, the sputtered atoms are diffusely scattered during transit and therefore reach the anode with randomized directions and energies. Also, due to collisions, the energetic ions hit the cathode at high oblique angles, which is helpful in increasing the yield.

At constant pressure and constant applied voltage, the deposition rate is low at large distances from the cathode and shows a decided maximum at the centre. As this distance is decreased, a more uniform deposit first results which then becomes annular in nature with a maximum thickness on a circle slightly smaller than the target. The optimum conditions of deposition with uniformity of deposit extending to about half the area of the target are obtained when the cathode-anode distance is about twice the length of the cathode dark space.

(c) Current and Voltage Dependence: The sputtering rate is proportional to the current for a constant voltage which is thus a very conveniently controllable parameter. The voltage dependence is non linear, but for a certain range of applied voltages, depending on the gas and the target material, the sputtering rate is proportional to the product of current and voltage. Typical conditions employed for plane cathode sputtering are 1 to 5 kV potential with a current density 1 to 10 mA/cm^2 .

(d) Cathode: A plane cathode of area about twice that required for a uniform deposit is used. The cathode material may be a plate, foil or electroplated deposit on a suitable target material. The bombardment of ions heats the cathode which rapidly reaches an equilibrium value. This heating does not significantly alter the sputtering yield, but it has other undesirable effects such as that of heating of the substrate, or heating of the gas resulting in changes in atomic density.

(e) Contamination Problem: Even if a leak proof sputtering system is initially pumped down to a high vacuum (say, 10 Torr) and then sputtering gas of high purity is admitted, contaminants may still appear from:

(i) the out gassing as a result of plasma-discharge heating of the walls and other components of the sputtering chamber.

(ii) the decomposition of oil vapours as a result of back streaming from the diffusion pump operated at high pressures.

Sputter deposition is carried out in wide range of chamber pressure, ranging from 100 Torr (high pressure) to less than a milli-torr (low pressure). However, some of the salient features of the low-pressure sputtering are: the decreasing influence of gas atoms, the lower concentration of the trapped gas atoms, the controlled direction and higher mean energy of the ejected atoms striking the substrate owing to smaller collision losses. Reasonable sputtering rates at low pressures may be obtained by increasing the ionization of the sputtering gas by

(1) increased ionizing efficiency of the available electrons,

(2) increased supply of ionizing electrons, and

(3) an ion-beam source.

A brief description of the various sputter deposition techniques are mentioned in the following paragraphs.

In magnetic field assisted or magnetron sputtering the ionizing efficiency may be increased very conveniently by increasing the path length of the ionizing electrons. A

longitudinal magnetic field (50 to 100 Gauss) is generally convenient to use for a diode geometry, i.e. cathode (target) and anode (substrate) system. Such a field has no effect on electrons moving parallel to the field, but it helps to concentrate the diffuse plasma by preventing lateral motion and also increases the path length of randomly moving electrons. Consequently, the current density is considerably increased and reasonable sputtering rate may be obtained at pressures down to a few millitorr.

In RF or AC sputtering, a RF voltage is applied to the cathode. The use of 13.56 MHz is international standard frequency for this purpose. RF sputtering is particularly suitable for the deposition of non-conducting materials and composites. Radio-frequency sputtering is a versatile technique and has several useful applications. If the rf power supply is coupled capacitively to a metal electrode, metals can also be rf sputtered. A combination of magnetron and RF sputtering is also used, especially for obtaining higher deposition rates of insulating materials.

Direct-current (DC) sputtering is commonly used for the deposition of metallic films. It is not recommended for the insulators because of the build-up of positive surface charges which would repel the energetic Ar ions. A high frequency alternating potential is used in RF sputtering to neutralize the insulator surface periodically with plasma electrons. Methods to neutralize this surface charge by injecting electrons from a gun, or by placing a metal screen over the cathode surface, thus producing a conductive sputtered metal film, have also been devised.

Most of the systems are ineffective below 10^{-3} Torr because of the scarcity of ions. By producing ions in a high-pressure chamber and then extracting them into a differentially pumped vacuum chamber through suitable apertures with the help of suitable electron and ion optics, a beam of ions may be obtained for sputtering in vacuum. This is called ion-beam sputtering.

4.2 FABRICATION OF HTSC THIN FILMS - A REVIEW

Since the discovery of high temperature superconducting oxides in 1986, there has been unprecedented research activity in the preparation of high quality thin films for device development. Owing to operation at liquid nitrogen temperature these materials have potential applications in superconducting electronics. As high T_c ceramic oxides are superconducting only when an optimum amount of oxygen is incorporated in these compounds, an appropriate amount of oxygen is included in argon to sputter the target material for thin film deposition. The properties of deposited film strongly depend on the substrate material, substrate temperature, the rate of deposition, etc. in addition to the elemental composition in the target.

4.2.1 Issues in substrate selection

One of the most important aspects in high temperature superconducting film growth is the choice of a substrate on which the films are deposited. This sub-section focuses on the issues related to the substrate selection. The compatibility of the crystal structures of the substrate and superconducting compound is an important criterion. However, each specific application requires different substrate material which offers an acceptable compromise for the purpose at hand. Some desirable substrate requirements are chemical compatibility, lattice and thermal expansion match, surface quality, buffer layer(s) compatibility, homogeneity and thermal stability. These issues limit maximum processing temperature, reactions at substrate-film interface, impurity incorporation in the film, film adhesion, microstructure, composition, morphology and uniformity of the film. Lattice mis-match, coincidence sites, surface quality and substrate structural quality are important considerations in substrate selection for the preparation of epitaxial films. All these substrate parameters profoundly influence superconducting properties of the films.

A number of materials have been explored as substrates for HTSC films, but most of them have met with limited success. In general, the search for a substrate that can support the growth of high quality high T_c films has centred on materials having the

perovskite crystal structure, usually oxides (Guo, et al., 1994). Strontium titanate ($SrTiO_3$) saw early success as an useful substrate (Chaudhari, et al., 1987), as it has small lattice mis-match with YBCO (its lattice constant is a = 0.3905 nm) and its ready availability. Its large dielectric constant (ε = 277, at room temperature) and unavailability in large sizes, has spurred the search for alternatives. Still, $SrTiO_3$ has supported high quality YBCO (Broussard, et al., 1992) and BSCCO films (Balestrino, et al., 1990). Lanthanum gadulate ($LaGaO_3$) with lattice constants, a = 0.5519 nm, b = 0.5494 nm and c = 0.777 nm and ε = 25 at room temperature (Sandstrom, et al., 1988) and Lanthanum aluminate ($LaAlO_3$), a pseudo-cubic with lattice constant 0.5377 nm and ε = 24 (Simon, et al., 1988; Young, et al., 1991), have also been successfully used as substrate for YBCO and BSCCO films (Balestrino, et al., 1990; Broussard, et al., 1992; Golden, et al., 1992). Some other perovskites were investigated and utilized as substrate for high T_c thin films include $NdGaO_3$ with ε = 20; a = 0.5417 nm, b = 0.5499 nm and c = 0.7717 nm (Simon, et al., 1988), NdAlO (Choi, et al., 1988), $YAlO_3$ (Asano, et al., 1990; Harshavardhan, et al., 1993), PrGaO (Sasura, et al., 1990), $KTaO_3$ (Feenstra, et al., 1989), $YbFeO_3$ (Ramesh, et al., 1989), Sr_2AlTaO_3 (Findikoglu, et al., 1992; 1993) and $GdBa_2NbO_6$ (Koshy, et al., 1994).

A number of problems have emerged with perovskite-related crystal structures. For example, high substrate cost, high dielectric constants, twinning, and presence of magnetic ions. These aspects have lead to extensive investigations of substrate materials that have other crystal structures. Magnesium oxide (MgO), with NaCl crystal structure has received a good deal of interest in light of its ready availability and its modest dielectric constant, ε = 9.65 and 9% lattice mis-match with YBCO (Moeckly, et al., 1990). It is one of the most popular substrates for the high T_c films (Gasparov, et al., 1990; Takeya and Takei, 1990; Hamet, et al., 1992a; 1992b; Awaji, et al., 1992; Agarwal, et al., 1993; Shekhawat, et al., 1995). Some other substrates which are considered interesting for HTSC film growth are sapphire (Al_2O_3) (Char, et al., 1990a; 1990b) and yttria-stabilized ZrO_2 (YSZ) (Broussard, et al., 1992; Alarco, et al., 1992). Some of these and others like ZrO_2 (Basovich, et al., 1993), CeO_2 (Wu, et al., 1991; Harshavardhan, et

al., 1993), YSZ (Broussard, et al., 1992), MgTiO (Haefke, et al., 1992; Hesse, et al., 1992; Lang, et al., 1992; Sum, et al., 1993), etc. have, also been successfully used as buffer layers between various substrates and HTSC films.

Semiconductors such as Si and GaAs have also received considerable attention as a substrate material due to possibilities of integrating semiconductors with superconductors. But these exhibited some serious problems like chemical reactivity and low temperature tolerance, especially for GaAs. However, there are few reports of YBCO films grown on bare Si (Chromik, et al., 1989; Fang, et al., 1992) and using buffer layers of YSZ (Fork, et al., 1990), CeO (Sanchez, et al., 1992), CaF_2 (Tiwari, et al., 1992) and TiN/Ti/Ag (Fang, et al., 1992). The buffer layers of CaF_2 , $AlGaO_3$, Indium tin oxide, Al_2O_3 , YSZ, YSZ/Si_3N_4 layers (Shewchun, et al., 1991; Tiwari, et al., 1991; Jia, et al., 1992) and MgO (Chang, et al., 1992) have also been explored to prepare superconducting films of GaAs substrate.

Attempts have also been made, to grow HTSC films on metallic substrates for specific applications where an alternative current- carrying path is required. The limited use of metal substrates is due to difference in crystal structures of metals and that of HTSC materials and chemical reactivity between the two (Agarwal et al., 1994). Silver has received the most attention as an HTSC substrate (Nasu, et al., 1989; Zhang, et al., 1990; Hazelton, et al., 1992; Tao, et al., 1993; Yuan, et al., 1993). However, gold has been used for the deposition of TBCCO (2212) films by MOCVD (Hu, et al., 1993). Copper with buffer layer of Ti, followed by a layer of MgO was used as substrate for YBCO films (Podkletnov, et al., 1992). Another potential HTSC substrate studied is Hastelloy (Ni-Cr-Mo alloy) (Yin, et al., 1992; Jia and Anderson, 1992a; 1992b; Umemura, et al., 1993; Aoki, et al., 1993; Kumar and Narayan, 1993; Kohno, et al., 1993; Fukutomi, et al., 1994) using various buffer layers such as YSZ, Pt, $SrTiO_3$, TiN and $BaTiO_3$. Nickel has also been investigated as an HTSC substrate (Iijima, et al., 1992; 1993; Golobov, et al., 1993).

4.2.2 High T_c thin films synthesis

Since the researchers involved in superconductivity area are from diverse disciplines such as structural chemistry, ceramic engineering, metallurgy, instrumentation, solid state electronics, condensed matter physics, etc., they have employed diverse and modified techniques, according to their expertise, to fabricate superconducting thin films. Almost all methods discussed in the section 4.1 have been explored for the preparation of HTSC films. It is also universally established that the substrates are needed to be kept at elevated temperatures (above 700°C) and during deposition of HTSC film, oxygen ambient is a must to obtain in situ superconducting films. This is done to give sufficient energy to depositing atoms, to obtain desired stoichiometry and crystallographic form. The following sub-sections give an overview of the various HTSC thin film preparation techniques employed the world over.

(i) Vacuum Evaporation

For the synthesis of high temperature superconducting oxide thin films by evaporation, the constituent elements (Narayana, et al. 1989) or their compounds (e.g., BaF_2) (Feenstra, et al., 1989) are co-evaporated by resistive heating and subsequently annealed in oxygen to obtain the superconducting phase. These are called post-annealed films. Y-Ba-Cu-O films have also been prepared by, layer-by-layer evaporation of Cu, BaF_2, and YF_3 using single resistive evaporation from tungsten boats onto $SrTiO_3$ substrates and post-deposition annealing (Azoulay and Goldschmidt, 1989). High T_c superconducting films of YBCO (123) have also been prepared by flash evaporation (Ece and Vook, 1989) and subsequent annealing in oxygen at 930°C for 60 minutes to achieve superconductivity.

(ii) Laser ablation

The pulsed laser evaporation technique is one of the most popular methods for the preparation of high quality HTSC thin films. A large number of reports have been published particularly on $YBa_2Cu_3O_{7-x}$ thin films synthesis by this method (Venkatesan, et al., 1988; Roas, et al., 1988; Fogarassy, et al., 1989; Ludorf, et al., 1989; Nortan, et al.,

1990; Wu, et al., 1990; Ohkubo, et al., 1990). Serbezov et al. (1990) have prepared YBCO thin films on poly-Al_2O_3, sapphire, $SrTiO_3$ and single crystal Si by nitrogen laser evaporation. The films were post annealed to achieve superconduction. However, in-situ superconducting $YBa_2Cu_3O_{7-x}$ films have been prepared by pulsed laser evaporation with $T_{c,zero}$ upto 87K on Si substrates with $MgAl_2O_4$ and $BaTiO_3$ double buffer layers (Hwang, et al., 1990). Laser deposited YBCO films with buffer layers of silver and platinum on stainless steel, platinum and several single crystal substrates (like MgO, $SrTiO_3$) also exhibited T_c upto 84K (Russo, et al., 1990).

(iii) Sputtering

Sputtering of HTSC is usually carried out in argon-oxygen mixture. Oxygen is almost universally accepted as a part of the sputtering gas, for the sputter deposition of oxide superconductors. However, one of the major disadvantages of oxygen incorporation in the sputtering gas is the formation of negative oxygen ions in the plasma. These negative oxygen ions etch the film which is being deposited on the substrates. To minimise film etching by negative oxygen ions, off-axis sputtering mode is employed for HTSC films deposition (Xi, et al., 1989; Newmen, et al., 1990). In off-axis configuration, substrates are usually held perpendicular to the target. Consequently, energetic negative oxygen ions do not directly strike the film surface and etching is avoided but the deposition rate is also highly supressed as most sputtered HTSC material species also move almost normal to the target. Nevertheless, off-axis has proven to be the most viable approach for the sputter deposition of HTSC films.

Quite a large number of sputtering techniques such as d.c. diode (Hong, et al., 1987; Poppe, et al., 1988; Hong, et al. 1988; Schubert, et al., 1989), d.c. and r.f. magnetron sputtering methods (Burbidge, et al., 1987; Hakuraku, et al., 1989a; Hakuraku, et al., 1989b; Scheib, et al., 1989; Subramanyam, et al., 1990; Agarwal, et al., 1993; Savvides and Katsaros, 1993) and their modifications like planer rf magnetron, compressed magnetic field (CMF) sputtering (Yoshimoto, et al., 1989), facing targets sputtering (FTS) (Hoshi, et al., 1977; Hirala and Naoe, 1990), ion beam assisted sputtering (Amean, et al., 1990; Klein, et al., 1990), electron cyclotron resonance (ECR)

plasma sputtering (Masumoto, et al., 1989; Doyle, et al., 1990), etc. have been used to produce high T_c superconducting films with or without post-deposition annealing. These systems are used in both on-axis and off-axis configurations to deposit HTSC films.

(iv) Ion assisted and ion beam deposition

An ion assisted laser deposition technique to prepare HTSC thin film was used by Witanachchi et al. (1988). A ring-shaped electrode was placed between the substrate and the target and it was held at +300V to trigger dc discharge. Due to dc discharge, the O_2^+ ions formed by electron impact between the ring electrode and the substrate were effective in enhancing and improving the film deposition by ion activation of the surface, where as those formed between the target and electrode were repelled. Also the O_2^+ ions tend to enhance the oxygen content of the deposited film, thereby improving the superconducting properties.

The low energy ion bombardment using electron cyclotron resonance (ECR) ion source during sputter deposition of BSCCO (Masumoto et al., 1989) and YBCO (Doyle et al., 1990) thin films have also been reported.

(v) Reactive deposition techniques

A number of compound thin films such as oxides, nitrates and carbides are typically prepared by reactive evaporation, reactive sputtering, and so on i.e. the metal is deposited in the presence of a reactive gas or component. To form certain oxides and nitrates, a high activation energy is needed for chemical reaction. This energy is obtained by the presence of ionized atoms which are also accelerated in the electric fields to further increase the energy of the ions. Such a process is known as activated reactive evaporation (ARE) technique. Preparation of YBCO superconducting films by reactive plasma evaporation method has been reported by Terashima et al. (1988). In their set-up, a mixture of $BaCO_3$, Y_2O_3 and CuO powders was fed into the rf plasma flame, with Argon as carrier gas. High temperature vapour mixtures generated in the plasma flame got deposited onto the (100) MgO single-crystal substrate placed in the tail of the plasma

flame. Prakash et al. (1989) have successfully deposited the YBCO superconducting films in situ by ARE. A reactive sequential deposition technique in which Bi, SrCu and CaCu were deposited using dc magnetron multitarget sputtering in an $Ar|O_2$ (5:1) atmosphere (3.5 Pa) to prepare the high T_c superconducting films (Setsune, et al., 1989). However, these films turned superconducting only after post annealing.

(vi) Epitaxial Film Deposition Techniques

Epitaxy is the oriented or single-crystalline growth of one substance over another having crystallographic relations between the deposit and the substrate. Epitaxial films are deposited by a variety of techniques from solution as well as from vapour. These methods include liquid phase epitaxy (LPE), molecular beam epitaxy (MBE), hot wall epitaxy (HWE), laser ablation and metal organic chemical vapour deposition (MOCVD).

MBE has been used by Kwo et al. (1988) to prepare epitaxial superconducting thin films. They have reported the in-situ preparation of highly oriented epitaxial $YBa_2Cu_3O_{7-x}$ thin films on MgO (100) by molecular beam epitaxy at a substrate temperature of 550-600°C. However, the major problem with MBE deposition is introduction of oxygen into the vacuum chamber as it is hard to operate electron gun in excessive oxygen environment. The in-situ low temperature growth was achieved by using a combination of MBE and a reactive oxygen source generated from a microwave discharge in a flow tube design. The films exhibited T_c (R=0) at 82K after annealing the as-grown films at 500°C in flowing oxygen.

Superconducting $YBa_2Cu_3O_{7-x}$ thin films with T_c (R=0) of 83K have also been grown by MOCVD on $SrTiO_3$ (100) substrate (Kanehori, et al., 1989). The main advantage of CVD technique is the possibility of deposition of films on large size substrates and on many substrates simultaneously. However, limited shelf life of organo-metallic compounds is a major problem of MOCVD technique.

(vii) Other Methods of Film Deposition

Some other film deposition techniques are being used for the synthesis of high temperature superconducting films. These are spray pyrolysis, spin-on coated, paint brush techniques etc. Spray pyrolysis involves a thermally stimulated chemical reaction between fine droplets of different chemical species. For the preparation of HTSC thin films, a solution containing soluble salts (usually nitrates) of the constituent atoms of the compound is sprayed onto a heated substrate in the form of fine droplets by a nozzle sprayer with the help of a carrier gas (Gupta, et al., 1988; Langlet, et al., 1989; Hsu, et al., 1989; Ban, et al., 1990). In spin-coating and paint brush techniques, fine powder of HTSC compound is mixed in an organic vehicle and coated on the substrates. The organic material evaporates at temperatures well below annnealing point of the film. Generally thicker films (thickness above one micron) are produced by these techniques.

4.3 FABRICATION OF YBCO AND BSCCO THIN FILMS

This section describes the techniques and procedures, we have developed and employed for the preparation of YBCO and BSCCO films. Firstly, we prepared polycrystalline BPSCCO and YBCO films by spin-on process, an innovative and very simple technique. Subsequently, RF magnetron sputtering (in on-axis and off-axis mode) was employed to fabricate superconducting films of these compounds. A new approach for the preparation of in-situ superconducting films, by sputtering is discussed separately. The film characterization results are reported and discussed simultaneously with the description of each process in the following sections.

4.3.1 Spin-on Films

A simple technique, based on spin-on diffusion method of semiconductor technology, has been developed for the fabrication of thin films of high T_c superconductors (Gupta and Khokle, 1993). The spin-on source is prepared by mixing fine powder of a HTSC material in an appropriate organic vehicle. The important

properties considered to select the vehicle are: (i) adhesion to substrates (ii) chemical and thermal resistance (iii) volatility at a temperature well below the melting point of the superconducting compound. They examined many organic liquids through a large number of experiments and determined that a polymer of novolac-resin-family meets all above requirements. It evaporates at about 650-700°C in air or oxygen. The mixing was accomplished with the help of magnetic stirrer to obtain a homogeneous viscous fluid to be used as a spin-on source. It was spin-coated on the substrates at 2000-5000 rpm, dried in oven at 100°C for one hour and heated slowly in a furnace at 700°C for 10 minutes to burn-out the organic mass. Thus a film containing only particles of high T_c material was obtained. It was then subjected to an appropriate annealing cycle to obtain superconduction.

Film thickness was controlled via viscosity of the spin-on source and coating speed. To produce thick or dense films, the coating and burn-out cycles were repeated. An important feature of the technique is that the rotating substrate spins-off the large sized particles and only approximately same sized particles are retained in the coated layer. However, the ultimate thickness of the film depends, not only on the particle size but also on the subsequent annealing, as melting of particles was always preferred, according to the present technique. The melting has been found essential for better adhesion as well as to improve critical current density of superconducting films.

On the basis of the results acquired, the approach of annealing high T_c films in different gases was continued, to develop low temperature processing. The experiments revealed that these films melt even at lower temperatures in argon than in nitrogen. However, minimum melting temperatures were obtained in helium atmosphere. For example, YBCO (123) melted at 910°C in oxygen (Gupta, et al., 1988). Similarly melting point of BSCCO (2223) films was found to be 7900C in helium which is much lower than that observed in other gases (Gupta, et al., 1989). Therefore, helium treatment in annealing procedure was incorporated. Spin-coated YBCO films were heated in oxygen upto 910°C, exposed to helium for 10 minutes, annealed in oxygen at the same

temperature for 30 minutes and then slowly cooled to room temperature. The resultant R-T behaviour of the film is illustrated in Fig. 4.1, which depicts $T_{c,zero}$ of 76 K. Lead doped bismuth cuprate (BPSCCO) films were also prepared in same manner. However, helium treatment was performed at 800°C, in this case, followed by annealing in flowing air at 880-890°C for 30 minutes. Thick films exhibited $T_{c,zero}$ between 90K to 100K, while thin films (<1μm thickness) yield zero resistance temperature in the range of 75 to 80K. Typical results are demonstrated in Fig. 4.2 and 4.3. As is seen in inset of Fig. 4.3, the critical current density, J_c = 567 amp/cm^2 was measured by transport method and criterion of 1μV/cm in this film. The low J_c in these films may be attributed to polycrystallinity and poor connectivity among grains of the film.

4.3.2 Sputtered Films

From the semiconductor technologies, it can be easily recognized that for the deposition of thin films of a compound or dielectric material, sputtering is one of the most viable techniques. It is a production technique and is also suitable for large area deposition with high reproducibility. Therefore, we adopted this approach to prepare films of ceramic oxide superconductors.

The films were prepared in a rf magnetron sputtering system (CVC-UK) which is configured to sputter-up mode with eight inch diameter water cooled powder target and three inch diameter stainless steel hot substrate holder. The target has been specially designed by the manufacturer for sputtering the material in powder form. The schematic diagram of the assembly is shown in Fig. 4.4. This arrangement provided a fixed distance of about 12 cm between the substrate holder and the target. As indicated in the Fig.4.4, oxygen was showered directly onto the substrates during deposition through a shower mounted on the substrate holder. Substrate plate was heated by a pair of quartz lamps placed on the back of the plate and its temperature was measured by a thermocouple fitted on the holder plate. The temperature was controlled to an accuracy of ±5°C with the aid of temperature controller of the system. Two stainless steel shutters, one positioned on

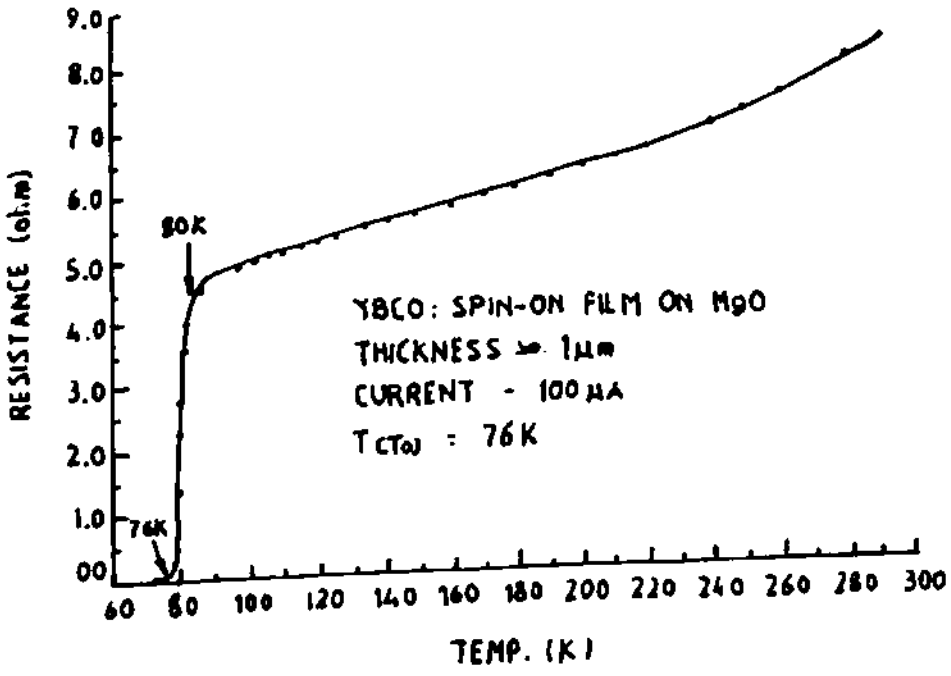

Figure 4.1: Resistance variation of YBCO spin-on film on MgO with temperature variation

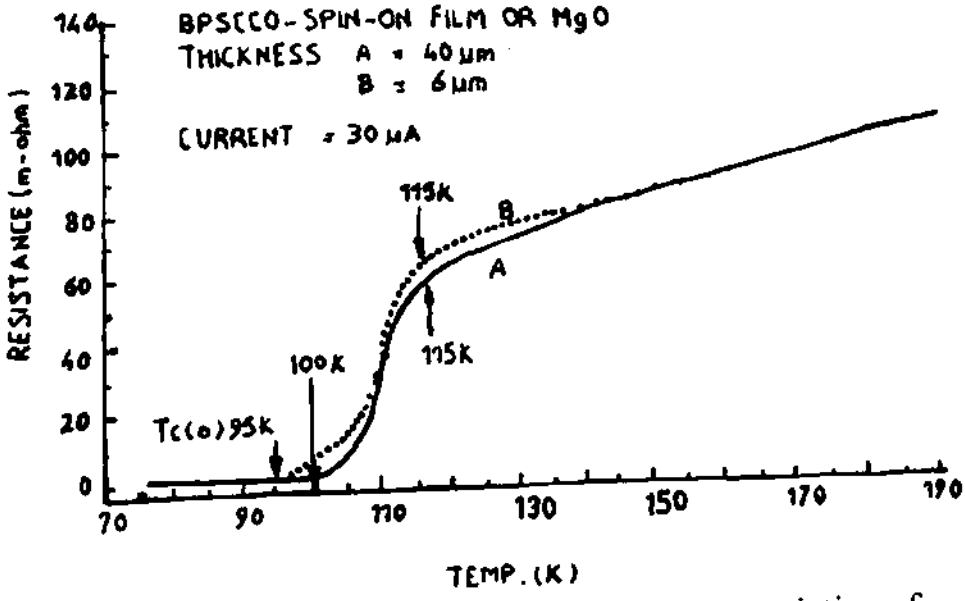

Figure 4.2: Resistance vs. temperature characteristics of BPSCCO (2223) spin-on film on MgO, film thickness (A) 40 µm (B) 6 µm

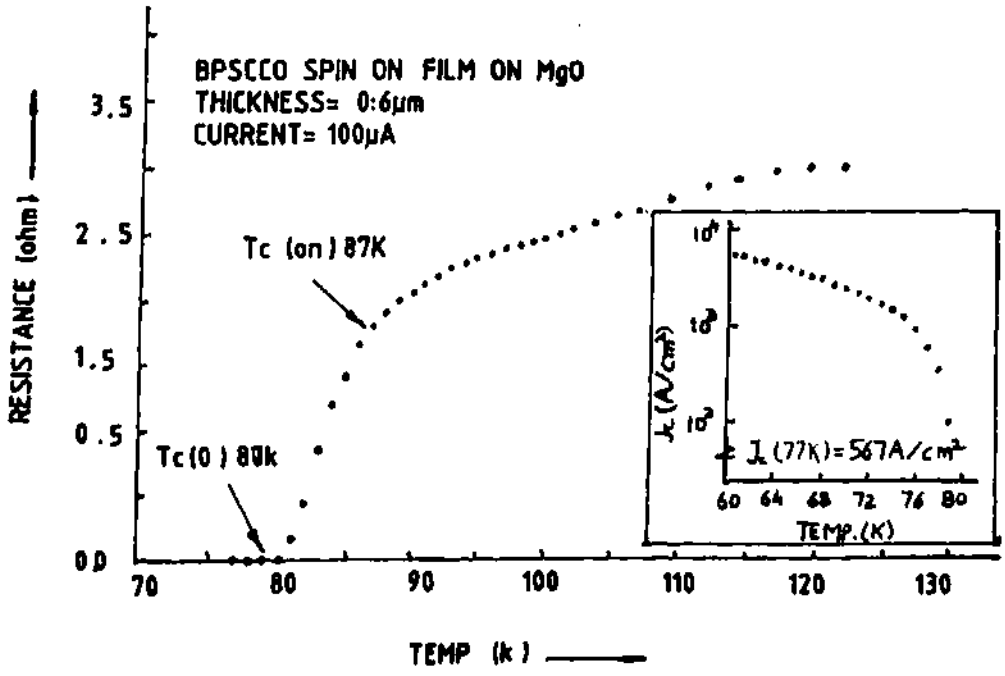

Figure 4.3: Resistance vs. temperature characteristics of BPSCCO (2223) spin-on film (0.6μm thick) on MgO. Inset shows temperature dependence of critical current density of the film

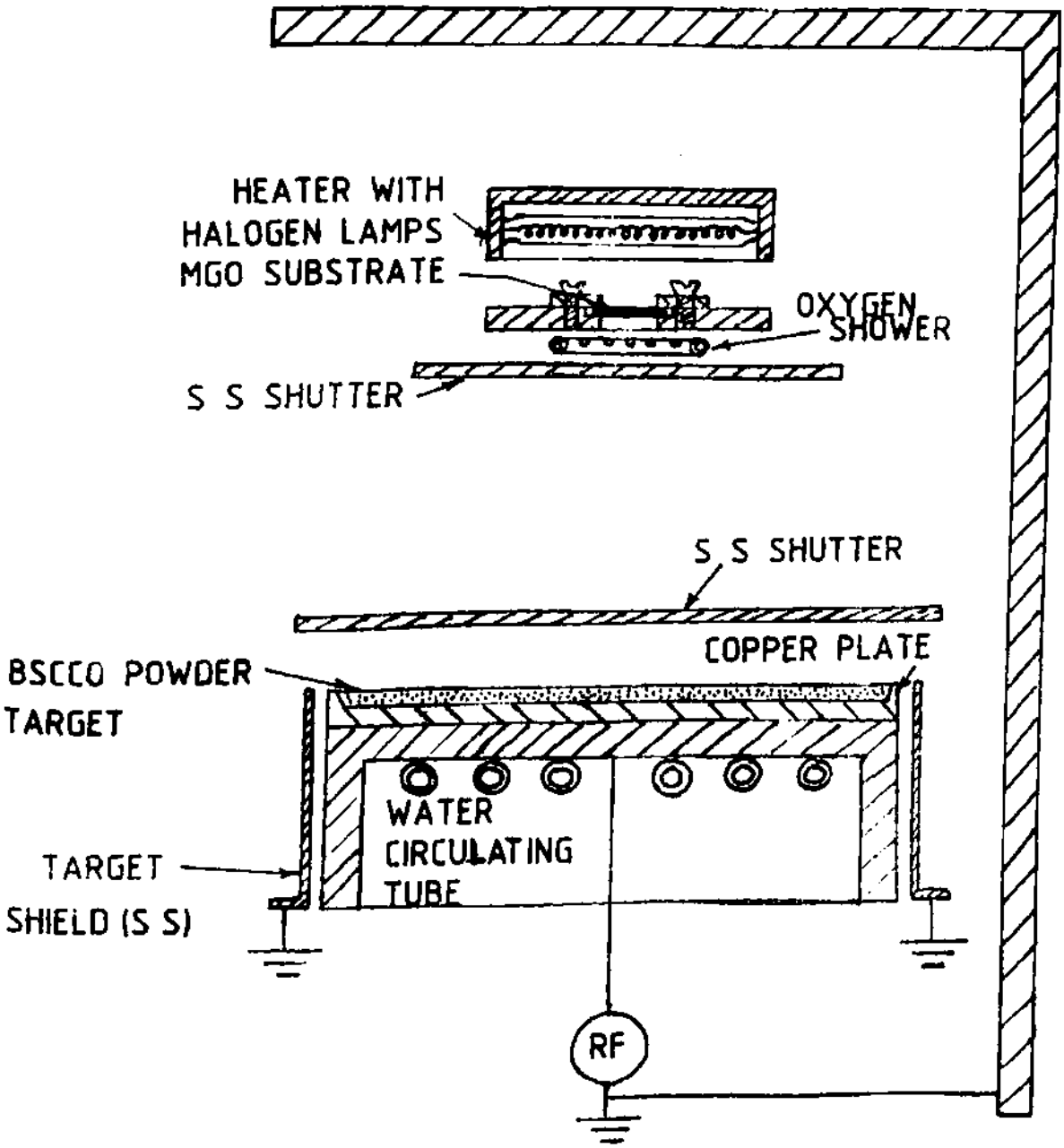

FIG 44 SCHEMATIC DIAGRAM OF THE RF MAGNETRON SPUTTERING ASSEMBLY

the target and the other covering the substrate holder, as shown in Fig. 4.4, were employed for pre-sputtering before actual deposition.

The target preparation was accomplished by mixing fine powders of Bi_2O_3 , PbO, $SrCO_3$, $CaCO_3$ and CuO for BSCCO system and Y_2O_3, $BaCO_3$ and CuO for YBCO system in an appropriate amount. The well mixed powder was heat treated at 840°C and 800°C for 10 hours and 15 hours respectively in air in case of Bi-cuprates while Yittrium cuprate was heat treated at 940°C for 18 hours in flowing oxygen. The materials thus produced were pulverized and sieved to obtain fine powders, which were uniformly spread and pressed on a copper plate to obtain the desired target for sputtering. The substrates were mounted on the holder which was covered with a clean copper foil to avoid deposition during target conditioning.

The chamber was evacuated to a vacuum level of 10^{-7} torr using cryo pump. The target conditioning was done for about 10 hours in argon and oxygen gas mixture to ensure chemical equilibrium on the target surface. The substrates cover was subsequently removed and the chamber was re-evacuated. The substrates were then heated to a desired temperature and the pre-sputtering was carried out. The pre-sputtering for about an hour was found necessary to obtain a stable cathode voltage. The shutters were then removed for the deposition of film on the hot substrates. The initial target composition and sputtering conditions for the fabrication of YBCO and BPSCCO films are illustrated in Table 4.1.

Table 4.1 Initial sputtering conditions for BSSCO and YBCO films

Target	$Bi_{1.7}Pb_{0.3}Sr_2Ca_3Cu_y$	$YBa_2Cu_3O_{7-x}$
Sputtering gas	Ar/O_2 (1:3)	Ar/O_2 (3:1)
Gas pressure	4 m Torr.	4 m Torr.
RF input power	500 Watt.	300 Watt.
Substrate temp.	600°C	650°C
Growth rate	40 Å/min.	25 Å /min.
Film thickness	1.0 μm	1.0 μm
Post-annealing	910°C/30 min/air	970°C/5min/ O_2

As-grown YBCO films were semiconducting and superconduction was achieved after annealing at 970°C for 5 min. in flowing oxygen. The films showed $T_{c,zero}$ of 65 K. As-deposited BPSCCO films were black, shiny and marginally conducting (resistance 10-15 M-ohm for a typical 1μm thick films at room temperature). These films turned superconducting after annealing in air at 910°C with $T_{c,zero}$ in the range of 70K-77K. Resistance dependence on temperature of a typical 65K YBCO film and 77K BPSCCO film is depicted in Fig.4.5. Surface morphology of the BPSCCO film before and after annealing is shown in Fig.4.6. As is seen in the SEM image of Fig.4.6 (a), the surface of as-deposited film appears smooth and featureless. However, after annealing at 910°C, the surface turns rough and porous. Formation of long needles or rod like structures is apparent in Fig.4.6 (b). The needles are about 20μm in length and 2 to 3 μm in diameter. These do not show any orientation with relation to substrate plate. The composition analysis of this sample was carried out by means of EDAX. The results are listed in Table 4.2. It is interesting to note that although Pb is present in the as-deposited film, it is not detected in superconducting needles of the film. This suggests either complete or partial loss of Pb by evaporation, below detection limit of EDAX, during post annealing process. Further it is important to compare elemental contents of needles and that of pores or opening between them. From this characterization, it can be inferred that the phase responsible for 77K is contained within the needles only. These results evince that further optimization of process parameters and target composition is required to obtain uniform composition of high T_c phase (2223) in the BSCCO films.

Table 4.2 Elemental composition of BSCCO film

	Atomic percentage				
	Bi	Pb	Sr	Ca	Cu
As deposited film	6.18	3.88	21.64	18.46	49.84
Needles	9.41	---	21.41	9.74	59.44
Pores	0.64	---	20.29	13.17	65.90

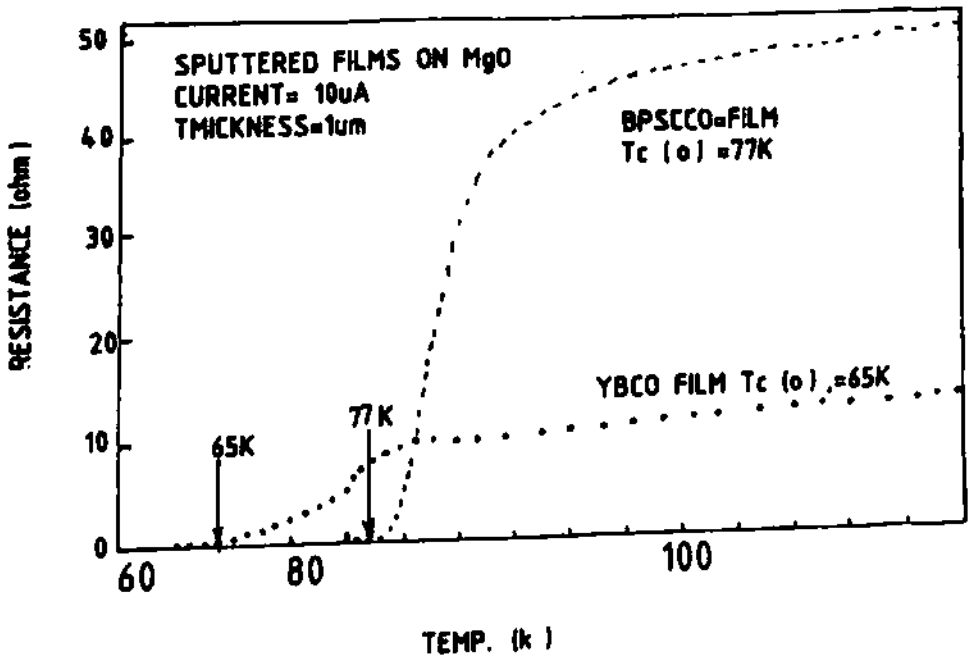

Figure 4.5: Resistance dependence on temperature of a typical 65K YBCO and 77K BPSCCO post annealed films (deposition done by sputtering)

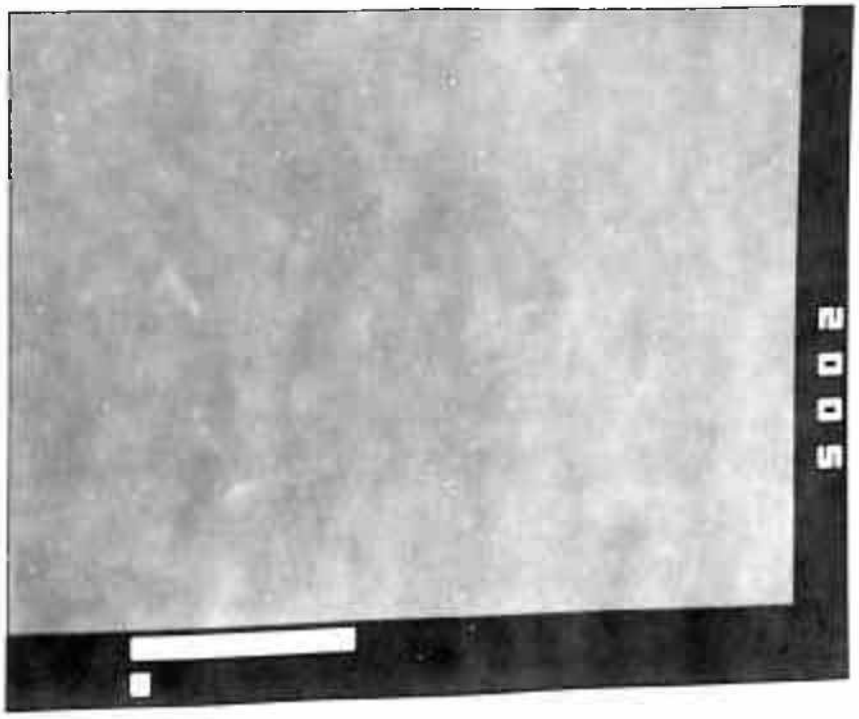

Figure 4.6(a): SEM picture of an as-deposited film (the bar measures 1μm)

Figure 4.6(b): SEM micrograph of an annealed film (the bar measures 10μm)

4.3.3 Preparation of insitu Superconducting Films

(A) BSCCO Films: Films were prepared by r.f. magnetron sputerring technique as described in previous sub-section using CVC-U.K. system. In order to optimize the target composition, the targets of varying elemental composition were used. For each target composition, about ten processes were employed to prepare films. The elemental contents of various targets and the films, thus produced were determined by EDAX. The data listed in Table 4.3 clearly indicates that the target F produced the films with elemental ratio of (Bi,Pb):Sr:Ca:Cu = 1.77:2.3:2.1:2.83, which is nearly equal to BSCCO high T_c phase (2:2:2:3).

Using this target, we concentrated on the optimization of the process parameters. Hence, after a number of deposition runs, we devised a tecnique to realize insitu superconducting BSCCO film with high-T phase (Agarwal et al., 1993). A conventional low-pressure on-axis sputter deposition as discussed in previous section, was followed by high-pressure oxygen plasma treatment (OPT) to prepare the films. For OPT, after depositing films as per deposition parameters in Table 4.4, the RF power was reduced to about 50W and the argon supply was switched off to produce pure oxygen plasma in the chamber. Oxygen supply was adjusted to manitain the chamber pressure at about 80mTorr. Under these conditions of oxygen plasma, the samples were quickly heated to a maximum temperature (830±5°C) for 5 min. The heaters were then switched off and the oxygen plasma treatment was continued until the substrate temperature dropped below 100°C.

Table 4.3 Elemental ratio of various BSCCO targets and corresponding films (averages of the data taken from ten sputtering processes for each target)

Process	Target Composition					Average film Composition				
	Bi	Pb	Sr	Ca	Cu	Bi	Pb	Sr	Ca	Cu
A	1.84	0.34	1.91	2.03	3.06	1.23	0.09	2.38	1.86	3.45
B	1.49	0.69	1.28	2.43	3.59	0.83	0.15	1.64	2.296	4.08
C	1.60	1.95	1.82	2.40	3.30	0.50	0.0	1.895	2.38	4.22
D	1.95	1.50	1.82	2.22	3.20	1.18	0.06	2.17	2.13	3.44
*E	2.40	0.71	1.82	2.20	3.20	1.39	0.06	1.95	1.98	3.61
F	2.40	0.96	1.82	2.10	3.50	1.66	0.11	2.30	2.10	2.83

Table 4.4 Sputter Deposition Parameters for insitu BSCCO films.

Target	$Bi_{2.4}Pb_{0.96}Sr_{1.82}Ca_{2.1}Cu_{3.5}O_x$
Substrate	MgO
Substrate temperature	755°C
Gases(Ar+O)	28m Torr with 1% O
Target to substrate separation	12cm
Deposition rate	12.5 Å/min
Sputtering time	4 hrs
Effective RF power	400 W

As-deposited BSCCO films produced after OPT were shiny, black and featureless with room temperature resistence in the range of 15 to 50Ω. The zero-resistence temperature of the films varied from 20 to 33K. Figure 4.7 is a typical R-T plot of one of the films, showing T_c = 33K and T_c about 100K. The onset of transition in the vicinity of 100K indicates the pressure of a high-T_c phase in the film. The fact is further supported by the XRD data of the film, in Figure 4.8, which distinctly shows the peaks corresponding to the 2223 phase. 2θ values of various peaks in Fig. 4.8 and the phases/compounds indicated by them are listed in Table 4.5.

Table 4.5 X-ray diffraction pattern (CuKα) of the 33K in-situ superconducting film.

Seq.	2θ	Phase(s) indicated; (plane)
1.	4.941	2223; (002)
2.	10.858	unidentified
3.	14.382	2201;
4.	19.298	2223; (008)
5.	21.505	2201;
6.	24.115	2223; (0010) & 2212; (008)
7.	29.014	2223; (0012) & 2212; (0010)
8.	34.008	2223; (0014)
9.	37.628	unidentified
10.	38.283	CuO
11.	43.113	MgO; (100)
12.	49.221	2223; (0020)
13.	59.968	2223; (0022)
14.	64.645	unidentified
15.	67.836	unidentified

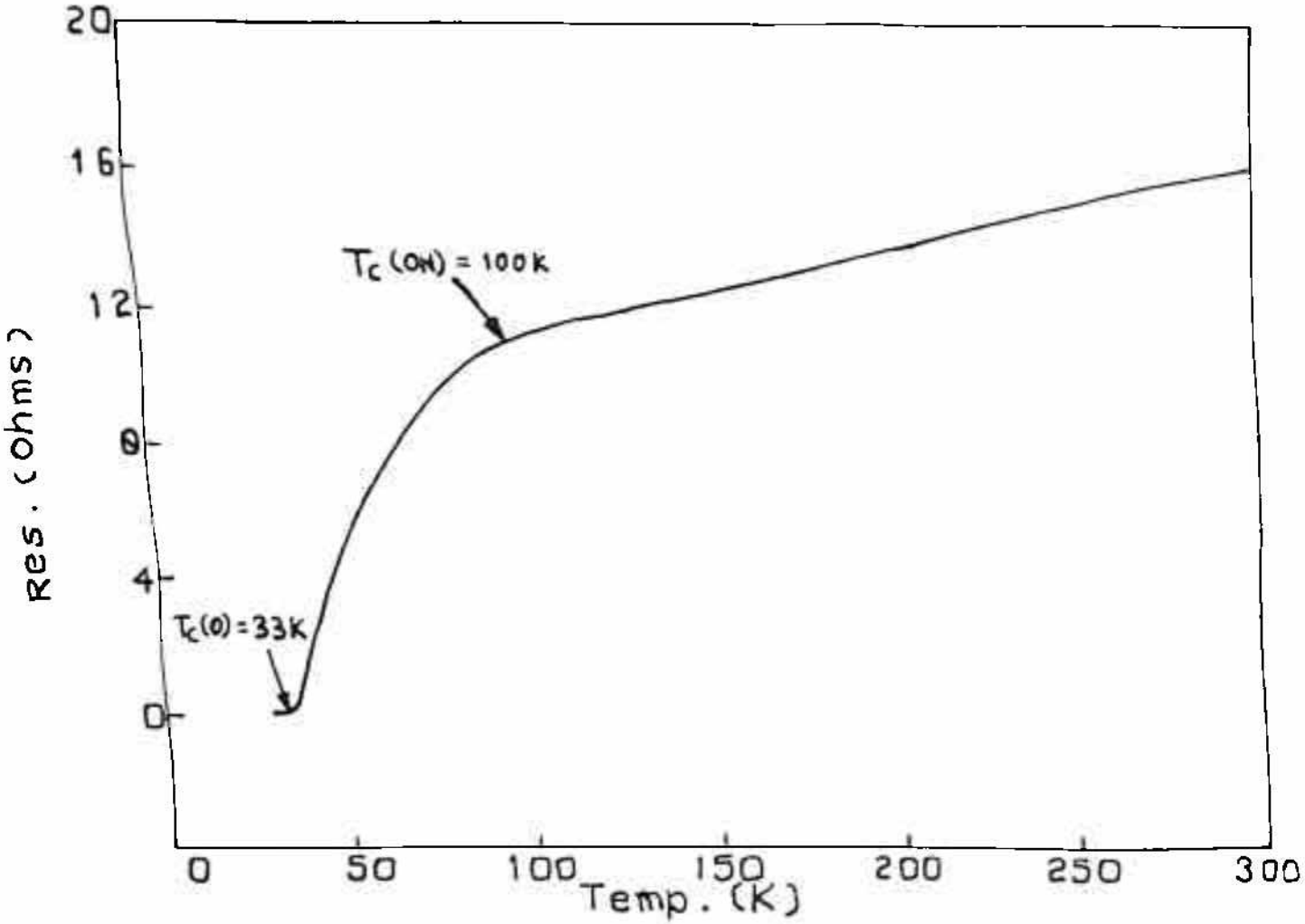

Figure 4.7: Resistance vs. temperature plot of an as-deposited BSCCO film

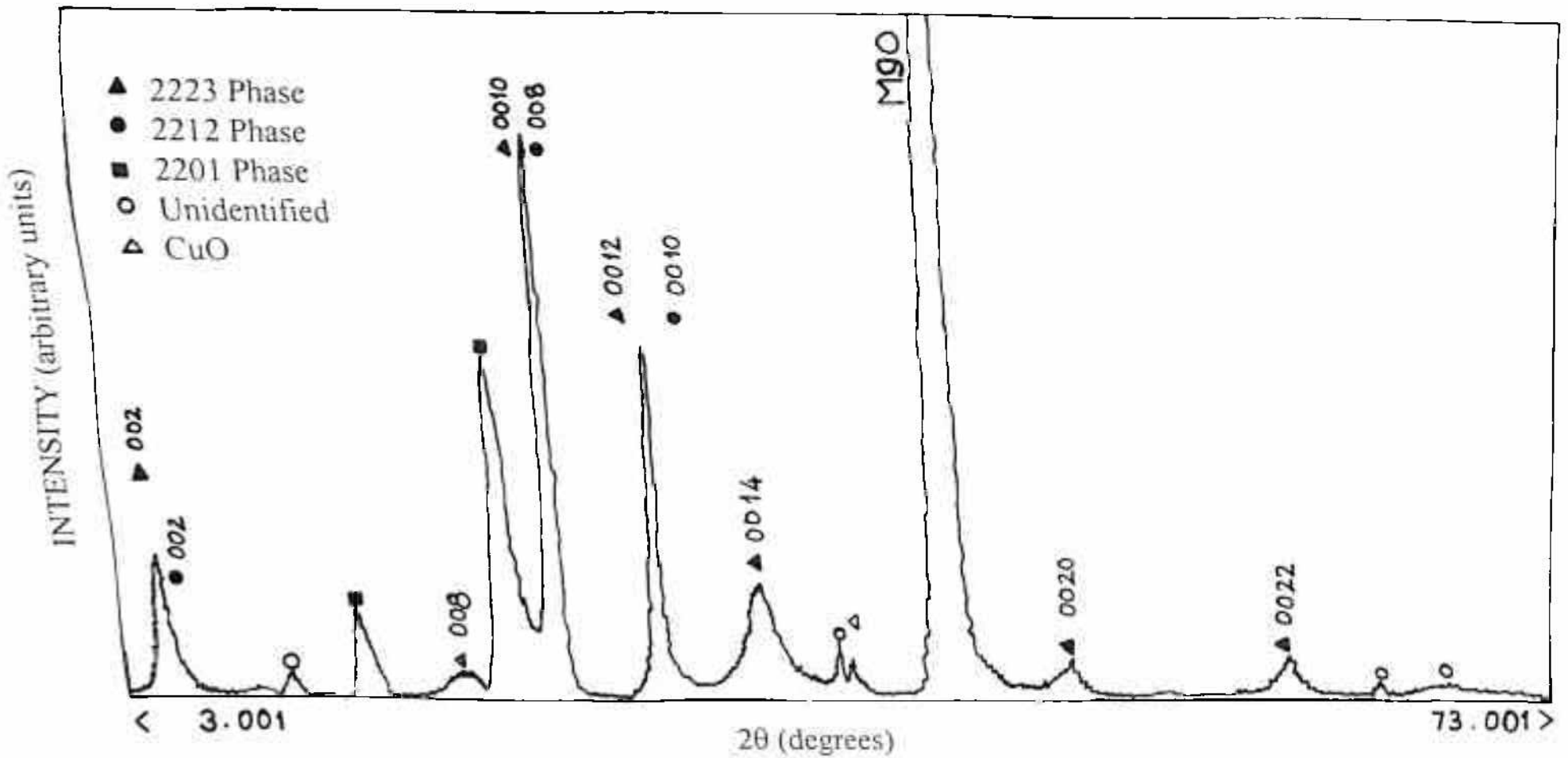

Figure 4.8: X-ray diffraction data of the 33K zero resistance film

After annealing at about 900°C in air, these films also showed zero-resistence critical temperature above liquid nitrogen temperature. This suggests that a sufficient amount of oxygen was still not incorporated into the films by OPT. Further optimization of the oxygen plasma parameters is likely to yield insitu superconducting films with a pure high-T_c phase and higher transition temperature. However, we did not succeed in it and terminated out efforts on BSSCO system to start work on YBCO films for device applications.

(B) YBCO Films: YBCO films deposition was initiated in the same system with various argon-oxygen gas mixtures. The total sputtering gas pressure was varied from few milli-torrs to few tens of milli-torrs and the substrates used were *MgO*, $SrTiO_3$ and sapphire. The separation between the target and the substrates was also changed from about 6 inch to 1 inch, but insitu superconduction could not be achieved in the films in on-axis configuration. Hence, the substrate-holder assembly along with heater was modified for off-axis sputtering, as shown in Figure 4.9. Using off-axis sputtering configuration, insitu superconducting YBCO films were produced with $T_{c,zero}$ above the boiling of liquid nitrogen (77K).

The surface topography of As-grown YBCO films, on MgO and $SrTiO_3$ single-crystal (100) substrates, have been investigated by scanning tunnelling microscopy (STM) which was operated in air at ambient temperature. Deposition temperature and some characteristics of the films, used for STM study, are listed in Table 4.6. STM images of YBCO films deposited on STO (sample1) and MgO (sample2) substrates are depicted in Fig.4.10(a) & (b) respectively. The bright regions correspond to higher surface areas while the dark portions correspond to lower surface areas. These pictures also clearly indicate that the surface is granular and the type of substrate influences the grain orientations. Figure 4.10 (a) shows compact columnar grains, varying from 380 to 600 nm in length and from 200 to 250 nm in width. Some dark spots are also visible in the image which may be holes. In Figure 4.10 (b), the grain size varies from 150 to 250 nm in length and 75 to 170 nm in width. The variation in grain size may be attributed to

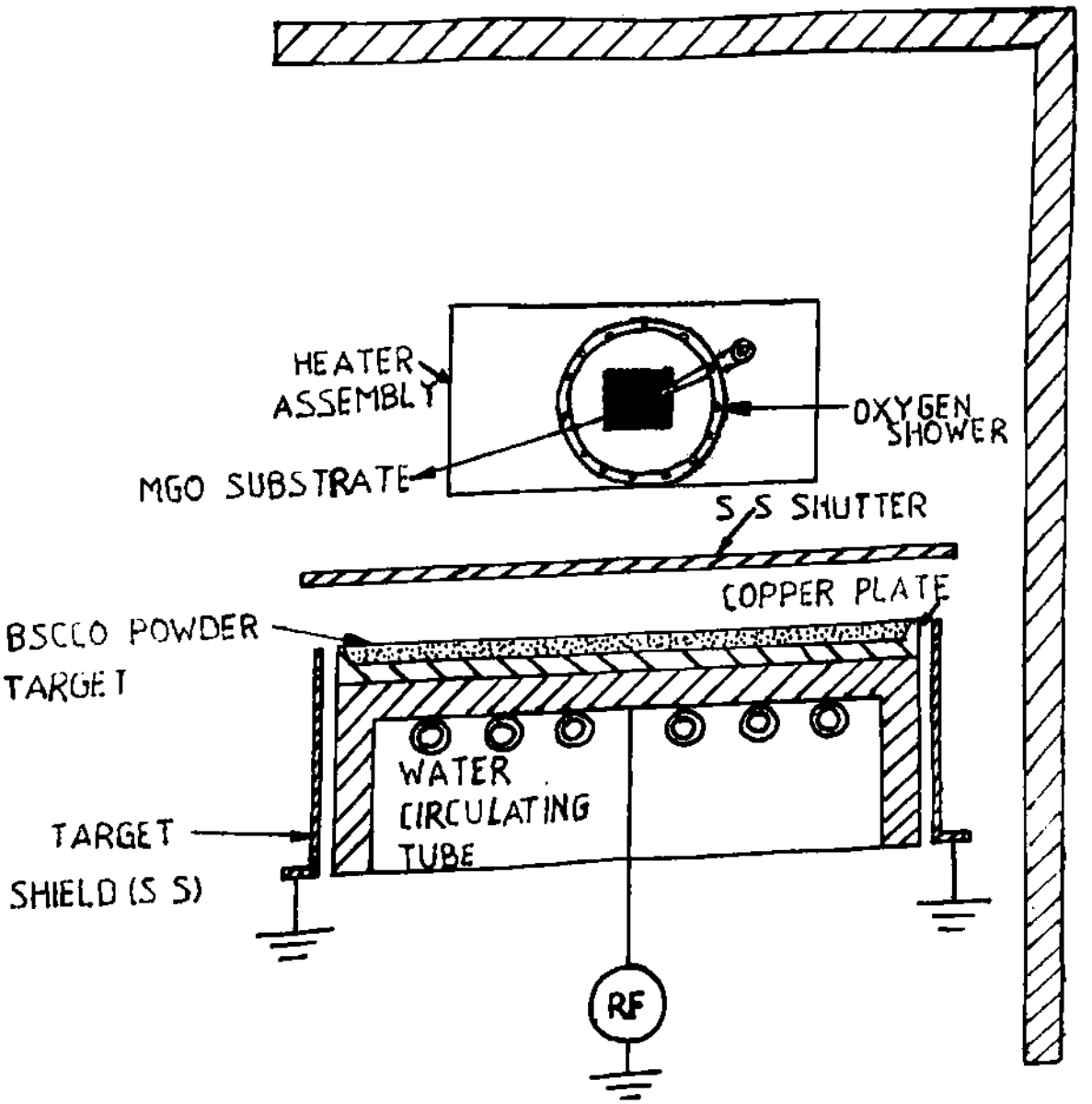

Figure 4.9: Modified substrate-holder assembly along with heater for off-axis sputtering

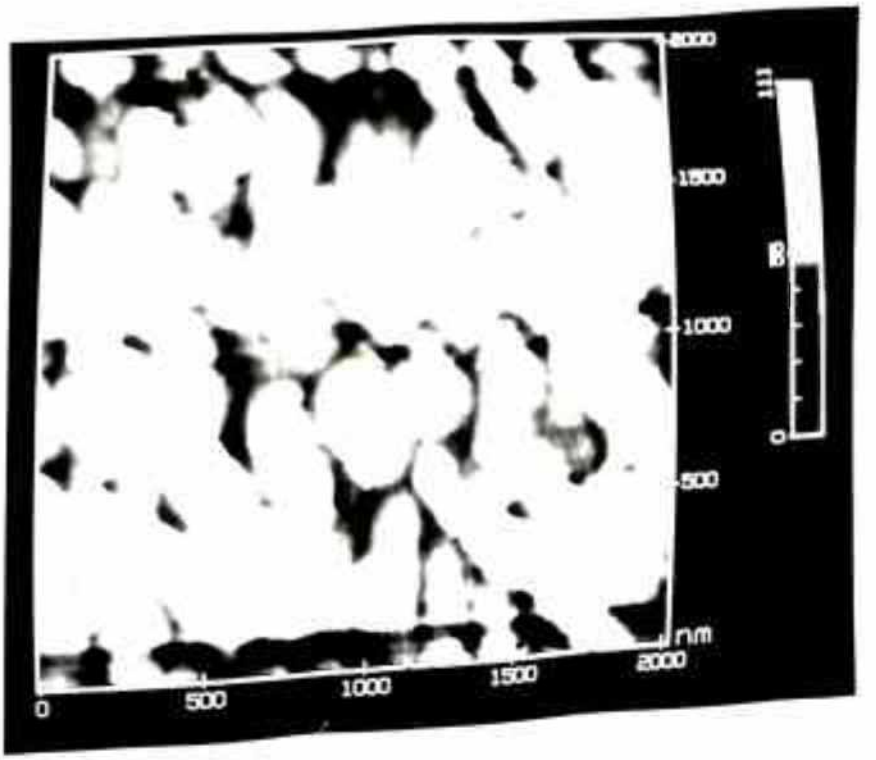

Figure 4.10(a): A 2000nm×2000 nm STM image of a YBCO thin film deposited on STO substrate (sample 1)

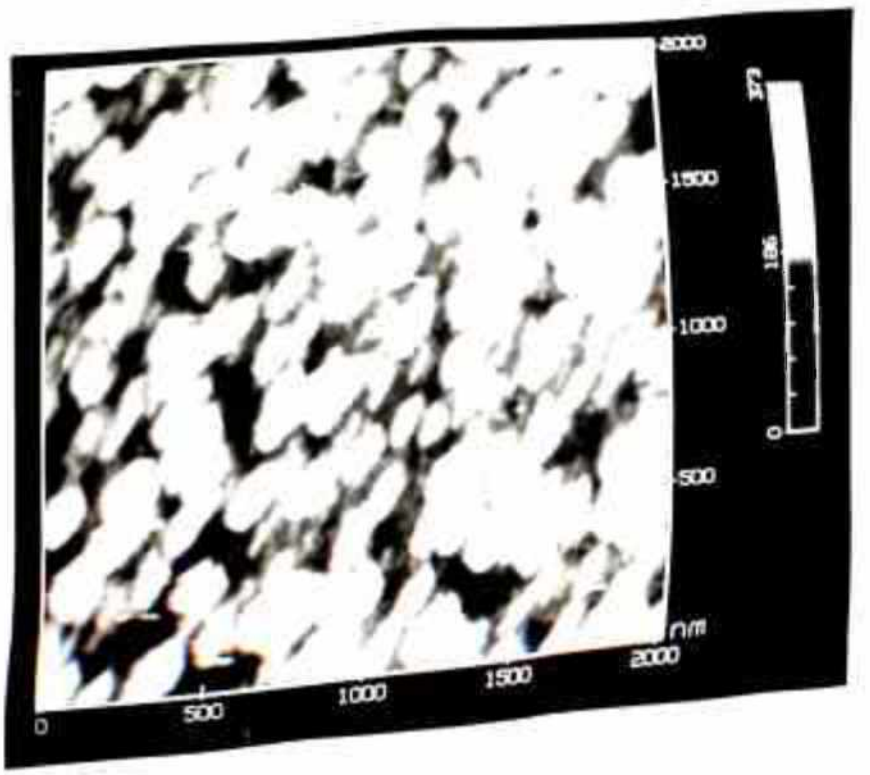

Figure 4.10(b): A 2000nm×2000 nm STM image of a YBCO thin film deposited on MgO substrate (sample 2)

the difference in lattice constants of STO/MgO and YBCO. The good matching of the lattice constants of YBCO with STO is responsible for the larger grain than that in case of MgO, which has poor matching.

Table 4.6 Deposition conditions and characteristics of the selected films

Sample	Substrate	Deposition Temp. (°C)	Thickness (Å)	RMS Roughness (Å)[a]	$T_{c,zero}$ (K)
1	STO	830	2000	36	82
2	MgO	830	2000	45	78

a Standard deviation

Small-area STM scans obtained on the flat surfaces of individual grains revealed the spiral growth pattern of each grain. Figure 4.11(a) & (b) depicts highly repetitive and stable real time (unfiltered) images of spirals on YBCO grains deposited on STO and MgO substrates (sample 1 and 2) respectively. The above images of the spiral structure are pyramidal type with the central point being at the highest point. The steps of about 1.12 nm in height separating atomically flat plateaus are also evident. These plateaus or terraces havea width of about 10-15 nm and flatness within ~ 0.2 to 0.5 nm. An atomic image in an area of 4×4 nm, along one of the terraces, is shown in Fig. 4.12, which depicts square lattice of 0.38 nm in length.

These results suggest that by further optimization of the process parameters, specially deposition temperature, the very high quality (nearly epitaxial) YBCO films can be produced by off-axis RF magnetron sputtering. However, these films with $T_{c,zero}$ in the vicinity of 80K also proved to be useful for the device application.

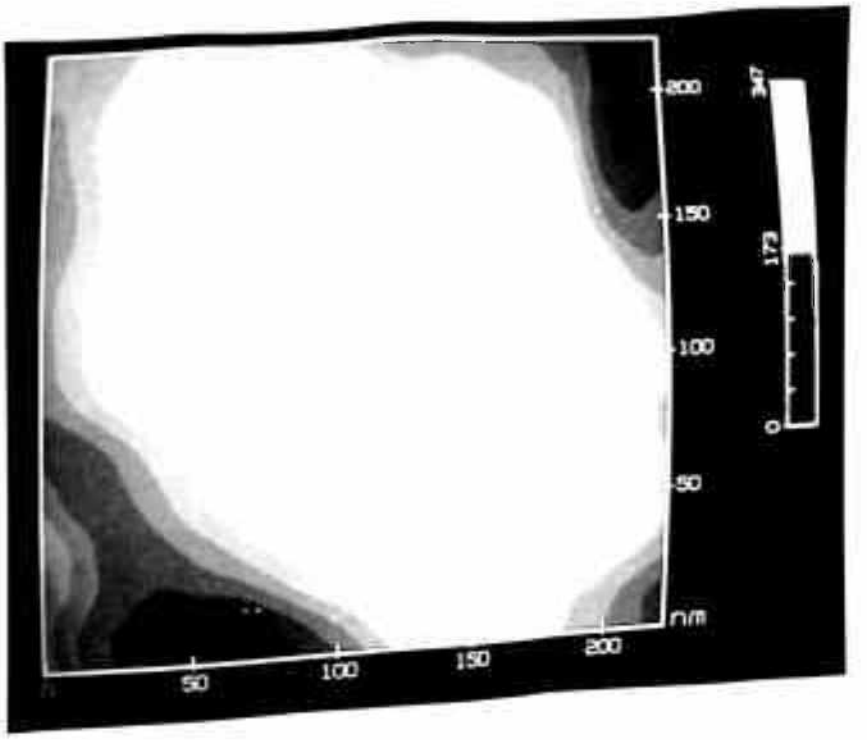

Figure 4.11(a): An STM image of a single grain of a YBCO film grown on STO (sample 1). The image size is 220 nm×220nm. The grey scale is about 15 nm from black to white

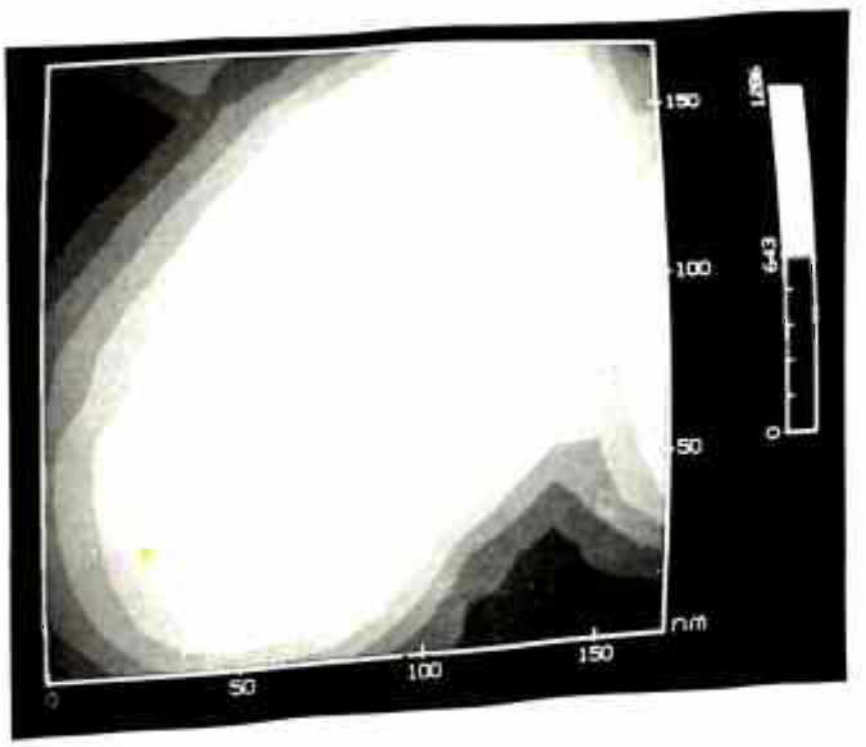

Figure 4.11(b): An STM image of a single grain of a YBCO film grown on MgO (sample 2). The image size is 170 nm×170nm. The grey scale is about 15 nm from black to white

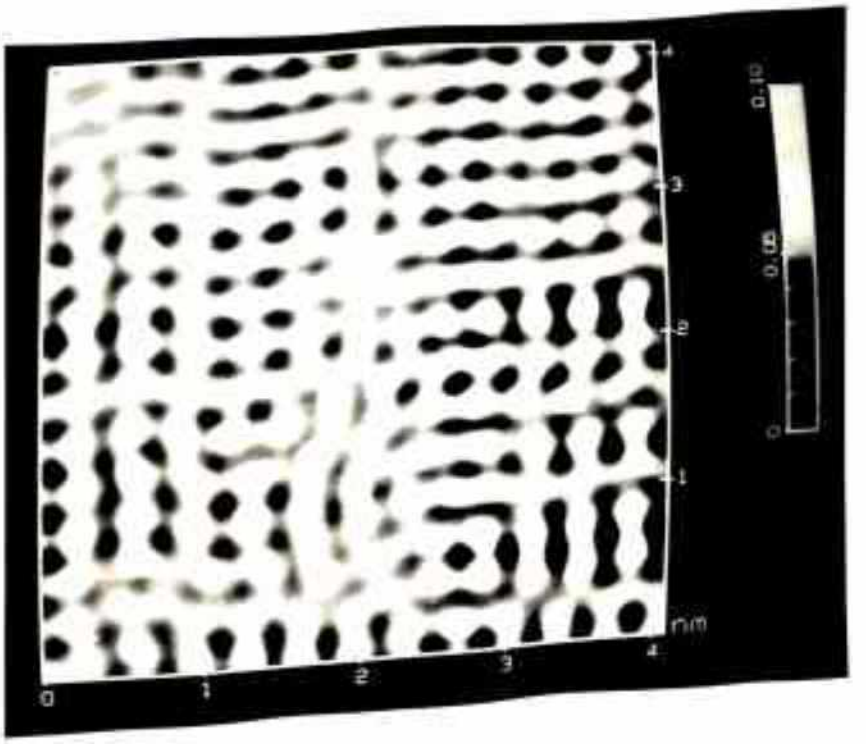

Figure 4.12: The square lattice of lattice constant 0.38nm = |a| = |b| seen on YBCO. The image measures 4nm on a side

CHAPTER-FIVE

OHMIC CONTACTS ON HIGH T_c FILMS

To realise the high temperature superconducting devices, the development of stable metal contacts to superconductors is essential. A thermodynamic criterion for the reliability of contact metals on high temperature superconductors (HTSC) is discussed in the first section of this chapter. The second section deals with the study of metal-superconductor interface using x-ray photo emission spectroscopy. And in the last section, we report contact resistance measurements carried out on silver contacts on YBCO films.

5.1 RELIABILITY OF HTSC METAL CONTACTS - A THERMODYNAMIC CRITERION

A thermodynamic criterion has been applied, in this section, to determine the reliability of contact metals such as silver, aluminium, gold, chromium and titanium on BSCCO and YBCO compounds (Agarwal, et al., 1994). The chemical stability is presumed for positive heat of reactions, i.e. $\Delta H_{reaction} > 0$, when a metal reacts with all the possible oxides present in the superconducting materials. Based on these calculations, metals for reliable contacts to BSCCO and YBCO superconductors are proposed.

5.1.1 Introduction

As in the case of semiconductors, some of the generic requirements for stable metal contacts are: low contact resistance, good adhesion, reasonable matching of thermal expansion coefficient and high electrical conductivity. In addition to these, the study of

Lau, et al. (1985) suggests that the chemical stability between two materials in contact is also very important for reliable operation of a device. Following this work, a thermally stable metallization procedure for making ohmic contacts to GaAs has been developed (Gupta, et al., 1990). This approach has been applied to determine the stability of metals on superconductors. Calculations based on chemical reactions between metals and HTSC materials are reported to determine chemical stability of a superconductor metal couple. Phase diagrams from various references (Brick, 1954; Smithells, 1955; McQuillan and McQuillan, 1956) are used to determine the possible metallic compounds and other phases that are likely to form when a metal is in contact with a HTSC compound/material. The relevant data on heats of formation of oxides and metal alloys are taken from Smithells (1955) to calculate heats of reaction between HTSC materials and some of the commonly used metals such as Ag, Al, Au, Cr, and Ti. Miedema's model (Miedema, 1976) is used to estimate the heat of formation, where experimental data was not available. Some of the possible alloys that are likely to form in the reactions considered here and for which data could be obtained are listed in Table 5.1. As it is known that the high T_c compounds are mainly oxides of cations, arranged in layers, the possibility of the ternary and higher order oxide phases is negligible.

Table 5.1: Metal or alloys which are considered as one of the reaction products for calculations of heat of reactions.

M / X_aO_b	Ag	Al	Cr	Ti
Bi_2O_3	Bi	Bi	Bi	Bi
CaO	AgCa	Al_3Ca	Ca	Ca
CaO_2				
SrO	AgSr	Sr	Sr	Sr
SrO_2				
PbO				
Pb_3O_4	Pb	Pb	Pb	PbTi
PbO_2				
Cu_2O	Cu	$AlCu_3$, $AlCu_2$, AlCu & Al_2Cu	Cu	CuTi
CuO				
Y_2O_3	AgY	Y	Y	Y
BaO	AgBa	Ba	Ba	Ba
BaO_2				

The compounds with positive heats of formation are not formed in actual practice (Lau, et al., 1985), hence such compounds are not considered for the reactions involved here. All possible oxides of the metals (e.g., in the case of a titanium contact its oxides are TiO, Ti_2O_3, Ti_3O_5, and TiO_2) are considered to investigate chemical reactions.

Model calculations for some of the superconductor metal couples are presented to illustrate the method of calculation used to deduce the heats of reaction. The reactions of silver with the oxides of lead-doped bismuth cuprate superconductor are :

$$Bi_2O_3 + 6Ag = 3Ag_2O + Bi \quad \ldots\ldots \quad (5.3)$$
(-138 kcal/mol) 6(0) 3(-7.3 kcal/mol) 2(0)
ΔH_{298} = +116.1 kcal

$$CaO + 3Ag = AgCa + Ag_2O \quad \ldots\ldots \quad (5.4)$$
(-151.9 kcal/mol) 3(0) (-21.0 kcal/mol) (-7.3 kcal/mol)
ΔH_{298} = +123.6 kcal

$$CaO_2 + 5Ag = AgCa + 2Ag_2O \quad \ldots\ldots \quad (5.5)$$
(-156.7 kcal/mol) 5(0) (-21.0 kcal/mol) 2(-7.3 kcal/mol)
ΔH_{298} = +121.1 kcal

$$SrO + 3Ag = AgSr + Ag_2O \quad \ldots\ldots \quad (5.6)$$
(-141.0 kcal/mol) 3(0) (-19.56 kcal/mol) (-7.3 kcal/mol)
ΔH_{298} = +121.1 kcal

$$SrO_2 + 5Ag = AgSr + 2Ag_2O \quad \ldots\ldots \quad (5.7)$$
(-153.0 kcal/mol) 5(0) (-19.56 kcal/mol) 2(-7.3 kcal/mol)
ΔH_{298} = + 118.83 kcal

$$PbO + 2Ag = Ag_2O + Pb \quad \ldots\ldots \quad (5.8)$$
(-52.0 kcal/mol) 2(0) (-7.3 kcal/mol) (0)
ΔH_{298} = +44.7 kcal

$$Pb_3O_4 + 8Ag = 4Ag_2O + 3Pb \quad \ldots\ldots \quad (5.9)$$
(-175 kcal/mol) 8(0) 4(-7.3 kcal/mol) 3(0)
ΔH_{298} = +145.8 kcal

$$PbO_2 + 4Ag = 2Ag_2O + Pb \quad \ldots\ldots \quad (5.10)$$
(-65 kcal/mol) 4(0) 2(-7.3 kcal/mol) (0)
ΔH_{298} = +50.4 kcal

$$Cu_2O + 2Ag = Ag_2O + 2Cu \quad \ldots\ldots \quad (5.11)$$
(-40 kcal mol) 2(0) (-7.3 kcal/mol) 2(0)

$$\Delta H_{298} = +32.7 \text{ kcal}$$

$$CuO + 2Ag = Ag_2O + 2Cu \quad \ldots\ldots \quad (5.12)$$
(-38 kcal mol) 2(0) (-7.3 kcal/mol) 2(0)

$$\Delta H_{298} = +30.7 \text{ kcal}$$

All the reactions of aluminium with this system are :

$$Bi_2O_3 + 2Al = Al_2O_3 + 2Bi \quad \ldots\ldots \quad (5.13)$$
(-138 kcal/mol) 2(0) (-7.3 kcal/mol) 2(0)

$$\Delta H_{298} = -262.0 \text{ kcal}$$

$$CaO + 11/3Al = Al_3Ca + 1/3Al\,O \quad \ldots (5.14)$$
(-151.9 kcal/mol) 11/3(0) = (-56.4 kcal/mol) 1/3(-400 kcal/mol)

$$\Delta H_{298} = -37.4 \text{ kcal}$$

$$CaO + 13/3Al = Al_3Ca + 2/3Al_2O_3 \quad \ldots (5.15)$$
(-156.9 kcal/mol) 13/3(0) = (-56.4 kcal/mol) 2/3(-400 kcal/mol)

$$\Delta H_{298} = -165.9 \text{ kcal}$$

$$SrO + 2/3Al = 1/3Al_2O_3 + Sr \quad \ldots\ldots \quad (5.16)$$
(-141.1 kcal/mol) 2/3(0) 1/3(-400 kcal/mol) (0)

$$\Delta H_{298} = +7.6 \text{ kcal}$$

$$SrO_2 + 4/3Al = 2/3Al_2O_3 + Sr \quad \ldots\ldots \quad (5.17)$$
(153 kcal/mol) 4/3(0) 2/3(-400 kcal/mol) (0)

$$\Delta H_{298} = -113.6 \text{ kcal}$$

$$PbO + 2/3Al = 1/3\,Al_2O_3 + Pb \quad \ldots\ldots \quad (5.18)$$
(-52 kcal/mol) 2/3(0) 1/3(-400 kcal/mol) (0)

$$\Delta H_{298} = -81.3 \text{ kcal}$$

$$Pb_3O_4 + 8/3Al = 4/3\,Al_2O_3 + 3Pb \quad \ldots\ldots \quad (5.19)$$
(-175 kcal/mol) 8/3(0) 4/3(-400 kcal/mol) 3(0)

$$\Delta H_{298} = -358.3 \text{ kcal}$$

$$PbO_2 + 4/3Al = 2/3\,Al_2O_3 + Pb \quad \ldots\ldots \quad (5.20)$$
(-65.9 kcal/mol) 4/3(0) 2/3(-400 kcal/mol) (0)

$$\Delta H_{298} = -201.6 \text{ kcal}$$

$$Cu_2O + 4/3Al = 2/3AlCu_3 + 1/3\ Al_2O_3 \ldots (5\ 21)$$
(-40 kcal mol) 4/3(0) 2/3(-16.4 kcal/mol) 1/3(-400 kcal/mol)
ΔH_{298} = -106.9 kcal

$$Cu_2O + 5/3Al = AlCu_2 + 1/3\ Al_2O_3 \ldots (5\ 22)$$
(-40 kcal mol) 5/3(0) (-16.05 kcal/mol) 1/3(-400 kcal/mol)
ΔH_{298} = -112.3 kcal

$$Cu_2O + 8/3Al = 2AlCu + 1/3\ Al_2O_3 \ldots (5\ 23)$$
(-40 kcal mol) 8/3(0) 2(-9.5 kcal/mol) 1/3(-400 kcal/mol)
ΔH_{298} = -112.5 kcal

$$Cu_2O + 14/3Al = 2Al_2Cu + 1/3\ Al_2O_3 \ldots (5\ 24)$$
(-40 kcal mol) 14/3(0) 2(-9.6 kcal/mol) 1/3(-400 kcal/mol)
ΔH_{298} = -112.5 kcal

$$CuO + 14/3Al = 1/3AlCu_3 + 1/3\ Al_2O_3 \ (5\ 25)$$
(-38.9 kcal/mol) 14/3(0) 1/3(-16.4 kcal/mol) 1/3(-400 kcal/mol)
ΔH_{298} = -100.8 kcal

$$CuO + 7/6Al = 1/2AlCu_2 + 1/3\ Al_2O_3 \ldots (5\ 26)$$
(-38 kcal/mol) 7/6(0) 1/2(-16 kcal/mol) 1/3(-400 kcal/mol)
ΔH_{298} = -103.4 kcal

$$CuO + 5/3Al = AlCu + 1/3\ Al_2O_3 \ldots (5\ 27)$$
(-38 kcal/mol) 5/3(0) (-9.5 kcal/mol) 1/3(-400 kcal/mol)
ΔH_{298} = -104.8 kcal

$$CuO + 8/3Al = Al_2Cu + 1/3\ Al_2O_3 \ldots (5\ 28)$$
(-38 kcal/mol) 8/3(0) (-9.6 kcal/mol) 1/3(-400 kcal/mol)
ΔH_{298} = -104.9 kcal

Similarly calculated values of heat of reaction for the reactions between metals like chromium or titanium with the oxides of Bi, Ca, Sr, Pb, or Cu are listed in Table 5.2.

Table 5.2: Heat of reaction (kcal) when one of oxide (X_aO_b) reacts with metal (M) to give oxide (M_eO_f) and alloy (X_cM_d) or metal (X).

	M	Ag	Al	Cr	Ti			
(X)	M_eO_f+* X_aO_b	Ag_2O+*	Al_2O_3+*	Cr_2O_3+*	TiO+*	Ti_2O_3+*	Ti_3O_5+*	TiO_2+*
Bi	Bi_2O_3	+116.1	-262.0	-131.0	-286.2	-277.4	-266.6	-252.8
Ca	CaO	+123.6	-37.4	+62.2	+28.0	+30.9	+34.5	+39.15
	CaO_2	+121.1	-165.9	-22.6	-91.1	-85.2	-78.1	-68.8
Sr	SrO	+114.1	+7.6	+51.3	+17.1	+20.1	+23.6	+28.25
	SrO_2	+118.8	-113.6	-26.3	-94.8	-88.9	-81.7	-72.5
Pb	PbO	+44.7	-81.3	-37.6	-92.9	-89.97	+86.5	-81.7
	Pb_3O_4	+145.8	-358.3	-183.6	-383.6	-670.5	-357.4	-339.0
	PbO_2	+50.4	-201.6	-114.3	-203.8	-197.0	-190.7	-282.5
Cu	Cu_2O	+32.7	**	-49.6	-109.6	-106.7	-103.1	-98.6
	CuO	+30.7		-51.6	-98.8	-95.8	-92.3	-87.6
Y	Y_2O_3	+380.3	+50.1	+181.0	+78.3	+87.1	+97.8	+111.7
Ba	BaO	+105.1	-0.3	+43.3	+9.1	+12.0	+15.6	+20.2
	BaO_2	+117.5	-114.4	-27.1	-95.6	-89.7	-82.5	-73.3

Note: * *represents coresponding metal or metallic alloy listed in Table 5.1*
** *data in Table 5.3.*

Table 5.3: Heat of reaction (kcal) for reactiopns between oxides of copper and aluminium metal

X_cM_d / X_aO_b	$AlCu_3$	$AlCu_2$	AlCu	Al_2Cu
Cu_2O	-106.9	-109.4	-112.3	-112.5
CuO	-100.8	-103.4	-104.8	-104.9

The reactions between Ag or Al and oxides of YBCO superconductors are given as

$$Y_2O_3 + 8Ag = 3Ag_2O + 2AgY \quad \ldots \quad (5\ 29)$$
(-450 kcal/mol) 8(0) 3(-7.3 kcal/mol) 2(-23.87 kcal/mol)
$$\Delta H_{298} = +380.36 \text{ kcal}$$

$$BaO + 3Ag = Ag_2O + AgBa \quad \ldots\ldots \quad (5\ 30)$$
(-133 kcal/mol) 3(0) (-7.3 kcal/mol) (-20.05 kcal/mol)
$$\Delta H_{298} = +105.65 \text{ kcal}$$

$$BaO_2 + 4Ag = 2Ag_2O + AgBa \quad \ldots\ldots \quad (5\ 31)$$
(-152.2 kcal/mol) 4(0) 2(-7.3 kcal/mol) (-20.05 kcal/mol)
$\Delta H_{298} = +117.55$ kcal

$$Y_2O_3 + 2Al = Al_2O_3 + 2Y \quad \ldots\ldots \quad (5\ 32)$$
(-450 kcal/mol) 2(0) (-400 kcal/mol) 2(0)
$\Delta H_{298} = +50$ kcal

$$BaO + 2/3Al = 1/3\ Al_2O_3 + Ba \quad \ldots\ldots \quad (5\ 33)$$
(-133 kcal/mol) 2/3(0) 1/3(-400 kcal/mol) (0)
$\Delta H_{298} = -0.3$ kcal

$$BaO_2 + 4/3Al = 2/3\ Al_2O_3 + Ba \quad \ldots\ldots \quad (5\ 34)$$
(-152.2 kcal/mol) 4/3(0) 2/3(-400 kcal/mol) (0)
$\Delta H_{298} = -114.46$ kcal

Similarly calculated values of ΔH_{298} for the reactions between Cr or Ti with Y_2O_3, BaO, and BaO_2 are listed in Table 5.2.

5.1.3 Results

The positive ΔH_{298} values of reactions between silver and cationic oxides of the BSCCO and YBCO systems suggest that these reactions are thermodynamically unfavourable. This indicates that silver is likely to form a stable metal contact on these high temperature superconducting materials. On the other hand, reactions of aluminium with oxides of HTSC elements demonstrate negative values of enthalpy, except for SrO and Y_2O_3. This illustrates the possibility of occurrence of chemical reaction and, consequently, instability of superconductor aluminium couples. Following these arguments, it can be predicted from the ΔH_{298} values listed in Table 5.2, that chromium is also likely to yield unstable contacts on these HTSCs. The table further reveals that titanium is likely to react with most of the oxides except CaO, SrO, Y_2O_3, and BaO. Therefore, a slight possibility of formation of unstable contacts with titanium on YBCO exists, provided that its reactions with oxides of copper (for which enthalpy values are negative) do not influence the interface properties.

Although the reactions of oxides of HTSCs with gold are not discussed here, gold is likely to yield stable contacts for two reasons. First, gold is known to form no oxide, and, secondly, it can be easily calculated that the heat of formation of the compounds of gold and the elements of HTSCs are positive or much less negative than the values corresponding to the oxides of these elements. This excludes the possibility of any reaction between gold and the elemental oxides of BSCCO and YBCO superconductors.

We have made silver, gold, and chromium contacts on yttrium- and bismuth-based superconducting films to fabricate SQUID devices. We have experimentally observed that the electrical characteristics of the devices are unaltered after formation of Ag and Au contacts, whereas chromium contacts resulted in the deterioration of superconducting properties. Thus, our experimental results also support the thermodynamic stability of Ag and Au contacts, as predicted by the present work. Silver and gold contacts are also widely being reported in the literature for HTSC-based devices.

5.1.4 Conclusions

On the basis of the thermodynamic criterion of positive heat of reactions, the present study concludes that silver and gold constitute stable metallization for contacts to BSCCO and YBCO superconductors. Our experimental results and reports in the literature substantiate this prediction. The suitability of these metals for HTSC contacts is further strengthened by close matching of thermal coefficients of expansion. These are 1.44×10^{-5}/°C for YBCO (Doss, 1989) compared to 1.42×10^{-5}/°C for Au (Weast, et al., 1984) and 1.9×10^{-5}/°C for Ag (Weast, et al., 1984). In addition to the chemical instability predicted for Al, Cr, and Ti, the thermal coefficient mismatch (Al, $\alpha = 2.5 \times 10^{-5}$/°C; Cr, $\alpha = 6.0 \times 10^{-6}$/°C and Ti, $\alpha = 8.5 \times 10^{-6}$/°C) (Weast, et al., 1984; Murarka, 1983) further suggests that these materials do not appear promising for contact formation on HTSCs.

5.2: PHOTO EMISSION STUDY OF SUPERCONDUCTOR-METAL INTERFACE

X-ray photo emission measurements were performed on $Bi_2Sr_2CaCu_2O_{8-x}$ single crystals coupled with gold films and $YBa_2Cu_3O_y$ thin films coated with silver over-layers. Gold and silver films were progressively removed by sputtering the couples with Ar ions. The change in the line-shapes and binding energy position of the valance and core levels of the constituent atoms of the superconductor and metal were studied to ascertain the possible reaction between the superconductor and the metal.

5.2.1 Introduction

Photo emission spectroscopy with its versatility and characteristic surface sensitivity is an ideal technique for the study of interfaces in UHV conditions (Srivastava, et al., 1994). If chemical reactions occur in the interface region, the valance and core levels of the constituent atoms undergo changes in their binding energies and relative intensities reflecting modification of their local environment and valence charge distribution. A number of studies of different metallic and semiconductor over-layers on substrate of high temperature superconductors have been reported (Lindberg, et al., 1990). Metallic over-layers of Au and Ag on high T_c superconductors are discussed here.

Bi (2212) superconductors are well suited for electron spectroscopy studies due to their oxygen stability and the relative ease cleavage i.e. the possibility to obtain a clean well defined high quality surface. Cu over-layer on Bi (2212) leads to segregation of Bi towards the near surface region and both O 1s and Cu 2p core level spectra also get changed (Hill, et al., 1988; Bernhoff, et al., 1991). However, Bi atoms seem to be less disruptive than Cu in which Cu 2p spectra remain unchanged and O 1s and Bi 4f core levels show a shift of 0.2 eV towards higher binding energies (Meyer, et al., 1988). More drastic changes take place as Al is deposited on Bi (2212) single crystal (Wells, et al., 1989). Al deposition adversely affects the metal-oxygen bonds. The Cu 2p satellite

disappears at 2Åcoverage and the O 1s core levels shift towards higher binding energy. The Bi 4f core levels show a multi component structure at coverages above 7Å, suggesting the formation of metallic Bi at the surface. On the other hand, Rb deposited on Bi (2212) single crystalline surfaces only show a small shift (0.5 eV) in O 1s and Bi 4f core level spectra (Lindberg, et al., 1988a; 1989). It shows that only Bi and O states show appreciable reaction with Rb atoms. Deposition of Pb gives rise to the formation of metallic Bi and oxidized Pb at the interface (Bernhoff, et al., 1992). The largest surface reactivity is found for metals with incomplete d-shell like Ti, Cr and Fe which tend to disrupt metal-oxygen bonds (Balzarotti and ptalla, 1992). Ag deposition on Bi (2212) compound shows a clear reduction of Cu^{2+} to Cu^{1+} (Lindberg, et al., 1988b). Also, the O 1s states show evidence of weak interaction with Ag adsorbate. However, the most suitable material for passivating the Bi (2212) material appears to be Au (Wells, et al., 1989; Balzarotti and Ptalla, 1992). No sign of reaction can be observed for any of the core levels, even at coverages upto 12Å (Wells, et al., 1989). We examined BSCCO(2212) Au and YBCO-Ag interface for the present study.

5.2.2 Experimental details

Single crystals of $Bi_2Sr_2CaCu_2O_{8+x}$ grown by flux method were obtained from H.Ohkubo and M.Akinaga, Fukuoka Univ., Japan where as $YBa_2Cu_3O_y$ thin films were grown in our laboratory. Gold and Silvers film were deposited by thermal evaporation after cleaving the crystal in $\sim 10^{-6}$ Torr.

The XPS measurements were carried out using a VG Microtech MT 300 system. The spectra were recorded with an unmonochromatised Al Kα (1486.6 eV) radiation at room temperature under a pressure of 3×10^{-9} Torr. The total instrumental resolution was 0.85 eV. The Ar ion sputtering was performed in the preparation chamber ($\sim 10^{-6}$ Torr) with argon ions of 2 KV.

5.2.3 Results and discussion

(A) BSCCO - Au interface

Figure 5.1 shows Au 4f spectra after successive sputterings. It is evident that relative intensities of both the peaks ($4f_{5/2}$, $4f_{7/2}$) attenuate with increasing sputtering time. As can be seen from figure 5.2, this decrease is exponential in nature. The lower intensity of the unsputtered surface (not shown in figure 5.1) is because of the contamination as the sample was exposed to air after Au deposition. However, there is no change in the binding energy positions and line shapes. This can be understood by taking into account the large and positive heat of formation of Au_2O_3 (8.65 kcal/mole) i.e. its inert nature and large size of Au atom. The large and positive heat of formation of Au_2O_3 prevents Au to form any oxide which, if present, would definitely reflect in the Au 4f spectra and due to large size of its atoms Au preferentially stays at the surface of the substrate i.e. Bi (2212) without any penetration into the bulk even on sputtering. However, the long tail (marked as ↔ in figure 5. 2) at lower Au concentration is most likely due to atomic mixing effects (Macht, et al., 1989) because of sputtering by which some Au ions have been implanted on the surface but as would be seen in the following discussion of other core level spectra (Bi 4f, Cu 2p, Sr 3d, O 1s, Ca 2p) these implanted ions do not appear to react with the substrate.

It is now well established that the Bi-O plane is the cleavage plane of Bi (2212) single crystal and as Au is deposited on the cleaved surface, BiO plane is the one likely to be affected on reaction with Au. Figure 5.3 shows Bi 4f spectra on successive sputterings. It can be seen that only after four minutes of sputtering the interface could be reached as evidenced by appearance of the Bi 4f peaks. Thereafter, the relative intensities of both the components go on increasing and finally stabilize after sputtering for about 10 minutes (figure 5.4). But no modifications in the line shapes and binding energy position (which remains at 158.8 eV) is observed. To check it further Bi 4f spectra were deconvoluted. As can be seen from figure 5. 5 there is no change in the relative weightage of higher binding energy and lower binding energy doublets even on subsequent sputterings and there is no sign of appearance of a low binding energy doublet that may be attributed to metallic Bi.

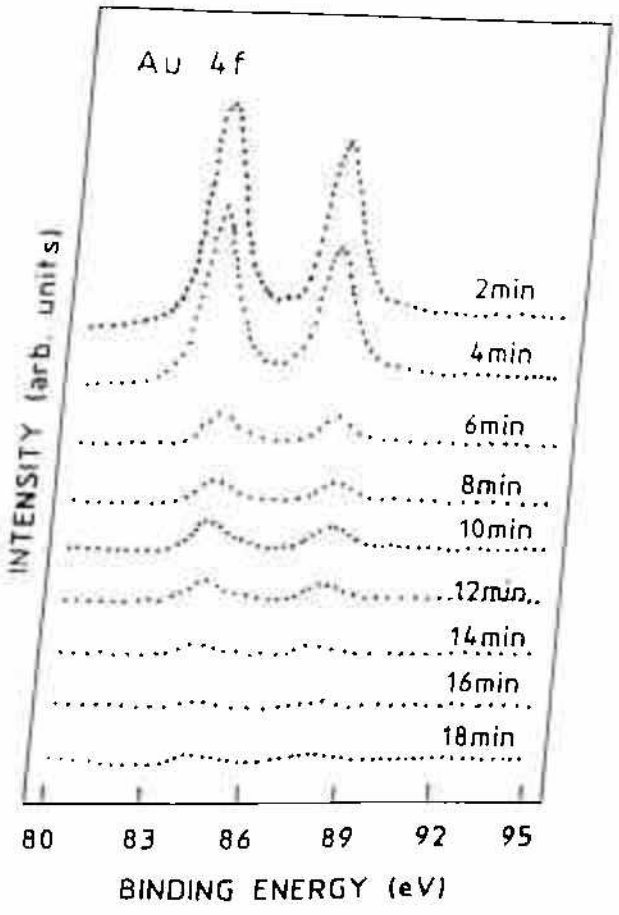

Fig.5.1: Au 4f spectra of Bi (2212) single crystal after progressive sputtering.

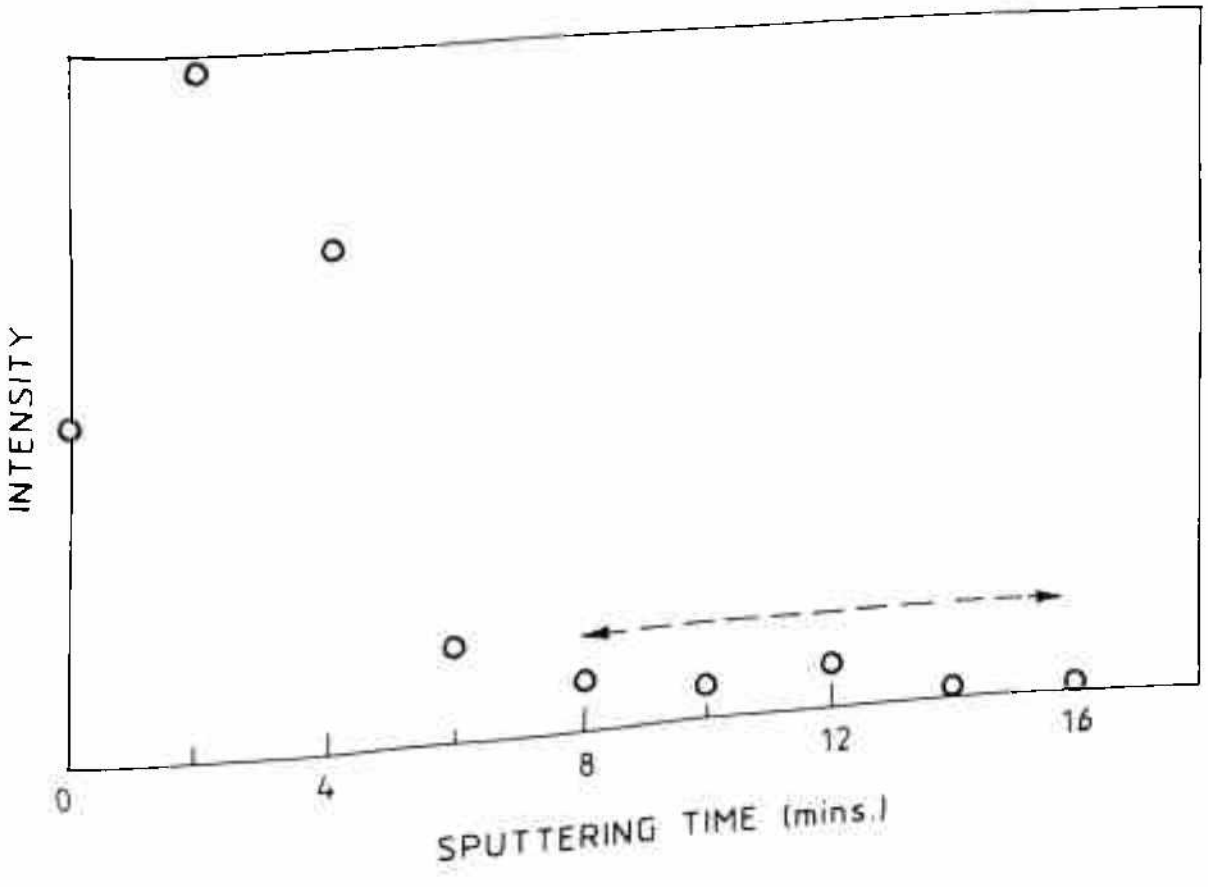

Fig.5 2: Intensity of Au $4f_{7/2}$ component after successive sputterings.

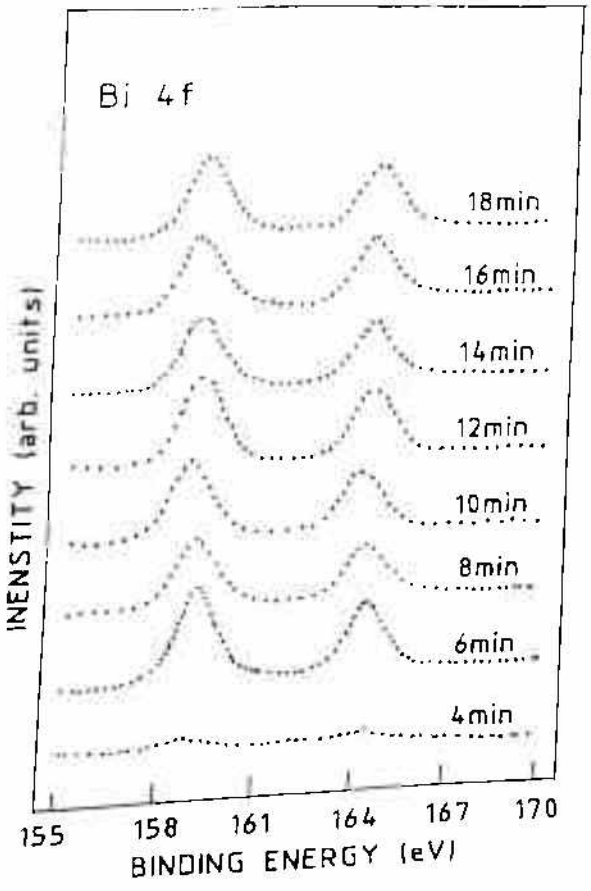

Fig.5.3: Bi 4f spectra of Bi (2212) single crystal after progressive sputtering.

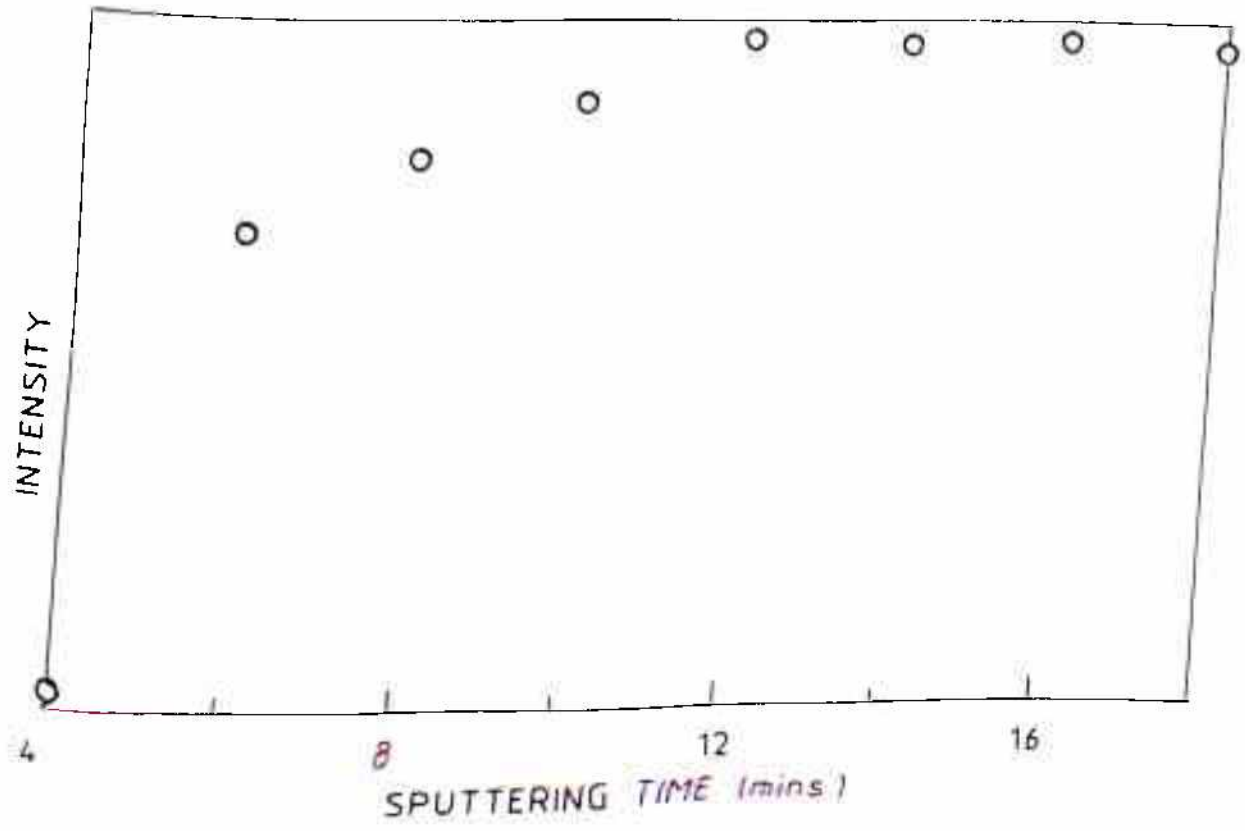

Fig.5.4: Intensity of Bi $4f_{7/2}$ component after successive sputtering

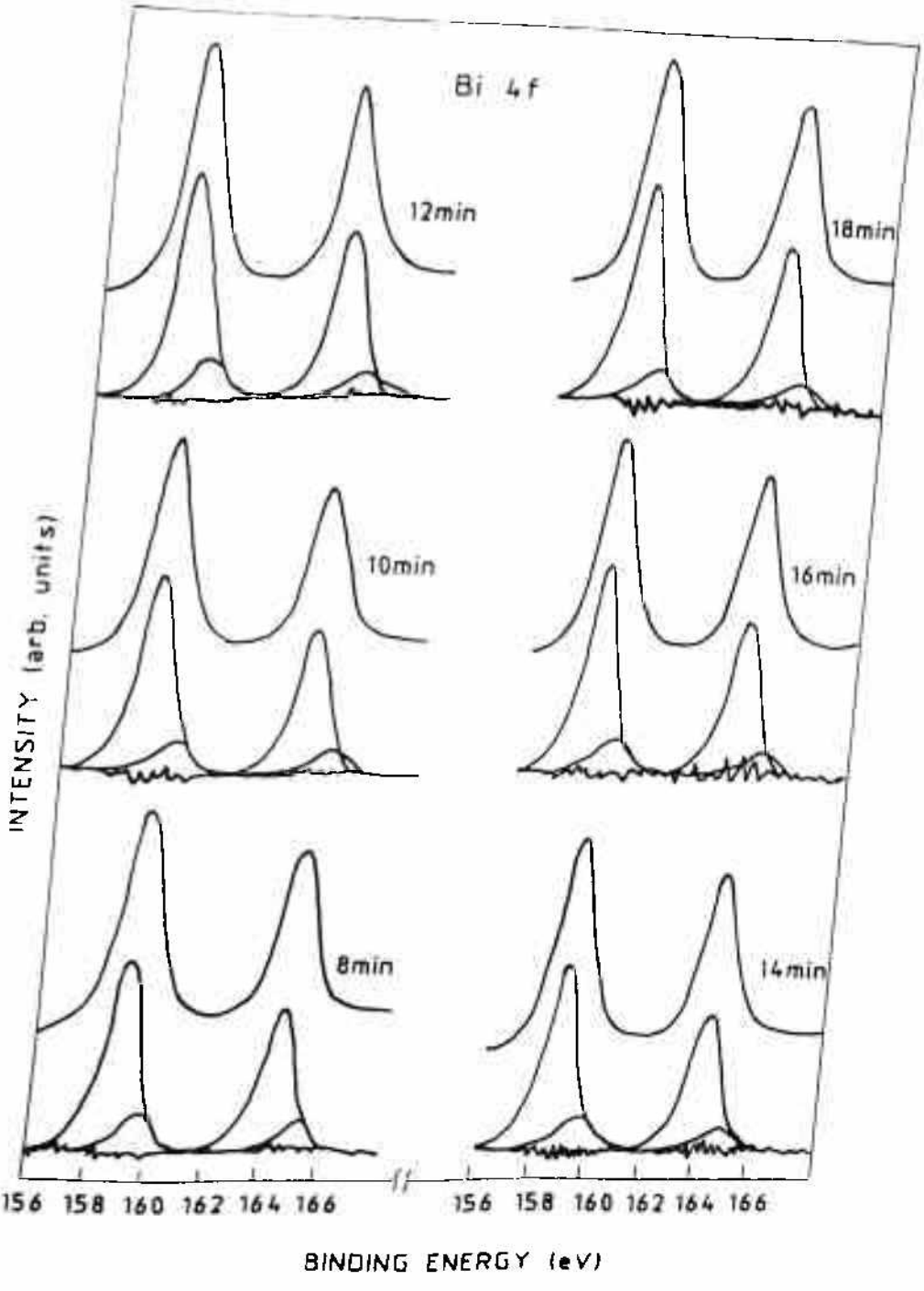

Fig 5.5: Bi 4f spectra of Bi (2212) single crystal along with the fitted components (solid line)

This further strengthens our conclusion that Au does not react with the substrate even on sputtering.

The Cu 2p spectra (figure 5.6) also does not show any changes on sputtering. There is no sign of formation of Cu and satellite to main peak ratio also remains the same (not shown in figure 5.6). No change is observed in Sr 3d (figure 5.7), O 1s and Ca 2p spectra (not shown) and hence one can rule out any possibility of interaction of Au with the substrate.

In conclusion, Au because of its inert nature (large and positive heat of formation) and large size of ions forms a passive layer on Bi (2212) single crystal and the small concentration of Au which gets implanted due to Ar sputtering also does not react with the substrate at room temperature.

(B) YBCO - Ag interface

YBCO-Ag interface was studied in three samples i.e.unannealed and annealed at 250°C and 350°C, using XPS. With successive sputterings for all three samples the intensity of $Ag_{3/2}$ peak, Cu 2p, Ba 3d, and Y 3d spectrum were studied. It was concluded that Ag forms a passive layer on $YBa_2Cu_3O_{7-x}$ thin film. However, the small concentration of it which gets implanted due to Ar ion sputtering seems to disrupt the Cu-O bonds which is reflected in Cu and O core level spectra. Annealing the interface up to 350°C does not seem to cause any further changes.

5.3 CONTACT RESISTANCE MEASUREMENT

The electrical evaluation of silver contacts on superconducting (YBCO) films was carried out, using modified version of the conventional three probe method. In the absence of a proper dielectric layer on superconductor the other methods known for the measurements of contact resistance to the semiconductors could not be applied.

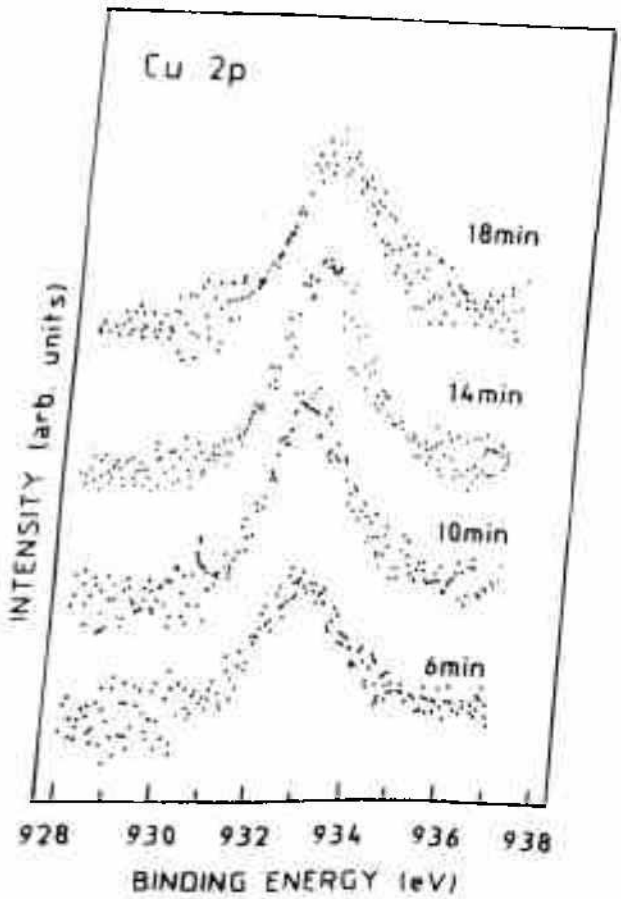

Fig.5.6: Cu 2p spectra of Bi (2212) single crystal after progressive sputtering

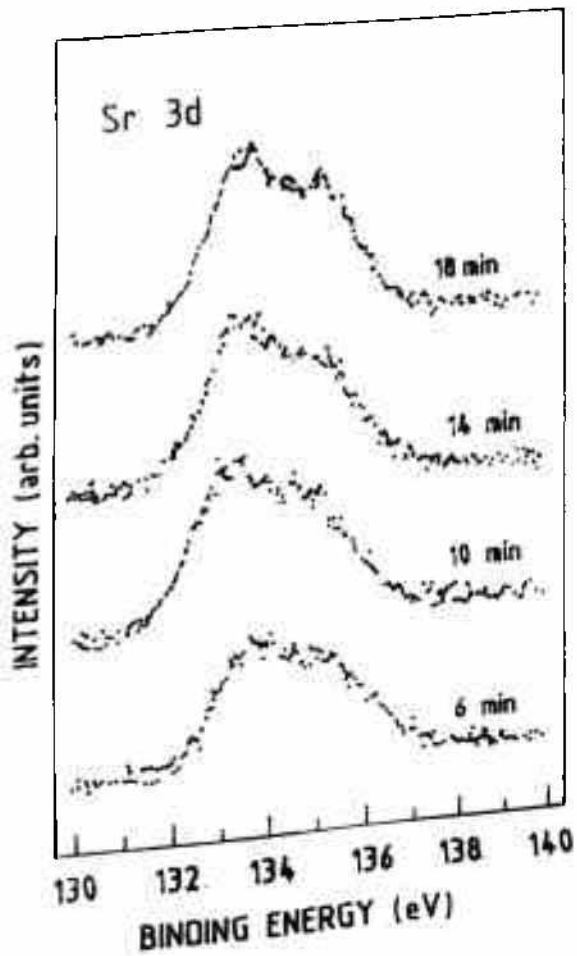

Fig. 5.7 Sr 3d spectra of Bi (2212) single crystal after progressive sputtering

5.3.1 Measurement Technique

A superconducting strip of desired width 200μm to 500μm was delineated in the superconducting films deposited on the substrates (mainly MgO), using conventional photo lithography and wet etching in dil. HCl (10%). Silver line contacts were formed perpendicular to the superconductor strip by lift-off technique or with the aid of a metal mask, during deposition. A schematic diagram of the scheme is shown in figure 5.8(a). The contact 1 and 7 were large area contacts (2mm×2mm) whereas width of contact lines 2 to 6, varied from 100μm to 350μm on the strip. Gold wires were bonded to the contact pads for electrical connections. Figure 5.8(b) depicts the measurement scheme to estimate resistance of contact no. 2. Here, a constant current was passed between pads 1 and 2 and voltage was measured across contacts 2 and 7 as is done in conventional three probe method i.e., contact 2 was made common for current supply and voltage-drop measurements. The ratio of measured voltage to current gives contact resistance of contact 2. Similarly, to determine resistance of contacts 3, 4, 5 and 6, the common probe was shifted to these contacts and their resistance was measured. Contact resistivity was calculated by multiplying the resistance value with area of intersection of the contact and superconducting strip. To isolate the contributions of bond wires, pads, metal line, etc. from the measured resistance, the approach of Gupta and Freyer (1979) was employed, wherein resistance (R) vs. inverse of contact area (A) was plotted. The slope of the resultant line gives specific contact resistivity and the intercept of the line with R-axis corresponds to resistance other than that of metal-superconductor interface. Since in the present case, the contact area can exactly be measured, the technique provides an accurate method for measurement of contact resistance.

5.3.2 Results and discussion

Using above procedure we measured contact resistance of silver on YBCO films. Silver was deposited by thermal evaporation as well as sputtering method. Contact resistivity data of thermal evaporated silver before and after sintering are listed in table 5.4. The as-deposited contact resistivity of the order of 10^{-3} ohm-cm^2 was obtained

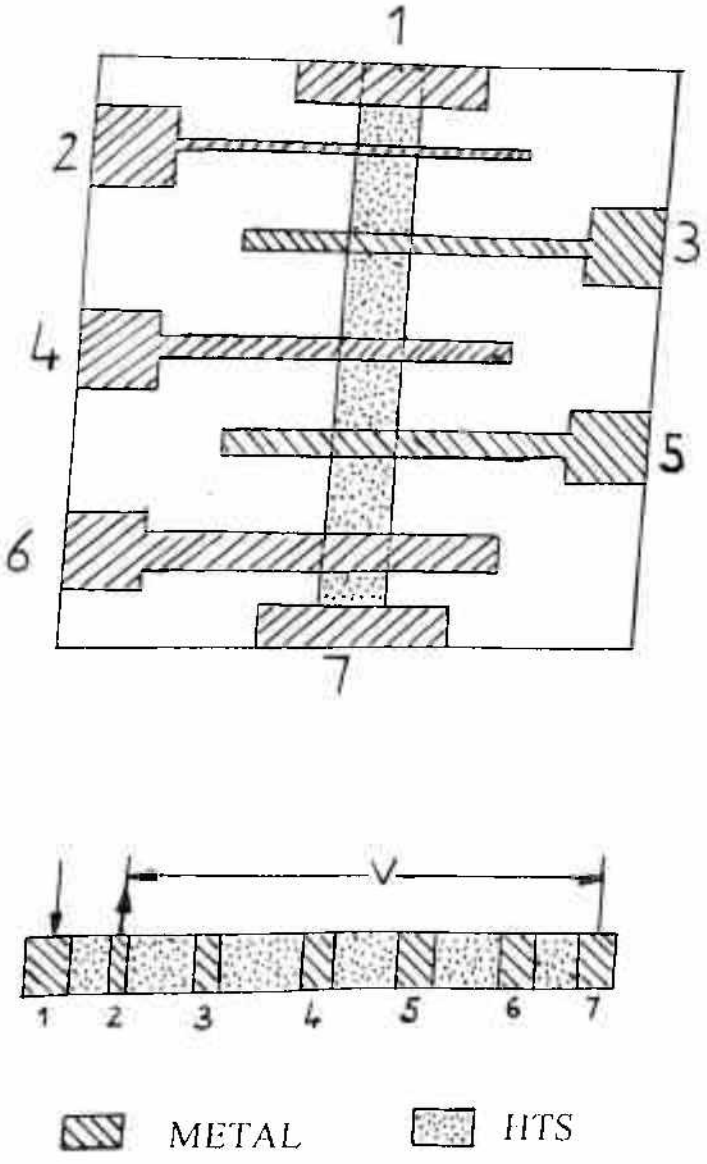

Figure 5.8: Schematic diagram of modified three-probe method for cotact resistance measurement of metal-high T_c film couple (a) Contacts Configuration (top view) (B) Measurement Scheme

whereas, it improved by two order magnitude after sintering in the temperature range of 300-350°C for 30 min. in flowing oxygen. Sintering temperature lower than 300°C could not effectively reduce the contact resistance and sintering above 350°C also failed to decrease it further. The minimum contact resistivity measured is ~2.3×10^{-5} ohm-cm^2. Contact resistance measurements on as-deposited sputtered silver contacts showed low resistivity ~10^{-4} ohm-cm^2. However, on sintering, it reduced to 10^{-5} ohm-cm^2.

Table 5.4: Contact resistivity of as deposited and sintered (300°C for 30 min. in O_2) silver contacts on YBCO films. (Measurement temperature: 30K)

Contact No.	Contact Area, A (cm^2)	Contact Resistance, R (Ω)		Contact Resistivity, ρ_c (Ω-cm^2)	
		As-deposited	Sintered	As-deposited	Sintered
2	4.9×10^{-4}	6.938	0.077	3.40×10^{-3}	3.8×10^{-5}
3	5.7×10^{-4}	2.965	0.040	1.69×10^{-3}	2.3×10^{-5}
4	8.6×10^{-4}	1.977	0.037	1.70×10^{-3}	3.2×10^{-5}
5	10.7×10^{-4}	1.645	0.034	1.76×10^{-3}	3.6×10^{-5}
6	11.7×10^{-4}	1.452	0.030	1.70×10^{-3}	3.5×10^{-5}

5.4 CONCLUDING REMARKS:

Gold and silver forms thermodynamically non-reactive contacts on YBCO and BSCCO films. The coefficient of thermal expansion for these metals and HTSCs also match closely, which is a criteria for the formation of stable contacts. XPS studies also reveal the fact that Au does not react with the high T_c films whereas some amount of Ag does penetrate, due to Ar-sputtering, and disrupt the Cu-O planes. Contact resistivity of the order of 10^{-5} ohm-cm^2 was also achieved for silver on YBCO films.

CHAPTER - SIX

SUPERCONDUCTING FIELD EFFECT TRANSISTORS

This chapter concerns with the device application of high T_c superconducting films. In the first section, importance of a three terminal device is described which is followed by electric field effects study in thin films. Second section reviews the recent progress in high T_c transistors. Following section describes the fabrication steps of MIS and Su-FET structures and our investigations on electric field effects in high T_c polycrystalline films. The last section deals with the measurement results, their discussion and concluding remarks in the end.

6.1 INTRODUCTION

6.1.1 Importance of three terminal device

Superconducting electronics has been explored extensively for several years, mainly around Josephson-Junction (JJ) as logic element. Despite high speed, low power consumption and high sensitivity of JJs, the dominance of semiconductors in modern electronics is attributed to unmatched characteristics of transistors. These are input-output isolation, inversion and well defined gain. Therefore, since last two decades research efforts are centred at the development of three terminal superconducting device, like a semiconductor transistor. The first three terminal superconducting tunnel junction transistor, analogous to the semiconductor junction transistor was demonstrated by Gray (1978). Subsequently, a large variety of superconducting three terminal devices were investigated The most promising among these structures are superconducting current injection transistors (super-CIT) (Zegbroeck, 1985; Hashimota et al., 1989; Kobayashi

and Kabasawa, 1989) and superconducting field effect devices (Su-FET) (Clark et al., 1980; Nishino et al., 1985, Takayanagi and Kawakami,1985, Yoshikawa et al., 1990 and 1991, Kabasawa et al., 1990; Xi et al., 1991 and 1992a, Mannhart et al., 1991a and 1993). Amongst these, a device based on electric field effect is preferred most due to its compatibility with other electronic components in integrated circuits.

6.1.2: Electric field effect in metallic/ metal-oxide films

Even before the discovery of superconductivity the effect of electrostatic charging on the conductivity of a metal film was investigated (Bose, 1906; Pohl, 1906). Later, Glover and Sherril (1960) examined the effect of charging on the superconducting transition temperature and the normal state conductivity of tin and indium. The same properties were investigated in the films of amorphous Bi and Ga, metastable crystalline Ga and in disordered crystalline Pb by Flesch and Glover (1971). However, it has been concluded that in the elemental superconductors the influence of electric field on superconducting properties is not significant enough for device development owing to high carrier concentration in them. Subsequently, large effects were observed in In/InO_x composite (Fiory and Hebard, 1985; Hebard et al., 1987) and doped $SrTiO_3$ (Gurevitch et al., 1986) where carrier current density is much smaller. These results are particularly significat in view of low carrier density in HTS materials, and is the principal reason for immense scientific interest on development of a electric field effect device in HTS immediately after the discovery of high temperature superconductors.

6.1.3 Electric field effect in high T_c films

The high T_c-copper oxide superconductors appear promising candidates for electric field effect devices as they have low concentration of mobile carriers and also because these cuparates have small coherence lengths and sizeable dielectric constants (Mannhart et al., 1992a; Xi et al., 1992; Mannhart et al., 1992b. Therefore, soon after their discovery in 1987, there has been active effort around the world in this area. The research is considered important for two reasons: one to understand the basic mechanism of superconductivity in oxide superconductors, (Shapiro, 1995; Gomeniuk et al., 1993;

Sergenkov, 1995; Burlachkov et al., 1993) and second to develop a three terminal superconducting device like semiconductor-field effect transistor (Mannhart et al., 1992a; Kleinsasser, 1992; Mannhart et al., 1991a; Xi et al., 1992b. Consequently, a number of reports were published, where in influence of external electric field on normal state and superconducting properties of these oxide compounds has been studied (Mannhart and Kleinsasser, 1992a; Fiory et al., 1990; Xi et al., 1992a; Mannhart et al., 1991a; Ogale et al., 1995). Inspite of tantalizing results a device for practical use is still awaited. It is believed that this may be due to insufficient effects of electric field on properties of oxide superconductors.

To enhance the effect of external electric field for percentage change in the carrier density, ultra thin films have also been used to fabricate superconducting-field effect transistor (Su-FET) (Xi et al., 1992a & 1991). However, in our opinion owing to low T_c of these ultra thin films and technological problems like forming reliable contacts on these films, a practical device has not yet been claimed. Recently, significant change in critical current density and transition temperature have been observed in films containing weak-links or grain boundaries (Mannhart et al., 1992a; Nakajima et al., 1994; Gupta and Khokle, 1993) but the progress in the development of grain boundary based FET remained limited probably due to localization of grain boundaries in the films. Nevertheless, grain boundary based device appears to be a possible approach to realize superconducting FET. We therefore concentrated our efforts to study electric field effects in granular films.

6.2 HIGH T_c TRANSISTORS

The unique potential benefits of superconducting transistors continued the interest of many scientists since discovery of superconductivity in 1911. A superconducting, and thus virtually loss-free, on-state of the source drain channel (SD channel) is the first most important example of such an advantage and its ability to sustain high current density is another. In addition, with regard to fabrication and operation, superconducting transistors

are compatible with other superconducting components, which may be required to interface with superconducting electronics.

This section reviews various three terminal devices built from high T_c superconductors and related materials. Particular emphasis is placed on the field effect transistors.

6.2.1 Superconducting Base Transistors (SBTs)

Superconducting Base Transistors (SBTs) are reminiscent of bipolar semiconducting transistors. From an emitter electrode, quasiparticles are injected as minority carriers into the superconducting base, in which Cooper pairs are the majority carriers. After traversing the base, the quasiparticales are gathered in the collector electrode. A major advantage these devices draw from superconductivity is the low resistivity of the superconducting base, which should allow ultra thin base layers to be used without having unacceptable resistances for gate current (I_G). Here, the base inductance is the performance limiting parameter. SBTs are classified in two variations: superconducting hot electron- transistors (SUPER-HETs) and superconducting-base-semiconductor- injection transistors (SUBSITs), both of which are discussed in detail by Kleinsasser and Gallagher (1990). In the SUPER-HET, quasiparticles have kinetic energy of $E_{kin} >>$ superconducting energy gap (Δ) and carriers traverse the base ballistically as hot carriers. While, in the SUBSIT, the kinetic energy of the quasiparticles is much lower, $E_{kin} \cong \Delta$, and particles move diffusively (Frank et al., 1985).

SUBSITs and SUPER-HETs have been fabricated using epitaxial Au/$Ba_{1-x}K_xBiO_3$/ Nb-doped $SrTiO_3$ (Suzuki et al., 1993; Usuki et al., 1993) and Nb-doped $SrTiO_3$/$Ba_xRb_{1-x}BiO_3$/In multilayers (Toda and Abe, 1994; Abe 1994; and Toda et al., 1994) as E/B/C configurations. Switching speeds in the terahertz range (Tazoh, 1991) is the most attractive feature for SBTs. However, device performance crucially depends on the height of the base-collector barrier, the control of which is a serious technological challenge (Kleinsasser and Gallagher, 1990).

6.2.2 Dielectric Base Transistors (DBTs)

The original concept of dielectric base transistors (DBTs) is based on resonant tunnelling from a superconducting emitter to a superconductor collecting electrode (Tamure et al., 1991). The charge carriers tunnel resonantly through a dielectric barrier that contains defect states of a well defined energy. For these devices, switching delays of only 0.5 psec have been predicted but the difficulties are associated with the growth of the tunnelling barrier. However, modified versions of DBTs have been fabricated successfully (Yoshida et al., 1991, 1992; Tamura et al., 1992; Hota et al., 1994). DBTs impress with their high current and voltage gains and their compatibility with high T_c superconductors. However, these devices derive no advantages from superconductivity except having superconducting contacts.

6.2.3 Vortex Flow Transistors (VFTs)

In vortex flow transistors a small magnetic field generated by a controlled current is used to inject magnetic vortices into one or more superconducting bridges connected in parallel, which are used as a source-drain (SD) channel. Usually, the vortices suppress the critical current of the bridge, and, once they flow, enhance the bridge resistance. If the bridge contains a Josephson junction, then the active flux quanta are Josephson vortices and the device is called a Josephson vortex flow transistor (JVFT), otherwise it would be an Abrikosov vortex flow transistor (AVFT). Besides these standard VFTs, other structures include, one having only one contact dedicated exclusively to the input line, the other one being connected directly to the drain or the source.

Planar Josephson junctions controlled by magnetic fields were investigated as amplifiers by numerous groups (Mitisoo, 1961; Likharev et al., 1979) but the first JVTs were demonstrated by T.V.Rajeevakumar (1981) and B.J.van Zeghbroeck (1983). Experimental investigations of high T_c VFTs were first reported by J.S.Martens and co-workers (Martens et al., 1989, 1991, 1993a, 1993b, 1993c), who demonstrated the captivating performance of high speed VFTs based on $YBa_2Cu_3O_{7-x}$ and $Tl_2Ca_2Ba_2Cu_3O_y$

films. These films did not contain Josephson junctions. Their results were not reproduced by other groups but model calculations were performed by Davidson and Petersen (1994). Alternative concepts or materials, like $Nd_{2-x}Ce_xCuO_4$, were also used to realize AVFTs (Miyahara et al., 1994).

For the fabrication of JVFTs, step edge junctions, bicrystal junctions and nanobridges have been used as Josephson junctions (Koelle et al., 1995; Dimos et al., 1988; Gerdemann et al., 1995a, 1995b; Alff et al., 1994; Satchell et al., 1992, 1993; Wen and Abe, 1994; Zhang et al., 1994; Schneider et al. 1993, 1994; Martens et al., 1989, 1991, 1993a, 1993b, 1993c). Their investigations have further revealed the fact that the speed of AVFTs is lower, probably due to slower Abrikosov vortices. However, no fundamental limitations have been identified to prevent operation of JVFTs at frequencies of the order of 500 GHz.

Further experimental work is necessary to obtain data on magnetic cross talk, on the sensitivity of the devices to external dc and rf magnetic fields to measure noise figures, and to reveal potential difficulties that may arise from the narrow biasing regime.

6.2.4 Quasiparticle Injection Devices (QPIDs)

In QPIDs, quasiparticles are injected through a barrier layer into a superconducting film to alter the superconducting order parameter by modifying the quasiparticle spectrum and the phonon distribution. In most cases the distributed quasiparticle and phonon distribution depress T_c and the critical current.

As far as high T_c superconductors are concerned, QPIDs are probably the least explored, may be due to difficulties associated with the fabrication of the multilayed structures. Also, QPIDs are inherently better suited for operation at liquid helium temperature than in the liquid nitrogen temperature range, because the high temperature background of thermal quasiparticles requires a correspondingly higher density of injected quasiparticles to create the desired nonequilibrium.

The response times of high T_c films due to ultra short light or supercritical current pulses have been studied by various groups (Chwalek et al., 1990; Eesley et al., 1990; Ghis et al., 1993; Han et al., 1990; Frenkel et al., 1989, 1990; Zeuner et al., 1992; Shi et al., 1993; Semenov 1992; Lindgren et al., 1994; Danerud et al., 1994; Sergeev et al., 1994; Karasik et al., 1995). However the first exploration of high T_c QPIDs was carried out in Japan in 1989 (Higashino et al. 1989a, 1989b, 1990; Kobayashi et al., 1989). They used polycrystalline $Bi_2Sr_2CaCu_2O_{8-x}$/$Bi_2Sr_2Ca_2Cu_3O_{10-x}$ SD channel with Au gate and (Y/Er)$Ba_2Cu_3O_{7-x}$ channels with Al gates to measure current gain. They used natural oxide layers as gate barriers. Subsequently, various bilayer and trilayer structures were used employing MgO or natural oxide as gate barriers (Lin et al., 1994; Boguslavskij et al., 1993, 1994a, 1994b; Schneider et al., 1995; Wang and Iguchi, 1994; Iguchi et al., 1994). As only very limited work has been done in the field of high T_c non-equilibrium device, its potential application is yet to be explored.

6.2.5 Electric Field-Effect Transistor (Su-FETs)

In superconducting field effect transistors (Su-FETs), an electric field is applied to a superconductor via an insulating barrier which changes the density of Cooper pairs in a layer extending parallel to the insulator/ superconductor interface. As the pair potential of a superconductor is a function of the Cooper pair density, all superconducting properties in the field penetrated layer depends on the applied electric field, if electric penetration depth (λ_{el}) is atleast comparable to the coherence length (ξ) (Shapiro, 1985; Mannhart, 1992):

$$\lambda_{el}(T) \geq \xi(T)$$

In high T_c superconductors, this condition is generally fulfilled but in low T_c counterparts $\lambda_{el}(T) << \xi(T)$ (Glover and Sherrill, 1960; Hilsch and Naugle, 1967; Berlincourte, 1969; Steenbeck, 1971; Fiory and Hebard, 1984; Stadler, 1965; Gurvitch et al., 1986). The field penetration depth is small due to high carrier density.

Yoshikawa et al., 1994; Han et al., 1993) and in bulk ceramics (Smirnov et al., 1992, 1993, 1994; Oriova and Smirnov, 1994).

Theoretical descriptions of the field effects on high T_c superconductors have also been reported (Shapiro, 1984, 1985, 1993, 1995; Burlachkov et al., 1993; Shapiro and Khalfin, 1993; Ghinobker et al., 1995a, 1995b; Kechiantz, 1990, 1992,; Konsin, 1994; Sorkin and Konsin, 1994; Jiang et al., 1991).

The ability to alter T_c and to modulate critical currents by applying electric fields suggests the use of the field effect to fabricate superconducting-FETs. For the fabrication of these structures, dielectric films like $SrTiO_3$ and $Ba_xSr_{1-x}TiO_3$ (Frey et al., 1995), PMMA or Kapton (Fiory et al., 1990, 1991; Mishonov, 1991; Levy et al., 1992), MgO (Kabasawa et al., 1990), SiO_2 (Jager et al., 1993; Villegier et al., 1991), CeO_2 (Wang and Iguchi, 1993; Walkenhorst et al., 1994), Al_2O_3 (Gupta and Khokle, 1993), and $PrBa_2Cu_3O_{7-x}$ (Ohmameuda and Okabe, 1995) have been used as gate barriers. These materials are attractive not only due to their small losses, but also because of their small permitivity, achievable field effects are modest, in addition to their compatibility with these materials.

In Su-FETs, the applied electric field is electrostatically screened by the mobile charge carriers. Therefore, enhanced field effects are expected for samples with reduced electrostatic screening which is attained by incorporating weak links with a reduced carrier density into SD channel (Mannhart et al., 1993; Chen et al., 1991; Nakajima et al., 1993, 1994; Yamashita et al., 1994; Ivanov et al., 1993; Dong et al., 1994; Moore et al., 1989). If the weak links are Josephson junctions, three terminal Josephson devices are obtained, the gate electrode of which can be used for switching and trimming purposes. Theoretical description of high T_c JOFETs are almost non-existent, and experimental data are only gradually becoming available. Nevertheless, given the low carrier density in the junction region, it is permissible to assume that such devices will be more sensitive

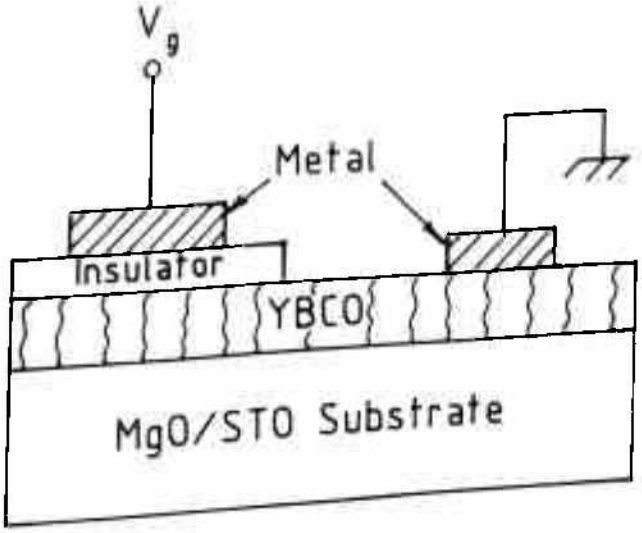

FIG 6.1 (a) METAL INSULALATOR SUPERCONDUCTOR (M-I-S) CAPACITOR

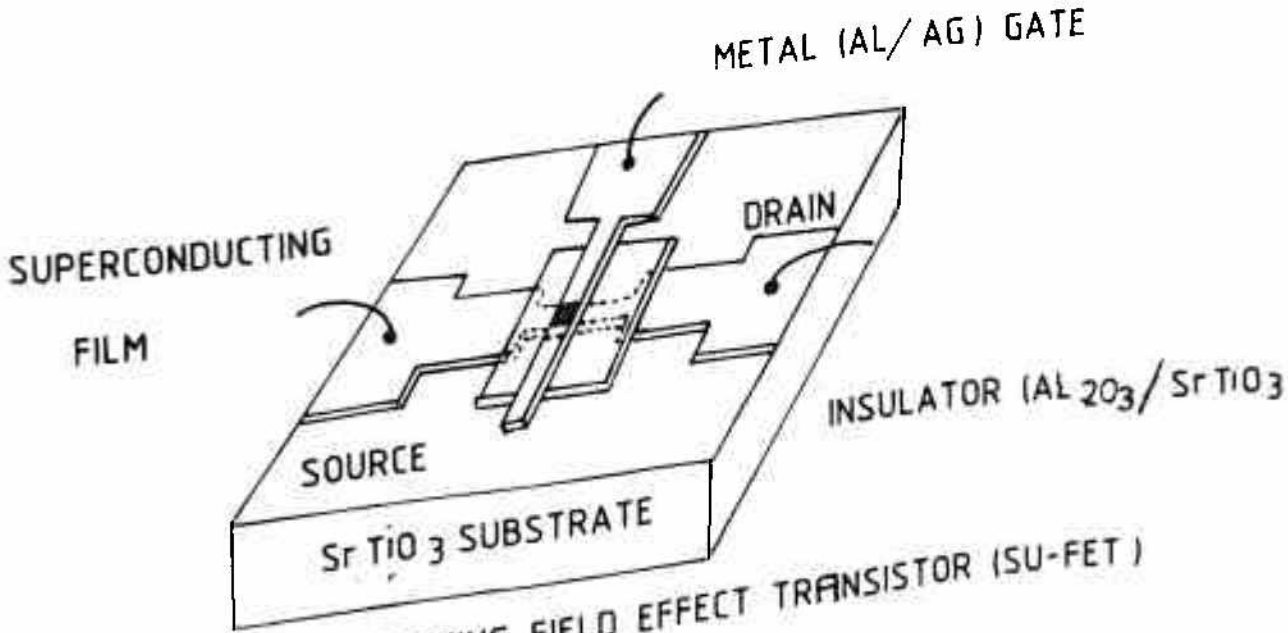

FIG 6.1(b) SUPERCONDUCTING FIELD EFFECT TRANSISTOR (SU-FET)

6.3.2 Areal charge density measurements

For the measurement of areal charge density at YBCO-insulator interface, the M-I-S structure was mounted on the cold finger of a CTI-cryogenics closed cycle helium refrigerator (model CCS-350). Temperature of the sample was monitored with the aid of a silicon diode sensor attached to the Lake Shore 330 auto-tuning temperature controller. Gate voltage, V was applied to the device through a Keithley 228A voltage source and the charge induced at the YBCO-insulator interface was measured by a Keithley 617 electrometer. The measured charge divided by gate area and electron charge gives areal charge density. For each observation, the gate current was monitored precisely, after application of the gate voltage. During these measurements low gate current (below 10 pico-ampere) was maintained to eliminate effect of injected charges at the interface. Thus the measured carrier density values represent the actual charges induces at the interface, due to applied field at the gate electrode. The results are illustrated in Fig.6.2 and 6.3 for Al- Al_2O_3-YBCO and Ag-STO-YBCO structures. Above measurements were also done on MIS structures fabricated in epitaxial films. However, no measurable change in areal density could be recorded. This appears justified as due to large thickness (>2000Å) of these films electric field effects may not be appreciable.

6.3.3 Results And Discussion

Electric field effect measurements were done on many samples, however, the results illustrated in Fig.6.2 and 6.3 are typically a set of results. The charge readings obtained on the application of gate voltage, in a particular range, was found reproducible and reversible. Also, the same set of charge readings were achieved on varying the gate potential from negative to positive and vice-versa. The important features of these curves are as follows:

i) For positive gate voltage, the negative charge was recorded at the YBCO-insulator interface signifying the electron accumulation. Positive charge corresponding to holes was only recorded on the application of negative gate voltage.

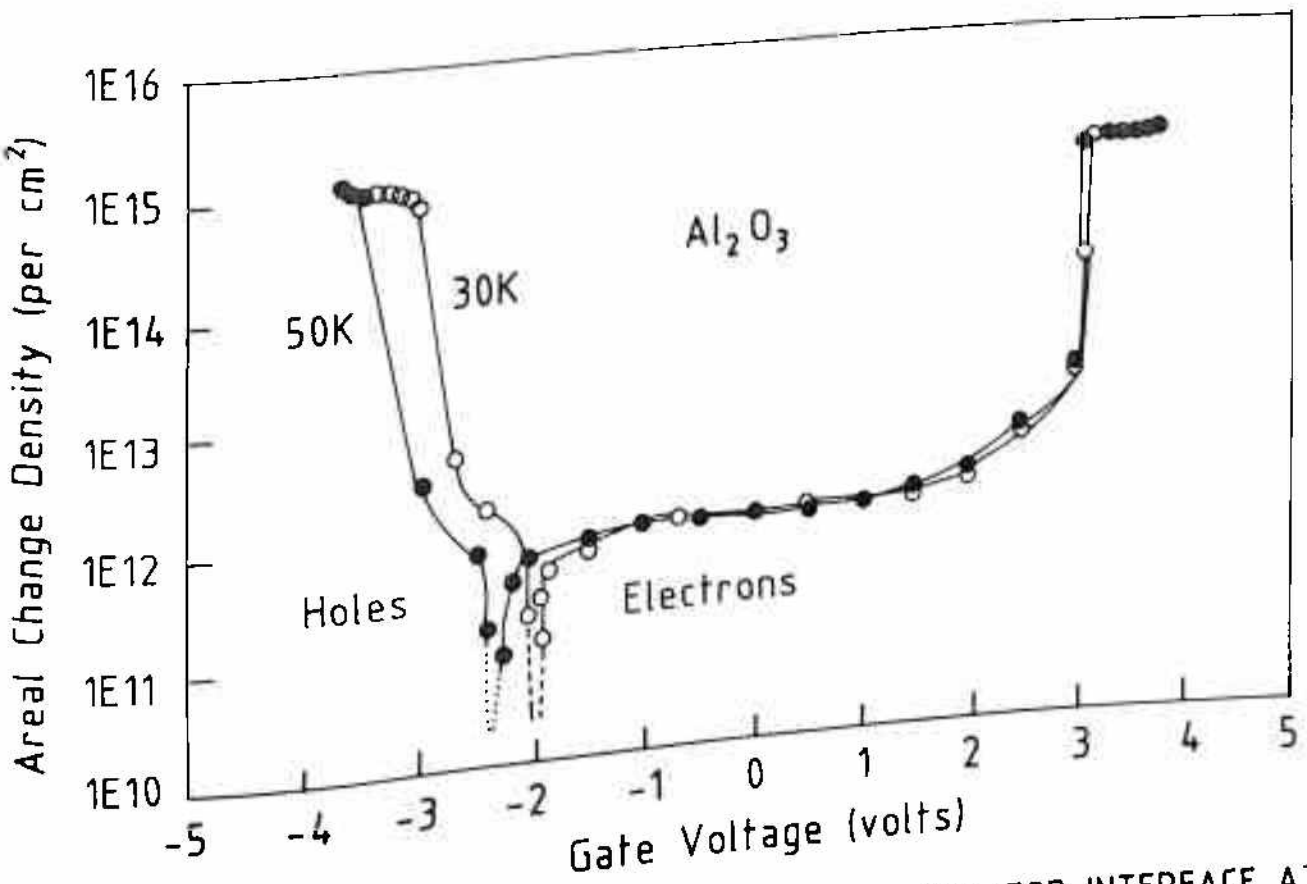

FIG. 6.2 AREAL CHARGE DENSITY AT YBCO INSULATOR INTERFACE AT VARIOUS GATE VOTTAGES WITH Al_2O_3 DIELECTRIC LAYER AND 30K &50K TEMPERATURES

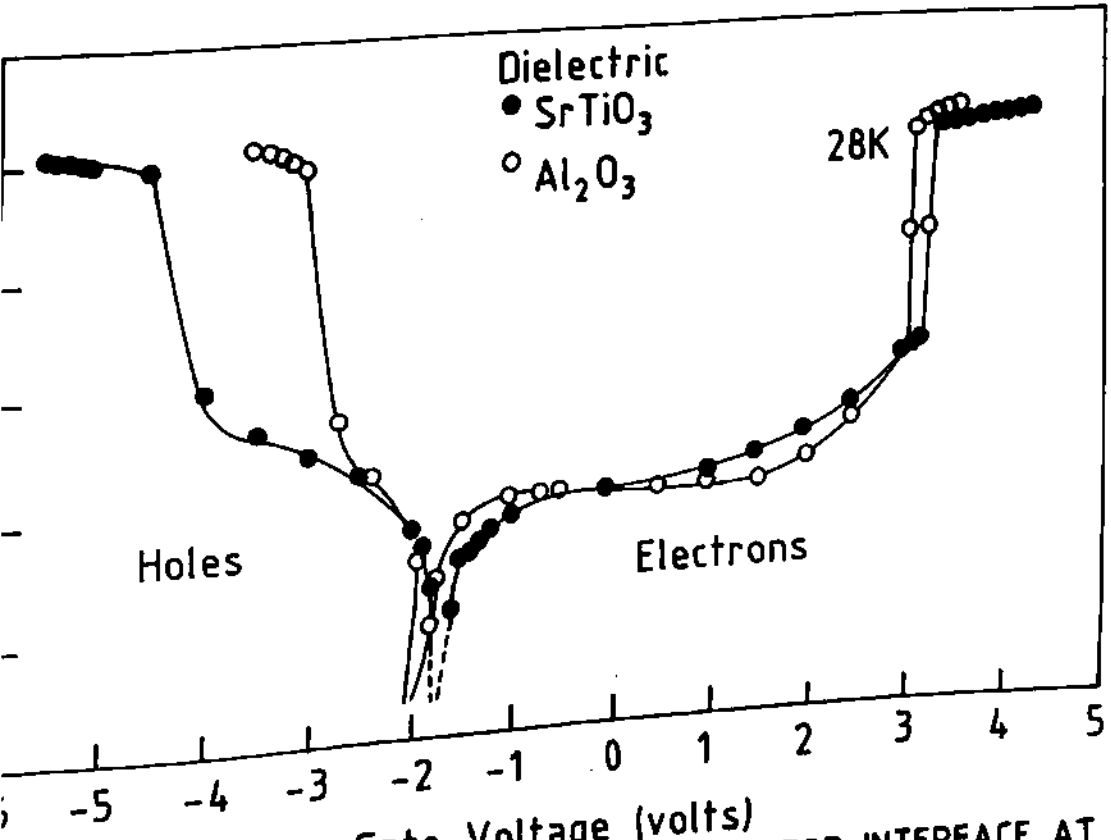

INSULATOR INTERFACE AT VARIOUS

ii) The electron density varies slowly over a longer span of voltage compared to that for holes. For example, in case of M-I-S structure with Al_2O_3 as insulator, areal charge density of holes varies from $10^{12}/cm^2$ to $10^{15}/cm^2$ as gate voltage changes from -2.5V to -3.5V whereas, areal charge density due to electrons varies in this range, when the gate potential increases from -2.0V to +3.0V.

iii) The cross-over voltage (V_{cross}) i.e. the gate voltage at which transition from

It is expected that like other cuprate superconductors, YBCO contains hole pairs in superconducting state. So, in case of M-I-S structures, cooled below the critical temperatures and at zero gate voltage there should be presence of holes at the YBCO-insulator interface. But our measurements suggest accumulation of electrons at the interface even for some -ve gate voltage upto V_{cross}. This is not clear but in our view, this may be analogous to silicon-silicon dioxide interface, where silicon dioxide always contain mobile and immobile positive charges (Sze, 1969). Due to these charges electron accumulation always exists at Si-SiO_2 interface. Perhaps, STO and Al_2O_3 also contain positive charges which are responsible for the accumulation of electrons at YBCO-Al_2O_3/STO interface, even at zero applied voltage. To deplete these electrons some negative voltage is always required and only after that holes or positive charge start accumulating at the interface. This argument also seems plausible through results in figure 6.3, where cross-over voltage for STO is higher than that for Al_2O_3. This suggests that values of possible positive charges in STO is higher than that in Al_2O_3. The lower value of cross-over voltage at 30K in Fig.6.2, compared to that at 50K can be easily understood. This may be attributed to increase in superconducting pair density with reduction in temperature, as at lower temperature more number of hole pairs are available and thereby an early cross-over results.

6.4 DEVICE FABRICATION AND FIELD EFFECT MEASUREMENTS

6.4.1 Fabrication of Su-FET

Superconducting field effect transistor (Su-FET) was fabricated (Fig. 6.1(b)) in the similar fashion using polycrystalline BPSCCO films on MgO, prepared by spin-on technique. $T_{c,zero}$ of the films was in the range of 75K to 80K. The structure was patterned in the films using standard positive photoresist photolithography. The gate length of 70μm and width of 250μm was defined by etching in 10% diluted hydrochloric acid.

Dielectric layer of Al_2O_3, gate metal Al and silver contacts were made as described for MIS capacitors.

6.4.2 Su-FET characteristics

Current-voltage characteristics of a Su-FET at 68K and effect of gate voltage on the transition temperature were measured using same set-up. The effect of gate field on drain i.e current-voltage (I_D-V_D) characteristics, at 68K, of a typical Su-FET having gate oxide thickness of the order of 500Å and $T_{c,zero}$ of 75K is shown in fig. 6.4. Due to large softening of I_D-V_D curve, it is difficult to estimate the suppression in the critical current on application of gate bias from the figure. Further, it is also apparent that to record the influence of field on I_D-V_D characteristics, a relatively large gate voltage of 15 volts was applied. On account of repeated measurements the micro bridge of the device failed. Therefore, another device (with gate oxide thickness of about 100 Å) was fabricated to study the influence of gate voltage on zero resistance temperature of the transistor. Fig. 6.5 illustrates that on application of 380mV to the gate, $T_{c,zero}$ of the device was reduced to 64K from 69K. In principle, these results demonstrate the change in superconductivity on application of electric field to gate of the device. In the absence of a proper theory of superconductivity in high T_c materials it is difficult to expain the observed field effect in Su-FET. However, as the areal charge density measurements suggest, there is a negative charge accumulation at the superconductor-insulator interface for positive gate voltage. Hence, more number of holes pairs are required to compensate these excess electrons. This can be easily achieved by reducing the temperature of the Su-FET. In other words, on the application of positive gate voltage the T_c should reduce. It will be interesting to see if T_c can be increased by the application of negative gate voltage.

6.5 CONCLUSION

In conclusion, this chapter deals with the quantitative measurements on areal charge at YBCO-insulator (Al_2O_3 and STO) interface and its dependence on external electric field. The effect of gate voltage on I_D-V_D characteristics and transition

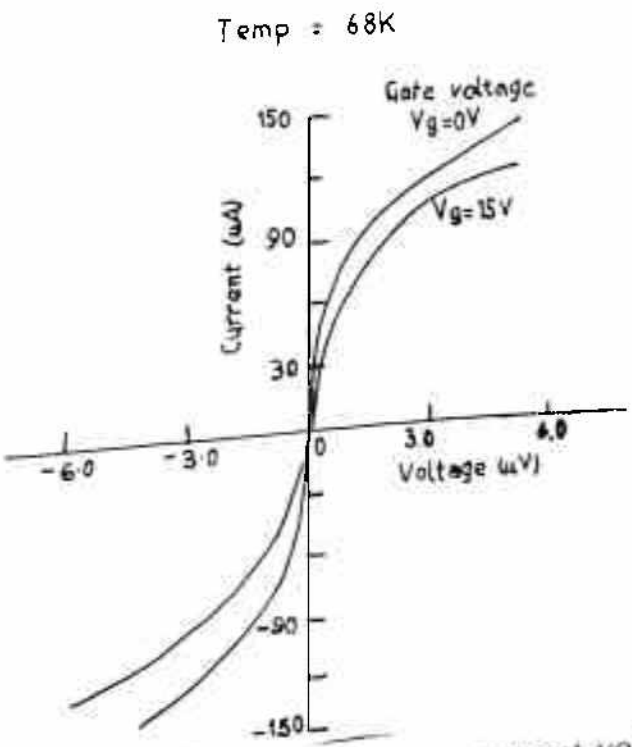

Figure 6.4: Effect of gate voltage on current-voltage curve of Su-FET

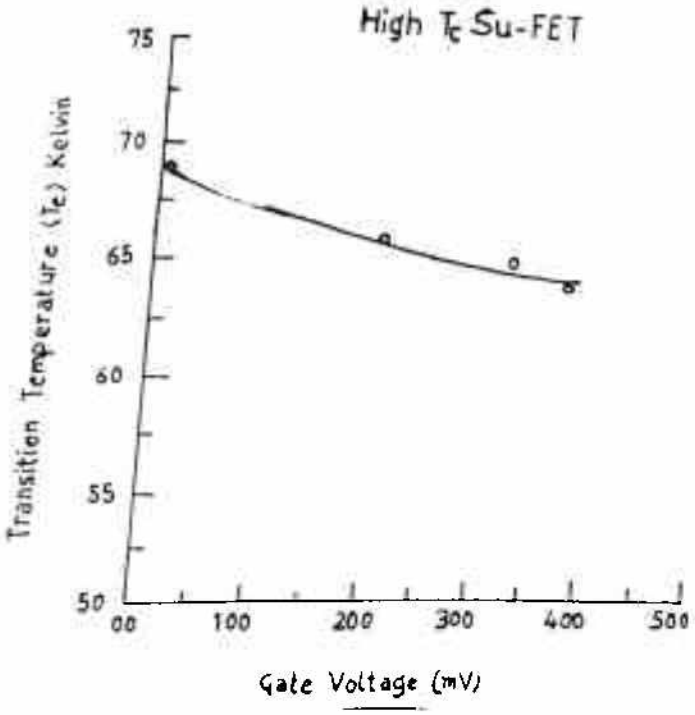

Figure 6.5: Effect of gate voltage on transition temperature of Su-FET

temperature of Su-FET is also prsented. The possibility of modifying the carrier concentration in YBCO films exists in reversible and controlled manner. This type of modifications do not affect the stoichiometry of the superconducting compound. These effects have implication on understanding the basic mechanism of superconductivity in copper oxides and likely to provide the basis for applications of high T_c superconductor in three terminal devices, which can be used as logic element in semiconducting electronics.

CHAPTER-SEVEN

CONCLUSION AND SCOPE FOR FUTURISTIC WORK ON HTS DEVICES

Last ten years of research has almost established the technology for the synthesis of YBCO, BSCCO and TBCCO bulk materials and films. Although technology for many other HTSC compounds has also matured but only above three compounds are common to all research groups. Device quality superconducting films of these materials are now components and

We strongly feel that the grain boundary based field effect transistor is likely to be a useful futuristic device, provided gate of the Su-FET is exactly located on single grain boundary. The understanding of physics of grain boundary in HTSC is also likely to provide insight into the behaviour of FET. Therefore, research on grain boundary based Su-FET offers technological challenges as well as understanding of transport mechanism in HTSC materials. Electric field effect studies on these materials are of immense interest to obtain information regarding variation in transition temperature with change in carrier concentration, coherence length, etc. We hope that in next five years, Su-FETs will be available for the practical applications if technological problems described above are circumvented.

Device noise is also one of the major issues when one compares the performance of a device based on LTS and HTS materials. Evidently, thermal noise is higher in HTS devices then that in LTS. So in our opinion electric field effects can be used to minimise the noise in a HTS device. This ushers an interesting area of research, theoretical as well as experimental. In brief, although experimentally high temperature superconductivity is established but the understanding of its mechanism is still eluding the theorist. That is why, this subject of high temperature superconductivity has become so much fascinating. This is also true in the development of HTS active devices. Its technology is challenging and device physics is even more interesting.

REFERENCES

1. Abe, H, Extended Abstracts of the HTSED Workshop'94 May 26-28 Whistler, Canada, Research and Development Association for Future Electron Devices, p.83
2. Agarwal Ajay, Ram P Gupta, W S Khokle, K D Kundra, P R Deshmukh, M Singh and P D Vyas, 1993, Supercond. Sci. Technol., 6, p.670
3. Agarwal Ajay, Ram P Gupta, and W S Khokle, (1994), Microelectron. Reliab., 34, p.1273
4. Ahn, C H, J-M Triscone, N Archibald, M Decroux, R H Hammmond, T H Geballe, O Fischer and M R Beasley, 1995, Science, 269, p.373
5. Alarco, J A, G Brorsson, Z G Ivanov, P A Nilsson, E Olsson, and M Lofgren, 1992, Appl. Phys. Lett., 61, p.723
6. Alff, L, B Mayer, S Schuster, O Frohlich, R Gerdemann, A Beck and R Gross, 1994, J. Appl. Phys., 75, p.1843
7. Alford, N Mc N, et al., 1991, Nature, 349, p.680
8. Alford, N Mc N and T W Button, 1991, Adv. Mater., 30, p.318
9. Alford, N Mc N, et al., 1997, Supercond. Sci. Technol., 10, p.169
10. Ameen, M S, O Auciello, A I Kingon, A R Krauss, and M A Ray, 1990 AIP Conf. Proc. (USA), 200, p.79
11. Antipov, E V, et al., 1993, Physica C, 215, p.1
12. Aoki, S, T Yamaguchi, Y Iijima, O Kohno, S Nagaya, and T Inoue, 1993, IEEE Trans. on Appl. Superconductivity, 3, p.1691

13. Asano, H, S Kubo, O Michikami, M Satoh, and T Konaka, 1990, Jap. J. Appl. Phys., 29, p. L1452

14. Awaji, T, K Sakuta, Y Sakaguchi, and T Kobayashi, 1992, Jpn. J. Appl. Phys., 31, p.L642

15. Azoulay, J and D Goldschmidt, 1989, J. Appl. Phys., 66, p.3937

16. Azuma, M, et al., 1992, Nature, 356, p.775

17. Babcock, S E, T F Kelly, P J Lee, J M Seuntjens, L A Lavanier, and D C Larbalestier, 1988, Physica C, 152, p.25

18. Bailey, A, et al., 1991, Bull. Mater. Sci., 14, p.111

19. Balestrino, G, V Foglietti, M Marinelli, E Milani, A Paoletti, and P Paroli, 1990, Appl. Phys. Lett., 57, p.2359

20. Ban, E, Y Matsuoka, and H Ogawa, 1990, J. Appl. Phys., 67, p.4367 Basovich, A J, S V Gaponov, L Jastrabik, M Jelinek, N A Kiseler, E B Kluenkov, O I Lebeder, L A Mazo, L Soukup, M D Strikovskij, V V Talanov, and A L Vasiliev, 1993, Thin Solid Films, 228, p.193

21. Battacharya, R N, et al., 1993, Physica C, 211, p.475

22. Bednorz, J G and K A Muller, 1986, Z Phys. B, 64, p.189

23. Benz, S P and C A Hamilton, 1996, Appl. Phys. Lett., 68, p.3171

24. Berkeley, D D, et al., 1993, Phys. Rev. B, 47, p.5524

25. Berkowitz, S J, et al., 1996, Appl. Phys. Lett., 69, p.2125

26. Berkowitz, S J, et al., 1996, Presented at the Applied Superconductivity Conf., Aug. 25-30, 1996, Pittsburg, PA

27. Berlincourt, T G, 1969, Phys. Lett., 29A, p.308 Boguslavskij, Yu M, K Joosse, F J G Roesthuis, G J Gerritsma and H Rogalla, 1993, Applied Superconductivity, Proc. of the First European Conference on Applied Superconductivity, October 4-9, 1993, Gottingen, DGM Informationsgesellschaft Verlag, Oberursel, H C Freyhardt Ed., p.1641

28. Bhattacharya, D, et al., 1993, Mater. Lett., 16, p.337

29. Boguslavskij, Yu M, K Joosse, A G Sivakov, F J G Roesthuis, G J Gerritsma and H Rogalla, 1994a, Physica C, 220, p.195

30. Boguslavskij, Yu M, K Joosse, F J G Roesthuis, G J Gerritsma and H Rogalla, 1994b, Physica B, 194-196, p.85

31. Borck, J, S Linzen, K Zach, and P Seidel, 1993, Physica C, 213, p.145

32. Bose, E, 1906, Physik. Z., 7, p.373

33. Bradley, P, 1993, IEEE Trans. Appl. Supercond., 3, p.2550

34. Brick, R M, 1954, Copper the Metal its Alloys and Compounds, Allison Butts (Ed.), Chap. 22, Reinhold, New York.

35. Brorsson, G, Yu Boikov, Z G Ivanov and T Claeson, 1993, IEEE Trans. Appl. Supercond., 3, p.2922

36. Broussard, P R, V C Cestone, L H Allen, and M E Reeves, 1992, Mat. Res. Soc. Symp. Proc., 275, p.507

37. Bulaevskii, L N, et al., 1992, Phys. Rev., B45, p.2545

38. Burbidge, D S, S K Dew, B T Sullivan, N Fortier, R R Parsons, P J Mulhern, J F Carolan and A Chaklader, 1987, Solid State Commun., 64, p.749

39. Burlachkov, L, I B khalfin and B Ya Shapiro, 1993, Phys. Rev. B, 48, p.1156

40. Button, T W, et al., 1991, IEEE Trans. Magn., 27, p.1434

41. Cambridge, J D Mc, et al., 1996, Presented at the Applied Superconductivity Conf., Aug. 25-30, 1996, Pittsburg, PA

42. Cardwell, D A, et al., 1994, Cryogenics, 34, p.671

43. Chang, L D, M Z Tseng, E L Hu, and D K Fork, 1992, Appl. Phys. Lett., p.1753

44. Char, K, D K Fork, T H Geballe, S S Laderman, R C Taber, R D Jacowitz, F Bridges, G A N Connell, and J B Boyce, 1990a, Appl. Phys. Lett., 56, p.785

45. Char, K, N Newman, S M Garrison, R W Barton, R C Taber, S S Laderman, and R D Jacowitz, 1990b, Appl. Phys. Lett., 57, p.409

46. Chaudhari, P, R H Koch, R B Laibowitz, T R McGuire, and R J Gambino, 1987, Phys. Rev. Lett., 58, p.2684

47. Chen, D-X, R B Goldfab, J Nogues, and K V Rao, 1988, J. Appl. Phys., 63, p.980

48. Chen, J, T Yamashita, H Sasahara, H Suzuki, H Kurosawa and Y Hirotsu, 1991, IEEE TRans. Appl. Supercond., 1, p.102

49. Chiang, Y M, J A S Ikeda, and A Roshko, "Ceramic Superconductors II", M. F. Yan, ed., 1988, American Ceramic Society, Westerville, Ohio, p.607

50. Choi, H K, R Hull, H Ishiwara, and R J Nemanich, eds., (1988), Mat. Res. Soc. Symp. Proc., 116, Pittsburgh, PA

51. Chromik, S, J Sith, V Strbik, J Schilder, V Smatko, S Benacka, V Kliment, and J Levarsky, (1989), J Appl Phys., 66, p.1477

52. Clarke, J, 1993, "SQUIDs: Theory Practice",in the New Superconducting Electronics, H Weinstock and R W Ralson, Eds., Kluwer Academic Publ., p.123

53. Chu, C W, et al., 1988, Phys. Rev. Lett., 60, p.941

54. Chu, C W, et al., 1993, Nature, 365, p.323

55. Chu, C W, 1997, IEEE Trans. Appl. Supercond., 7, p.80

56. Chwalek, J M, C Uher, J F Whitaker, G A Mourou, J Agostinelli and M Lelental, 1990, Appl. Phys. Lett., 57, p.1696

57. Clark, T D; R J Prance and A D C Grassie, 1980, J. Appl. Phys., 51, p.2736

58. Danerud, M, D Winkler, M Lindgren, M Zorin, V Trifonov, B S Krasik, G N Gol'tsman and E M Gershenzon, 1994, J. Appl. Phys., 76, p. 1902

59. Davidson, A, and N F Pedersen, 1994, Proc. of the Appl. Supercond. Conference 1994, EUE-5

60. Deng, Z J, et al., 1995, Extended Abs. , 5th Int. Superconductive Electronics Conf., (ISEC'95), Nagoya, Japan, Sep 18-21

61. Deng, Z J, et al., 1996. Presented at the Appl. Supercond. Conf., Aug. 25-30, Pittsburg, PA

62. Dimesso, L, et al., 1992, Physica C, 203, p.403

63. Dimos, D, P Chaudhari, J Mannhart and F K LeGouse, 1988, Phys. Rev. Lett., 61, p.219

64. Donaldson, G B, et al., 1993, The New Superconducting Electronics, H Weinstock and R W Ralston, Eds., Kluwer Academic Publishers, p.181

65. Dong, Z W, V C Matijasevic, P Hadley, S M Shao and J E Mooij, Proc. of the Appl. Supercond. Coference, 1994, EUE-5

66. Dong, Z W, 1995, "High T Superconducting Thin Film Devices", PhD thesis, Delft University Press, Stevinweg 1, 2628 CN Delft, The Netherlands

67. Doss, James D, 1989, Engineer's guide to high-temperature superconductivity, John Wiley & sons, New York

68. Dou, S X, et al., 1989, Physica C, 158, p.93

69. Doughty, C, C Kwon, Q Li, X X Xi, T Venkatesan, A Walkenhorst, K Petersen and H Adrian, Applied Superconductivity, Proc. of the first European Conference on Applied Superconductivity, Oct. 4-9, 1993, Gottingen, DGM Informationsgesellschaft Verlag, Oberursel, H C Freyhardt Ed., 1457

70. Doyle, J P, R A Roy, J J Cuomo, S J Whitehair, L Mahoney, and T R McGuire, 1990, AIP Conf. Proc. (USA), 200, p.102

71. Drung, D, et al., 1996a, Appl. Phys. Lett., 68, p.1856

72. Drung, D, et al., 1996a, Appl. Phys. Lett., 68, p.1421

73. Du, Z L, et al., 1989, in Proc. of the 10th Anniversary High T_c Supercond. Workshop on Phys., Mater., and Appl., Balogg et al., Eds. Singapore, World Scientific

74. Dubash, N D, et al., 1996, Presented at the Appl. Supercond. Conf., Aug. 25-30, Pittsburg, PA

75. Dubots, P, and J Cave, 1988, Cryogenics, 28, p.661

76. Duzer, T V, 1997, IEEE Trans. Appl. Supercond., 7, p.98

77. Duzer, T V, 1980, IEEE Trans. Microwave Theory and Tech., MTT-28, p.490

78. Edelman, H S, 1997, J Appl. Phys., 8, p.2296

79. Eesley, G L, J Heremans, M S Meyer, G L Doll and S H Liou, 1990, Phys. Rev. Lett., 65, p.3445

80. Ekin, JW, A I Braginski, A J Panson, M A Janoko, D W Capone II, N J Zaluzec, B Flandermeyer, O F de Lima, M Hong, J Kwo, and S H Liou, 1987, J. Appl. Phys., 62, p.4821

81. Er, G, et al., 1991, Physica C, 181, 206

82. Ezura, E, et al., 1993, Japan. J. Appl. Phys. Part I, 32, p.3435

83. Fang, Y K, K H Chen, S B Hwang, S J Wu, C R Liu, W T Lin, and J R Chen, 1992, Thin Solid Films, 208, p.228

84. Feenstra, R, L A Boatner, J D Budai, D K Christen, M D Galloway, and D B Poker, 1989, Appl. Phys. Lett., 54, p.1063

85. Feld, B A, et al., 1996, IEEE Trans. Appl. Supercond., 6

86. Felsch, W, and R E Glover, 1971, J. Vac. Sci. Technol., 9, p.333

87. Findikoglu, A T, C Doughty, S Bhattacharya, Z Li, X X Xi, T Venkatesan, R E Fahey, A J Strauss, and J M Phillips, 1992, Appl. Phys. Lett., 61, p.1718

88. Findikoglu, A T, S Bhattacharya, C Doughty, M S Pambianchi, A Li, X X Xi, S M Anlage, R E Fahey, A J Strauss, J M Phillips, and T. Venkatesan, 1993, IEEE Trans. on Appl. Superconductivity, 3, p.1425

89. Finnemore, D K, R N Shelton, J R Clem, R W McCallum, H C Ku, R E McCarley, S C Chen, P Klavins and V Kogan, 1987, Phys. Rev. B, 35, p.5319

90. Fiory A T and A F Hebard, 1984, Phys. Rev. Lett., 52, p.2057

91. Fiory, A T, and A F Hebard, 1985, Physica B, 135, p.124

92. Fiory, A T, A F Hebard, R H Eick, P M Mankiewich, R E Howard,

93. and M L P Malley, 1990, Phys. Rev. Lett., 65, p.3441

94. Fiory, A T, A F Hebard, R H Eick, P M Mankiewich, R E Howard, and M L P Malley, 1991, Phys. Rev. Lett., 67, p.3196

95. Fogarassy, E, C Fuchs, J P Stoquert, P Siffert, P Perriere, and F Rochet, 1989, J. Less. Common Mater., 151, p.249

96. Fork, D K, D B Fenner, R W Barton, J M Phillips, G A N Connell, J B Boyce, T H Geballe, 1990, Appl. Phys. Lett. 57, p.1161

97. Frank, D J, M J brady and A Davidson, 1985, IEEE Trans. Magn., 21, p.721

98. Frenkel, A, M A Saifi, T Venkatesan, C Lin, X D Wu and A Inam, 1989, Appl. Phys. Lett., 54, p.1594

99. Frenkel, A, T Venkatesan, C Lin, X D Wu and A Inam, 1990, J. Appl. Phys., 67, p.3767

100. Frey, T, J Mannhart, J G bednorz and E J Williams, 1995, Phys. Rev. B, 51, p.3257

101. Frey, T, J Mannhart, J G Bednorz and E J Williams, 1995, "High-T Superconductor-Insulator-Superconductor Hetrostructures with Highly Resistive Insulator Layers" preprint

102. Fukutomi, M, S Aoki, K Komori, R Chatterjee, and H Maeda, 1994, Physica C, 219, p.333

103. Fujii, T, K Sakuta, T Awaji, K Matsui, T Hirano, Y Ogawa and T Kobayashi, 1992, Japn. J. Appl. Phys., 31, p.L612

104. Gao, L, et al., 1993, Physica C, 213, p.261

105.Gao, L, et al., 1994, Phys. Rev. B "Rapid Communication",50, p.4260

106.Gao, L, et al., 1995, Mod. Phys. Lett. B, 9, p.1397

107.Garcia, J, C Rillo, F Lera, J Bartolome, R Navarro, D H A Blank and J Flokstra, 1987, J. Magn. Mater., 69, p.L225

108.Gasparov, V A, A F Dite, S F Kondakov, N M Sorokin, S S Khasanov, and V G Yaremenko, 1990, Superconductivity: Physics, Chemistry, Technology, 3, p.387

109.Gavala, J R, et al., 1974, Appl. Phys., 46, p.3009

110.George, Joy, 1992, Preparation of thin films, Marcel Dekker, Inc., New York

111.Gerber, Ch, et al., 1991, nature, 350, p.279

112.Gerdemann, R, T Bauch, L Alff, A Beck and R Gross, 1995a, Proc. of the HTS-Worhshop on Applications and New Materials, Twente University Enschede, The Netherlands, May 8-10, 1995

113.Gerdemann, R, L Alff, A BAck, O M Froehlich, B Mayer and R Gross, 1995b, Proc. of the Appl. Supercond. Conference 1994, EUB-13

114.Ghinovker, M, V B Sandomirski and B Ya Shapiro, 1995a, Sol. State Comm., 93, p.209

115.Ghinovker, M, V B Sandomirski and B Ya Shapiro, 1995b, Phys. Rev. B, 51, p.8404

116.Ghis, A, J C Villwgier, S Pfister, M Nail and Ph Gibert, 1993, Appl. Phys. Lett., 63, p.551

117.Ginzburg, V L, and D A Kirzhnitz, Eds., 1992, High Temperature Superconductivity, New York, Consultant Bureau

118.Glover, R E and M D Sherrill, 1960, Phys. Rev. Lett., 5, p.248

119.Golden, S J, F F Lange, D R Clarke, L D Chang and C T Necker, 1992, Appl. Phys. Lett., 61, p.351

120.Goldfarb, R B, A F Clark, A I Braginski and A J Panson, 1987, Cryogenics, 27, p.475

121.Golobov, E M, N A Prytkova, Zh M Tomilo, D M Turtsevich, and N M Shimanskaya, 1993, Superconductivity: Physics, Chemistry, Technology, 6, p.282

122.Golovashkin, A I, E V Ekimov, S I Krasnosvobodtsev, V P Martovitsky, E V Pechen and P N Lebedev, 1989, Physica C, 162-164, p.715

123.Gomeniuk, Yu V, N I Klyui, V Z Lozovski, V S Lysenko, A Yu Prokof'ev, B N Romanyuk, T N Sytenko and I P Tyagul'skii, 1991 Superconductivity, 4, p.671

124.Gomeniuk, Yu V, V Z Lozovski, V S Lysenkoand I P Tyagul'skii,

125.1993a, Physica C, 214, p.127

126.Gomeniuk, Yu V, V Z Lozovski, V S Lysenko and I P Tyagul'skii, 1993b, Solid State Communications, 85, p.643

127.Goshal, U, et al., 1993, IEEE Trans. Appl. Supercond., 3, p.2315

128.Goshal, U, et al., 1995a, IEEE Trans. Appl. Supercond., 5, p.2640

129.Goshal, U, et al., 1995b, Ext. Abs. , 5th Int. Superconductive Electronics Conf. (ISEC'95), Nagoya, Japan, Sept 18-21

130.Goto, T, S Iwabuchi, R Suzuki, X Y Cai, K Usami and T Kobayashi, Extended Abstracts of HTSED Workshop'94, May 26-28 Whistler, Canada, Research and Development Association for Future Electron Device, p.148

131.Gray, K E, 1978, Appl. Phys. Lett., 32, p.392

132.GuéP, et al., 1980, IBM J. Res. Develop., 24, p.155

133.Guo, R, A S Bhalla, L E Cross and R Roy, 1994, J. Mater. Res., 9, p.1644

134.Gupta, A, G Koren, E A Giess, N R Moore, E J M O' Sullivan, and E I ZCooper, 1988, Appl. Phys. Lett., 52, p.163

135.Gupta, R P and J Freyer, 1979, Intl. J. Electron., 47, p.459

136.Gupta, R P, W S Khokle, R C Dubey, S Singhal, K C Nagpal, G S

137.T Rao, and J D Jain, 1988, Appl. Phys. Lett., 52, p.1987

138.Gupta, R P, W S Khokle, C C Tripathi, J P Pachauri and S U M Rao, 1989, Supercond. Sci. Technol., 1, p.340

139.Gupta, R P, W S Khokle, J Wuerfl, and H L Hartnagle, 1990, J. Electrochem. Soc., 137, p.631

140.Gupta, R P, W S Khokle, A Agarwal, G S Virdi, B C Pathak and P D Vyas, 1990, (A report)

141.Gupta, R P, G S Shekhawat, R R Mishra, A Agarwal, W S Khokle, and P D Vyas, 1996, Proc. of Int. conf. on High Temp. Superconductors: Ten years after its discovery, Dec. 16-21, Jaipur, India, in press

142.Gupta, R P and W S Khokle 1993, in Mat. Sc. Forum, 137-139, Trans. Tech Publications Ltd. Switzerland, p.707

143.Gurvitch, M, H L Stormer, R C Dynes, J M Greybeal, and D C Jacobson, 1986, Bull. Am. Phys. Soc., 31, p.438

144.Gurvitch, M, H L Stormer, R C Dynes, J M Graybeal and D C Jacobson, MRS Proc., J Bevk and A I Braginski (eds.), 1986, p.47

145.Haetke, H, H P Lang, R Sum, H J Guntherodt, L Berthold, and D Hesse, 1992, Appl. Phys. Lett., 61, p.2359

146.Hagberg, J, et al., 1993, Appl. Supercond., 1, p.1091

147.Hakuraku, Y, S Higo and T. Ogushi, 1989, Appl. Phys. Lett., 55, p.1569

148.Hakuraku, Y, Y Aridome, D M Yagi, N G Suresha and T Ogushi, 1989, Jpn. J. Appl. Phys., 2(28), p.L819

149.Hakuraku, Y, et al., 1992, J Appl. Phys., 73, p.309

150.Hamet, J F, B Mercey, M Hervieu and B Raveau, 1992a, Physica C, 193, p.465

151.Hamet, J F, B Mercey, M Hervieu, G Poullain and B Raveau, 1992b, Physica C, 198, p.293

152.Hamilton, C A, et al., 1985, IEEE Electron Device Lett., EDL-6, p.623

153.Han, X, J-F Jiang and M Sugahara, 1993, IEEE Trans. Appl. Supercond., 3, p.2918

154.Han, S G, Z V Vardeny, K S Wong, O G Symko and G Koren, 1990, Phys. Rev. Lett., 65, p.2708

155.Harshavardhan, K S, S M Green, A Pique, K Patel, R Edwards, T Venkateshan, E Denlinger, D Kalokitis, A Fathy, V Pendrick, X D Wu, S Bhattacharya and M Rajeshwari, 1993, AIP Conference Proceedings, 208, p.607

156.Hase, Takashi, Hiromi Takahashi, Hirohiko Izumi, Katsumi Ohata, Katsumi Suzuki, Tadataka Morishita, and Shoji Tanaka, 1991, J. of Crystal Growth, 115, p.788

157.Hashimoto, K, U Kabasawa, M Tonouchi and T Kobayashi, 1981, Progress in high temperature superconductivity, Vol. 15, (Y Murakami, Ed.) World Scientific, Singapore, p.315

158.Hasoya, M, et al., 1996, Presented at Appl. Supercond. Conf., Aug 25-30, Pittsburg, PA

159.Hatano, Y. et al., 1989, DIG. Tech. Papers, Int. Solid-State Circuits Conf., New York, p.234

160.Hato, T, H Takauchi, A Yoshida, H Tamura and N Yokoyama, 1994, Extended Abstracts of the HTSED Workshop'94 May 26-28 Whistler, Canada, Research and Development Association for Future Electron Devices, p.122.

161.Hawley, M et al., 1991, Science, 251, p.1587

162.Hazelton, D W, L Chen, T W Piazza, A Sweeney and A E Kaloyeros, 1992, AIP Conf. Proc., 251, p.214

163.Hazen, R M, et al., 1988a, Phys. Rev. Lett., 60, p.1174

164.Hazen, R M, et al., 1988b, Phys. Rev. Lett., 60, p.1657

165.Hebard, A F, A T Fiory and R H Eick, 1987, IEEE Trans. on Mang., MAG-23, p.1279

166.Hein, R A, T L Francavilla and D H Liebenberg, eds., 1992, Magnetic Susceptibility of Superconductors and other Spin Systems, Plenum Press, New York.

167.Henhels, W H and H H Zappe, 1978, IEEE J. Sold-State Circuits, SC-13, p.591

168.Herr, Q P, et al., 1996, Presented at Appl. Supercond. Conf., Aug 25-30, Pittsburg, PA

169.Hesse, D, L Berthold, H Haefke, H P Lang, R Sum and H J Guntherodt, 1992, Physica C, 202, p.277

170.Higashino, H, K Setsune and K Wasa, 1989a, Proc. of the ISS'89, Tsukuba, Japan, 1989, p.981

171.Higashino, H, A Enokihara, K Mizuno, K Setsune and K Wasa, 1989b, Ext. Abstr. of FED 2nd Worhshop on High T Superconducting Electron Devices, p.257

172.Higashino, H, K Mizuno, T Matsushima, K Setsune and K Wasa, 1990, in Advances in Superconductivity III, Proc. of the ISS'90, Kajimura and Hayakawa (eds.), Springer 1991, p.1227

173.Hilsch, P and D G Naugle, 1967, Zeit. f. Phys., 201, p.1

174.Hirata, T and M Naoe, 1990, J. Appl. Phys., 67, p.4047

175.Holesinger, T G, et al., 1995, Physica C, 243, p.93

176.Hong, M, S H Liou, J Kwo and B A Davidson, 1987, Appl. Phys. Lett., 51, p.694

177 Hong, M, J Kwo, C H Chen, A R Kortan and D D Bacon, 1988, AIP Conf. PROC. (USA), 182, p.107

178 Hor, P H, et al., 1987, Phys. Rev. Lett., 58, p.1891

179 Hosoya, Y, M Naoe and S Yamanaka, 1977, Jpn. J. Appl. Phys., 16, p.1715

180 Hsieh, M H and H C Yang, 1990, Chin. J. Phys., 28, p.287 Hsu, H M, I Yee, J De Luca, C Hilbert, R F Miracky and L N Smith, 1989, Appl. Phys. Lett., 54, p.957

181 Hu, J, D J Miller, D L Schulz, B Han, D A Neumayer, B J Hinds and T J Marks, 1993, Physica C, 210, p.97

182 Huang, Z J, et al., 1993, Physica C, 217, p.1

183 Hwang, D W, R Ramesh, C Y Chen, X D Wu, A Inam, M S Hedge, B Wilkens, C C Chang, J Nazar, T Venkatesan, M S Matsubara, Y Miyasaka and N Shohata, 1990, J. Appl. Phys., 68, p.1772

184 Iguchi, I, K Nakui and K Lee, 1994, Phys. Rev. B, 50, p.457

185 Ihara, H, et al., 1994, Jpn. J Appl. Phys., 33, p.L300

186 Iijima, Y, N Tanabe, O Kohno and Y Ikeno, 1992, Appl. Phys.

187 Lett., 60, p.769

188 Iijima, Y, O Onabe, N Futaki, N Tanabe, N Sadakata, O kohno and Y Ikeno, 1993, IEEE Trans. Appl. Superconductivity, 3, p.1510

189 Ingle, N J C, et al., 1995, Supercond. Sci. Technol., B, p.282

190 Irwin, K D, 1995, Appl. Phys. Lett., 66, p.1988

191 Ishida, T and h Mazaki, 1981, J. Appl. Phys., 52, p.6798

192 Ivanov, Z G, E A Stepantsov, A Ya Tzalenchuk, R I Shekhter and T Claeson, 1993, IEEE Trans. Appl. Supercond., 3, p.2925

193 Jager, A, J C Villwgier, P Bernstein, J Bok and L Force, 1993, IEEE Trans. Appl. Supercond., 3, p.2933

194 Jeffery, M, et al., 1995, Appl. Phys. Lett., 67, p.1769

195 Jeffery, M, et al., 1996, Appl. Phys. Lett., 69

196 Jenks, w G and L R Testardi, 1993, Phys. Rev. B, 48, p.1293

197 Jia, Q X, S Y Lee, W A Anderson, and D T Shaw, 1992, Physica C, 190, p.266

198 Jia, Q X, and W A Anderson, 1992, Appl. Phys. Lett., 60,

199 Jia, Q X and W A Anderson, 1992, AIP Conf. Proc., 251, p.96

200 Jiang, J F, N Yoshikawa, X Y Han and M Sugahara, 1991, Supercond. Sci. Technol., 4, p.468

201 Jones, A R, et al., 1994, Appl. Phys., 76, p.1720

202 Jones, A R, et al., 1995, Appl. Supercond., 3, p.47

203 Joosse, K, Yu M Boguslavskij, G J Gerritsma and H Rogalla, 1993a, J. of Alloys and Compounds, 195, p.723

204 Joosse, K, Yu M Boguslavskij, G J Gerritsma and H Rogalla, 1993b, Applied Superconductivity, Proc. of the First European

205 Conference on Applied Superconductivity, October 4-9, 1993, Gottingen, DGM Informationsgesellschaft Verlag, Oberursel, H C Freyhardt Ed., p.861

206 Joosse, K, Yu M Boguslavskij, G J Gerritsma, H Rogalla, J G Wen and A G Sivakov, 1994, Physica C, 224, p.179

207 Josephson, B D.1962, Phys. Lett., 1, p.251

208 Kabasawa, U, K Asano and T Kobayashi, 1990, Jpn. J. Appl. Phys., 29, p.L86

209 Kanehori, K, N Sughii, T Fukazawa, and K. Miyauchi, 1989, Thin Solid Films, 182, p.265

210 Kaplunenko, V K, et al., 1995, Appl. Phys. Lett., 67, p.282

211 Karasik, B S, M A Zorin, I I Milostnaya, A I Elantev, G N Gol'tsman and E M Gershenzon, 1995, J. Appl. Phys., 77, p.4064

212 Kawai, M, T Kawai, H Masuhira and M Takahasi, 1988, in Materials Research Society Symposium proceedings, vol. 99, Merwyn B Brodsky, Robert C Dynes, Koichi Kitazawa and Harry L Tuller (Eds.), Materials Research Society, Pennsylvania, p.395

213 Kawashima, T, et al., 1994a, Physica C, 224, p.69

214 Kawashima, T, et al., 1994b, Physica C, 227, p.95

215 Kawecki, T G, 1996, The High Temperature Space Experiment (HTSSE-II) Design, IEEE Trans. Microwave Theory and Tech., 44, p.1198

216 Kechiantz, A M, 1990, in Progress in High-Temperature Superconductivity, 24, World Scientific, Singapore, p.556

217 Kechiantz, A M, 1992, Physica C, 196, p.48

218.Khokle, W S, 1988, Proc. 5th Intl. Workshop on Future Electron Devices, (FED Hi T -ED Workshop) Miyagi-Zao-Japan, FED-65, p.133

219.Khokle, W S and R P Gupta, 1990, Ind. J Radio & Space Phys., 19, p.309

220.Klein, J D, Y Yen, and S L Clauson, 1990, J. Appl. Phys., 67, p.6389

221.Kleinsasser, A W and W J Gallagher, 1990, in Superconducting Devices, S F Ruggiero and D A Rudman (Eds.), Academic Press, Boston, p.325

222.Kleinsasser, A W, 1992, The New Superconducting Electronics, Kluwer Academic Publishers, The Nitherland, NATO Advanced Studies Institute, 1

223.Kliuy, Yu V, V Z Lozovski, V S Iysenko, A Yu Prokofiev, B N Romaniuk, T N Svtenko and IP Tyagul'skii, 1991, Superconductivity: Physics Chemistry Technique, 4, p.762

224.Kobayashi T and U Kabasawa, 1989, Studies of high temperature superconductors, Vol. 1, (Anant Narlikar, Ed.) Nova Science Publishers, NY, p.211

225.Kobayashi, T, K Hashimoto, U Kabasawa and M Tonouchi, 1989, IEEE Trans. Magn., MAG-25, p.927

226.Kobayashi, T, 1994a, Electronics and Communications in Japan, 2, p.56

227.Kobayashi, T, T Ashida, M Taga and M Iwabuti, 1994, Extended Abstracts of the HTSED Workshop'94, May 26-28 Whistler, Cannada, Research and Development Association for Future Electron Devices, p.74

228.Koelle, D, R Kleiner, F Ludwig, A H Miklich, E Dantsaer and J Clarke, 1995, Appl. Phys. Lett., 66, p.640

229.Kohno, O, Y Iijima, K Onabe, N Futaki, N Sadakata, N Tanabe and Y Ikeno, 1993, Appl. Superconductivity, 1, p.645

230.Konsin, P, 1994 Physica C, 235-240, p.1437 Koshy, J, J Kurian, Y P Yadava, P K Sajith, A D Damodaran, S P Pai, Dhananjayakumar, R Pinto and R Vijayaraghavan, 1994, Physica C, 225, p.101

231.Koshy, J, et al., 1993, Physica C, 215, p.209

232.Koshy, J, et al., 1994, Bull. Mater. Sci., 17, p. 577

233.Kotani, S, et al., 1988, Digest Tech. Papers, Int. Solid-State Circuits Conf., San Francisco, p.150

234.Kotani, S. et al., 1990, Digest Tech. Papers, Int. Solid-State Circuits Conf., San Francisco, p.148

235.Kumar, A and J Narayan, 1993, Supercond. Science and Technol., 6, p.662

236.Kupfer, H, I Apfelstedt, W Schauer, R Flukiger, R Meier-Hirmer and H Wuhl, 1987, *Z Phys. B*, 69, p.159

237.Kurtan, J, et al., 1995, J. Solid State Chem., 116, p.163

238.Kwo, J, M Hong, D J Trevor, R M Fleming, A E White, R C Farrow, A R Kortan, and K T Short, 1988, Appl. Phys. Lett., 53, p.2683

239.Kwon, C, et al., 1993, published in Appl. Phys. Lett.

240.Lang, H P, H Haefke, R Sum, H J Guntherodt, L Berthold, and D Hesse, 1992, Physica C, 202, p.289

241.Langlet, M, E Senet, J L Deschanvres, G Delabouglise, F Weiss, and J C Joubert, 1989, Thin Solid Films, 174, p.263

242.Larbalestier, D C, M Daeumling, X Cai, J Seuntjens, J Mekinnell, D Hampshire, P Lee, C Meingast, T Wills, H Muller, R D Ray, R G Dillenburg,E E Hellstrom and R Joynt, 1987, J. Appl. Phys., 62, p.3308

243.Larbalestier, D C, et al., 1996, Proc. of 8th Int. Conf. on Critical Currents of Superconductors, Kitakyushu, Japan, Ed. K Yamafuji, World Scientific, 1996, p.87

244.Larbalestier, D C, 1997, IEEE Trans. *Appl. Supercond.*, 7, p.90

245.Lau, S S, W X Chen, E D Marshall, C S Pai, W F Tseng and T F Kuech, 1995, Appl. Phys. Lett., 47, p.1298

246.Lay, K W and J E Tkaczyk, 1994, Appl. Supercond., 2, p.677

247.Levy, A, J P Falck, M A Kastner, R J Birgeneau, A T Fiory, A F Hebard, W J Gallagher, A W Kleinsasser and A C Anderson, 1992, Phys. Rev. B, 46, p.520

248.Li, Q, et al., 1990, Phys. Rev. Lett., 64, p.3086

249.Li, Q, et al., 1992, Phys. Rev. Lett., 69, p.2713

250.Li, Q, et al., 1992b, Phys. Rev., 46, p.5957

251.Li, Q, et al., 1997, Appl. Phys. Lett., 70, p.1164

252.Likharev, K K, et al., 1985, in SQUID'S 85, Berlin, Germany: W de Gruyter, p.1103

253.Lin, H, N J Wu, K Xie, X Y Li and A Ignatiev, 1994, Appl. Phys. Lett., 65, p.953

271.Martens, J S, T E Zipperian, V M Hietala, D S Ginley, C P Tigges, J M Phillips and M P Siegal, 1993c, IEEE Trans. Electron Dev., 40, p.656

272.Masumoto, H, T Goto and T Hirai, 1989, Appl. Phys. Lett., 55, p.498

273.Matijasevic, V C, S Bogers, N Y Chen, H M Appelboom, P Hadley and J E Mooij,1994, Physica C, 235-240, p.2097

274.Matisoo, J, 1967, Proc. of the IEEE, 55, p.172

275.Matsui, K, T Awaji, T Hirano, T Fujii, K Sakuta and T Kobayashi, 1992, Jpn J. Appl. Phys., 31, p.3195

276.May, P, 1988, Supercond. Sci. Technol., 1, p.1

277.Mazaki, H and T Ishida, 1987, Jpn. J. Appl. Phys., 26, p.L1508

278.McQuillan, A D and M K McQuillan, 1956, Metallurgy of the Rarer Metals, No. 4, Titanium, Chapter 7, Butterworth, London

279.Meng, R L, et al., 1993, Physica C, 216, p. 21

280.Miedema, A R, 1976, Phil. Tech. Rev., 36, p.217

281.Mishonov, T M, 1991, Phys. Rev. Lett., 67, p.3195

282.Miyahara, K, S Kubo and M Suzuki, 1994, J. Appl. Phys., 76, p.4772

283.Moeckly, B H, S E Russek, D K Lathorp, R A Buhrman, J Li and J W Mayer, 1990, Appl. Phys. Lett., 57, p.1687

284.Moore, D F, 1989, in Proc. of the 2nd Workshop on High Temperature Superconducting Electron Devices, R&D Association for Future Electron Devices, June 7-9, 1989, Shikabe, Japan, p.281

285.Morosini, B, et al., 1988, Physica C, 152, p.413

286.Murarka, S P, 1983, Silicides for VLSI Applications, A. P., New York, p.29

287.Mukhanov, O A, 1993, IEEE Trans. Appl. Supercond., 3, p.3102

288.Myoren H, T Ishikawa and Y Osaka, 1991, Physica C, 185-189, p.2529

289.Nakajima, K, K Yokota, H Myoren, J Chen and T Yamashita, 1993, Appl. Phys. Lett., 63, p.683

290.Nakajima, K, K Yokota, J Chen, H Myoren and T Yamashita, 1994, Jpn. J. Appl. Phys.,33, p.L934

291.Nakamura, T, S Tanaka, H Tokuda, T Fujimoto and M Iiyama, 1994, Sumitomo Electric Technical Review, 38, p.35

314.Prakash, S, D M Umarjee, H J Doerr, C V Deshpandey and R F Bunshah, 1989, Appl. Phys. Lett., 55, p.504

315.Pradhan, A K, et al., 1995, IEEE Trans. Appl. Supercond., 5, p.2248

316.Putilin, S N, et al., 1991a, Matr. Res. Bull., 26 p.1299

317.Putilin, S N, et al., 1991b, Nature, 362, p.226

318.Putilin, S N, et al., 1993, Physica C, 212, p.266

319.Rajeevakumar, T V, 1981, Appl. Phys. Lett., 39, p.439

320.Ramesh, R, A Inam, W A Bonner, P England, B J Wilkens, B J Meagher, L Nazar, X D Wu, M S Hegde, C C Chang and T Venkatesan, 1989, Appl. Phys. Lett., 55, p.1138

321.Rao, C N R and J Gopalakrishnan, 1986, New directions in solid state chemistry, Cambridge University Press, Cambridge.

322.Remillard, S K, et al., 1990, Physica C, 177, p.345

323.Roas, B, L Schultz and G Endres, 1988, Appl. Phys. Lett., 53, p.1557

324.Russo, R E, R P reade, J M McMillan and B L Olsen, 1990, J. Appl. Phys., 68, p.1354

325.Rylov, S V, et al., 1996, Presented at the Appl. Supercond. Conf., Aug 25-30, Pitsburg, PA

326.Sanchez, F, M Varela, X Queralt, M V Garcia - Guenca, R Aguiar and J L Morenzza, 1992, Physica C, 195, p.47

327.Sandstrom, R L, E A Giess, W J Gallagher, A Segmuller, E I Cooper, M F Chisholm, A Gupta, S Shinde and R B Laibowitz, 1988, Appl. Phys. Lett., 52, p.1874

328.Sasura, M, M Mukaida and S Miyazawa, 1990, Appl. Phys. Lett., 57, p.2728

329.Satchell, J S, J A Edwards, N G Chew, R G Humphreys, 1992, Elect. Lett., 28, pp. 781

330.Satchell, J S, R G Humphreys, J A Edwards, N G Chew, 1993, IEEE Trans. Appl. Supercond., 3, pp. 2273

331.Sato, H, K Ayusawa, T Arai and K Kawamura, 1988, 5th International Workshop on Future Electron Devices - High Tenp. Supercond. Electron Devices, June 2-4, Miyagi-Zao, p.115

332.Savvides, N and A Katsaros, 1993, Thin Solid Films, 228, p.182

333.Scheib, M, H Goebel, L Hotman, D Lengeler, H Oechsner and G Zorn, 1989, Thin Solid Films, 174, p.5

334.Schilling, A, et al., 1993, Nature, 363, p.56

335.Schneider, C W, G J Gerritsma and H Rogalla, 1995, Proc. of HTS-Workshop on Applications and New Materials, Twente Univ., Enschede, The Nitherlands, May 8-10, 1995

336.Schneider, J, H Kohlstedt, and R Wordenweber, 1993, Appl. Phys. Lett., 63,2426

337.Scheider, J, A V D Hart, and R Wordenweber, 1994, Proceedings of the Appl. Supercond. Conference 1994, EUE-10

338.Schubert, J, U Poppe and W Sybertz, 1989, J. Less Common Met., 151, p.277

339.Schulz, D L, et al., 1995a, Mater. Res. Bull., 30, p.689

340.Schulz, D L, et al., 1995b, IEEE Trans. Appl. Supercond., 5 (part 2), p.1962

341.Semenov, A D, G N Gol'tsman, I G Gogidze, A V Sergeev, E M Gershenzon, P T Lang and K F Renk, 1992, Appl. Phys. Lett., 60, p.903

342.Semenov, V K, et al., 1996, Presented at Appl. Supercond Conf., Aug 25-30, Pittsburg, PA

343.Senda, M and O Ishii, 1991, J. Appl. Phys., 69, p.6586

344.Serbezov, V, S Benacka, D Hadgiev, P Atanasov, N Electronov, V Smatko, V Stribik and N Vassilev, 1990, J. Appl. Phys., 67, p.6953.

345.Sergeev, A V, A D Semenov, A Kouminov, V Trifonov, I G Goghidze, B S Karasik, G N Gol'tsman and E M Gershenzon, 1994, Phys. Rev. B, 49, p.9091

346.Setsune, K, M Kitabatake, T Matsushima, Y Ichikawa, H Adachi and K Wasa, 1989, Proceedings of the SPIE, Santa Clara

347.Shapiro, B Ya, 1984, Phys. Lett., 105A, p.374

348.Shapiro, B Ya, 1985, Sol. State Comm., 53, p.673

349.Shapiro, B Ya, 1993, Phys. Rev. B, 48, p.1672

350.Shapiro, B Ya, and I B Kholfin, 1993, Physica C, 209, p.99

351.Shapiro, B Ya, 1995, Phys. Lett., A 197, p.361

352.Shekhawat, G S, Ram P Gupta, A Agarwal, K B Garg and P D Vyas, 1995, Supercond. Sci. Technol., 8, p.291

353.Sheng, Z Z, and A M Hermann, 1988, Nature, 332, p.55

354.Sheng, Z. Z. et al., 1988, Phys. Rev. Lett., 60, p.937

355.Shewchun, J, Y Chen, J S Holder and C Uher, 1991, Appl. Phys. Lett., 58, p.2704

356.Shi, L. G L Huang, C Lehane, D H Kim and H S Kwok, 1993, Appl. Phys. Lett., 63, p.2830

357.Shokor, S. et al., 1995, Appl. Phys. Lett., 67, p.2869

358.Siegrist, T. et al., 1988, Nature, 334, p.231

359.Simon, R W, C E Platt, A E Lee, K P Daly, M S Wire, J W Luine and M Urbanik, 1988, Appl. Phys. Lett., 53, p.2677.

360.Smirnov, B I, S V Kristopov and T S Orlova, 1992, Sov. Phys. Solid State, 34, p. 1331

361.Smirnov, B I, T S Orlova and S V Kristopov, 1993, Phys. Solid State, 35, p. 1118

362.Smirnov, B I, T S Orlova and Kh-I Kaufmann, 1994, Phys. Solid State, 36, p. 252

363.Smith, M O, et al., 1991, Nature, 351, 549

364.Smithells, Colin J., 1955a, Metals Reference Book, Vol. 1, Butterworth, London, p.297

365.Smithells, Colin J., 1955b, Metals Reference Book, Vol. 2, Butterworth, London, p.580

366.Sorkin, B and P Konsin, 1994, Phys.Stat. Sol. (b), 185, p.K23

367.Special issue on the Microwave and Millimeter wave Applications of High Temp. Superconductivity, IEEE Trans. Microwave and Tech., July 1996

368.Spooner, A, et al., 1996, Presented at Appl. Supercond Conf., Aug 25-30, Pittsburg, PA

369.Srivastava, P, N L Saini, B R Sekhar, S Venkatesh, M Khaled, S K Sharma, K B Garg, A Agarwal, Ram P Gupta, W S Khokle, H Ohkubo and M Akinaga, 1994, Supercond. Sci. Technol., 7, p.940

370.Stadler, H L, 1965, Phys. Rev. Lett., 14, p. 979

371.Steenback, K, 1971, Journ. de Phys., C1, p. 1096

372.Subramanyam, G, F Radpour, V J Kapoor and G H Lemon, 1990, J. Appl. Phys., 68, p.1157

373.Suenaga, M, A Ghosh, T Asano, R L Sabatini and A R Moodenbaugh, in: "High Temperature Superconductors", D V Gubser and M Schlutter, eds., 1987, Materials Research Society, Pittsburg, EA-11, p.247

374.Sun, R, H P Lang, H Haefke, L Berthold, D Hesse and H J Guntherodt, 1993, J. Alloys and Compounds, 195, p.113

375.Suzuki, H, T Yamamoto, S. Suzuki, M. Iyori, K. Takahashi, T. Usuki, Y. Yoshisato and S. Nakano, *1993, Jpn J. Appl. Phys.*, 32, pp. 783

376.*Sze, H. et al., 1989, Bull Am. Phys. Soc.*, 34, p.517

377.Sze, S M, 1969, Physics of Semiconductor Devices, *Wiley Eastern Ltd.*, New Delhi, p.444

378.Tahara, S. et al., 1996, IEICE Trans. Electron, E 79-C, p.1193

379.Taheri, E H, K W Cochrane and G J Russell, 1995, J. Appl. Phys., 77, p.761

380.Takayanagi, H., T Kawakami, 1985, Phys. Rev. Letters, 54, p.2449

381.Takano, M, et al., 1992, Jpn. J Appl. Phys., 7, p.3

382.Takeuchi, K, T Yoshida, M Kawasaki, S Uchida, T Hirayama, M Yoshimoto, Y Saito, S Hayano and H Koniuma, 1989, Rep. Res. Lab. Eng. Mater., Tokyo Inst. Technol., 14, p.77

383.Takeya, H and H Takei, 1990, J. Cryst. Growth, 99, p.954

384.Tamura, H, A Yoshida, K Gotoh, S Hasuo and P Van Duzer, 1991, IEEE Trans. Magn., 27, p.2594

385.Tamura, H, A Yoshida, H Takauchi and S Hasuo, 1992, in Springer Proc. in Physics, Vol. 64, Superconducting Devices and their Appplications eds. H Koch and H Ltbbig, p.588

386.Tao, W, M P Yuan, H T Huang, X Z Liao, X M Xie, H L Zhou and Z L Wu, 1993, Appl. Phys. Lett., 62, p.894

387.Tarutani, Y, S Saitoh, T Fukazawa and U Kawabe, 1991, J Appl. Phys., 69, p.1778

388.Tazoh, Y, 1991, IEEE Trans. Magn., 27, p.79

389.Terashima, K, K Eguchi, T Yashida and K Akashi, 1988, Appl. Phys. Lett., 52, p.1274

390.Terashima, T, 1991, Phys. Rev. Lett., 67, p.1362

391.Thomas, J K, et al., 1995, Supercond. Sci. Technol., 8, p.525

392.Tiwari, P, S Sharan and J Narayan, 1991, Appl. Phys. Lett., 59, p.357

393.Tiwari, A N, S Blunier, H Zogg, Ph. Lerch, F Marcenat and P Martinoli, 1992, J. Appl. Phys., 71, p.5095

394.Toda, F and H Abe, 1994, Jpn. J. Appl. Phys., 33, p.L318

395.Toda, F, T Makita, R Kawasaki, Z Wen, T Yamada and H Abe, Extended Abstracts of the HTSED Workshop'94, May 26-28, Whistler, Canada, Research and Development Association gor Future Electron Devices, p.162

396.Tomita, N, et al., 1992, Jpn. J Appl. Phys., 31, p.L942

397.Toradi, C C, et al., 1988, Phys. Rev. B, 38, p.225

398.Tsabha, Y and S Reich, 1995, Physica C, 254, p.21

399.Umemura, T, S Matsuno, S Kinouchi, K Egawa, S Miyashita, F Uchikawa and Y Nakamayashi, 1993, Jpn. J. Appl. Phys., 32, p.L1513

400.Usuki, T, S Suzuki, M Iyori, K Yamano, H Suzuki, T Yamamoto and Y Yoshisato, 1993, Electr. and Communic. in Japan, 76, p73

401.Van Zeghbroeck, B J, 1983, Appl. Phys. Lett., 42, p.736

402.Vandriessche, I et al., 1994, Appl. Supercond., 2, p.391

403.Vanolo, M, et al., 1994, Nuovo Cimento Soc. Ital. Fis. D, 16, p.2119

404.Varma, H. K, K G K Warrier, K R Nair and A D Damodaran, 1988, Proceedings of the Seminar on Advanced Ceramics, Banaras Hindu Univ., Feb 16, p.16

405.Veblen, D R, 1988, Nature, 332, p.334

406.Venkatesan, T, X D Wu, A Lnam and J B Wachtman, 1988, J. Appl. Phys. Lett., 52, p.1193

407.Verghese, S, et al., J. Appl. Phys., 74, p.4251

408.Villégier, J C, A Jager, H Boucher, M Levis, H Moriceau, M Schwerdtfeger and M Vabre, 1991, SPIE, 1597, p.135

409.Wagner, P, et al., 1995, Phys. Rev. B, 51, p.1206

410.Walkenhorst, A, C Doughty, X X Xi, Q Li, C J Lobb, S N Mao and T Venkatesan, 1992, Phys. Rev. Lett., 69, p.2709

411.Walkenhorst, A, M Schmitt, H Adrian and K Petersen, 1994, Appl. Phys. Lett., 64, p.1871

412.Wang, J L, et al., 1994, Physica C, 230, p.189

413.Wang, J L, et al., 1996, J. Mater. Res., 11, p.868

414.Wang, Q and I Iguchi, 1993, IEICE Trans. Electron, E76-C, p.1271

415.Wang, Q and I Iguchi, 1994, Physica C, 228, p.393

416.Weast, R C, M J Astice and W H Beyer, 1984, CRC Handbook, CRC press, Florida

417.Wellhofer, F, et al., 1993, Mater. Sci. Eng. B, 21, p.19

418.Welp, U, et al., 1995, Appl. Phys. Lett., 66, p.1270

419.Wen, Z and H Abe, 1994, Jpn J Appl. Phys., 33, p.L1153

420.Wiegerink, R J, et al., 1995, IEEE Trans. Appl. Supercond., 5, p.3452

421.Wiegerink, R J, et al., 1996, Presented at the Applied Superconductivity Conf., Aug. 25-30, 1996, Pittsburg, PA

422.Witanachchi, S, H S Kwok, X W Wang and D T Sham, 1988, Appl. Phys. Lett., 53, p.234

423.Withers, R, 1996, Extended Abstracts, ISTEC Superconductivity Workshop, Iwate, Japan, June 1996

424.Worsham, A H, et al., 1996, Presented at Appl. Supercond. Conf., Aug 25-30, pittsburg, PA

425.Wu, K, S Kramer and G Kordas, 1988, in Materials Research Society Symposium proceedings, Vol. 99, Merwyn B Brodsky, Robert C Dynes, Koichi Kitazawa and Harry L Tuller (Eds.), Materials Research Society, Pennsylvania, p.395

426.Wu, M K, et al., 1987, Phys. Rev. Lett., 58, p.908

427.Wu, X, et al., 1995, Appl. Phys. Lett., 67, p.2397

428.Wu, X D, R E Miinchausen, S Foltyn, R C Estler, R C Dye, C Flamme, N S Nagar, A R Gracia, J Martin and J Tesmer, 1990, Appl. Phys. Lett., 56, p.1481

429.Wu, X J, et al., 1994, Physica C, 223, p.243

430.Xi, X X, J Geerk, Q Linker and O Meyer, 1989, J. Appl. Phys. Lett., 54, p.2367

431.Xi, X X, Q Li, C Doughty, C Kwon, S Bhattacharya, A T Findikoglu and T Venkatesan, 1991, Appl. Phys. Lett., 59, p.3470

432.Xi, X X, March meeting of the American Physical Society, Indianapolis, March 20, 1992

433.Xi, X X, C Doughty, A Walkenhorst, C Kwon, Q Li and T Venkatesan, 1992a, Phys. Rev. Lett., 68, p.1240

434.Xi, X X, C Doughty, A Walkenhorst, S N Mao, Q Li and T Venkatesan, 1992b, Appl. Phys. Lett., 61, p.2353

435.Xi, X X, 1993, FED Journal, 4, Suppl.1, p.10

436.Yamasaki, H, et al., 1993, IEEE Trans. Appl. Supercond., 3, p.1536

437.Yamashita, T, K Yokota, K Nakajima, H Myoren and J Chen, 1994, Extended Abstracts of the HTSED Workshop'94 May 26-28, Whistler, Canada, Research and Devepolment Association for Future Electron Devices, p.152

438.Yang, M, et al., 1994, Supercond. Sci. Technol., 7, p.378

439.Yin, E, M Rubin and M Dixon, 1992, J. Mater. Res., 7, p.1636.

440.Yoshida, A, H Tamura, H Takauchi and S Hasuo, 1991a, Appl. Phys. Lett., 59, p.1242

441.Yoshida, A, H Tamura, K Gotoh, H Takauchi and S Hasuo, 1991b, J. Appl. Phys., 70, p.4976

442.Yoshida, A, H Tamura, H Takauchi, T Imamura and S Hasuo, 1992, J. Appl. Phys., 71, p.5284

443.Yoshikawa, N, T Murakami and M Sugahara, 1990, Jpn. J. Appl. Phys., 29, p.1086

444.Yoshikawa, N, L Zhang and M Sugahara, 1991, IEEE Trans. Magn., MAG-27, p.3268

445.Yoshikawa, N, X Han, H Katoh and M Sugahara, 1994, Extended Abstracts of HTSED Workshop'94 May 26-28, Whistler, Canada, Research and Devepolment Association for Future Electron Devices, p.154

446.Yoshimoto, M, A Takano, H Nagata, M Kawasaki and H Komume, 1989, Res. Res. Lab., Eng. Mater., Tokyo Inst. Technol., 14, p.71

447.Young, K H, G V Negrete, M M Eddy, J Z Sun, T W James, McD, Robinson and E J Smith, 1991, Thin Solid Films, 206, p.116

448.Yuan, F, B Cheng, X Yiyuan, S Zhu, Y Wen, X Luo, J Chen and B Cui, 1993, Chinese J. Low Temp. Phys., 15, p.331

449.Zegbroeck, Bart J Van, 1985, IEEE Trans. Magn., MAG-21, p.916

450.Zeuner, S, H Lengfellner, J Betz, K F Renk and W Prettl, 1992, Appl. Phys. Lett., 61, p.973

451.Zhang, D, et al., 1995, IEEE Microwave and Guided wave Lett., 5 p.405

452.Zhang, J L, and J E Evetts, 1994, J. Mater. Sci., 29, p.778

453.Zhang, J M, B W Wessels, L M Tonge and T J Marks, 1990, Appl. Phys. Lett., 56, p.976

454.Zhang, Y M, D Winkler, P A Nillson and T Claeson, 1994, Appl. Phys. Lett., 64, p.1153

455.Zhang, Y M, et al., 1996, Presented at the Applied Superconductivity Conf., Aug. 25-30, 1996, Pittsburg, PA

456.Zhang, X Y, et al., 1992, Phys. Rev., B45, p.7584

LIST OF PUBLICATIONS

1. **Agarwal Ajay**, Ram P Gupta, W S Khokle, K D Kundra, P R Deshmukh, M Singh and P D Vyas, 1993, A new approach for the preparation of insitu superconducting BSCCO films, Supercond. Sci. Technol., 6, p.670

2. **Agarwal Ajay**, Ram P Gupta, and W S Khokle, 1994, Reliability of high temperature superconductor metal contacts, Microelectron. Reliab., 34, p.1273

3. Srivastava, P, N L Saini, B R Sekhar, S Venkatesh, M Khaled, S K Sharma, K B Garg, **A Agarwal**, Ram P Gupta, W S Khokle, H Ohkubo and M Akinaga, 1994, Photoemission study of influence of sputtering on Au-Bi(2212) interface, Supercond. Sci. Technol., 7, p.940

4. Shekhawat, G S, Ram P Gupta, **A Agarwal**, K B Garg and P D Vyas, 1995, The effect of sputter deposition conditions on the growth mechanism of $YBa_2Cu_3O_{7-\delta}$ thin films studied by scanning tunnelling microscopy, Supercond. Sci. Technol., 8, p.291

5. Shekhawat, G S, Ram P Gupta, **A Agarwal**, K B Garg and P D Vyas, 1995, Pattern generation on silicon surfaces and $YBa_2Cu_3O_{7-\delta}$ thin films by a scanning tunneling microscope, J. Appl. Phys., 78, p.127

6. Shekhawat, G S, Ram P Gupta, **A Agarwal**, P D Vyas, P Srivastava, N L Saini, S Venkatesh, and K B Garg, 1995, Observation of intercalation of excess oxygen in $Bi_2Sr_2CaCu_2O_{8+y}$ single crystal, Appl. Phys. Lett., 67, p.3343

7. Gupta, R P, G S Shekhawat, R R Mishra, **A Agarwal**, W S Khokle, and P D Vyas, 1996, Enhanced electric field effects in grain boundary based superconducting-FET,

Proc. of Int. conf. on High Temp. Superconductors: Ten years after its discovery, Dec. 16-21, Jaipur, India, in press

8. Srivastava, P, N L Saini, G S Shekhawat, B R Sekhar, S Venkatesh, **A Agarwal**, Ram P Gupta, and K B Garg, STM study of oxygen trapping in Bi-2212 single crystal, presented in DAE Symposium in Dec. 1993, BARC Bombay

9. **Agarwal Ajay**, Ram P Gupta, S A Mirji, P D Vyas, and W S Khokle, 1992, Sodium doped YBCO superconductor - A quest for room temperature superconductors, presented in National seminar on Phys. of Semiconductor Devices, Sept 21-22, CEERI, Pilani

10. Singh, G, **Ajay Agarwal**, S A Mirji, Ram P Gupta, P D Vyas, and W S Khokle, 1992, Study of silicon surface by scanning probe microscope, presented in National seminar on Phys. of Semiconductor Devices, Sept 21-22, CEERI, Pilani

11. Gupta, R P, *W S Khokle*, **Ajay Agarwal**, and P D Vyas,, 1992, High T_c Su-FET, Indo-US workshop on perspectives in materials, March 23-24, N Delhi

12. Gupta, R P, W S Khokle, **A Agarwal**, G S Virdi, B C Pathak and P D Vyas, 1990, (A report)